

Walt Lounsbery

CHAPTER V

STRUCTURES

## 5.1. STRUCTURES

- 5.1.1 Structural Requirements
- 5.1.2 Candidate Construction Methods
- 5.1.3 Wing
  - 5.1.3.1 Wing Configuration
  - 5.1.3.2 Wing Construction
- 5.1.4 Fuselage
  - 5.1.4.1 Fuselage Configuration
  - 5.1.4.2 Fuselage Construction
- 5.1.5 Tail
  - 5.1.5.1 Tail Configuration
  - 5.1.5.2 Tail Construction

## 5.2. WEIGHT AND BALANCE

- 5.2.1 Basic RPV
- 5.2.2 Mission A
- 5.2.3 Mission B

## 5.3. NASTRAN MODEL

- 5.3.1 NASTRAN Modeling
  - 5.3.1.1 Grid Points
  - 5.3.1.2 Elements
  - 5.3.1.3 Constraints
- 5.3.2 NASTRAN Results
  - 5.3.2.1 Weights and Moments of Inertia
  - 5.3.2.2 Displacements
  - 5.3.2.3 Stresses
  - 5.3.2.4 Final Structure

## 5.4. REFERENCES

## 5.1. STRUCTURES

### 5.1.1 Structural Requirements

The RPV structure had to be configured around many requirements including take-off and landing and maneuvering flight loads, propulsive system demands and stability and control while providing an excellent platform for the mission equipment. At the same time, it was necessary to keep the production costs to a minimum, build in a high degree of maintainability and keep the structural weight down to a point that allowed the mission objectives to be met. Obviously, trade-offs were necessary and these are presented here to indicate the philosophy used in this design phase.

From the beginning, a rocket-assisted take-off was used for take-off load estimation. A 3-5g acceleration gave the necessary take-off performance but produced large structural loads in the longitudinal direction. This indicated a need for internal bracing to support internal components (fuel tanks, electronics, power plant, etc.). Furthermore, the take-off load was applied by the rocket-powered sled (or hydraulic catapult) to a hook toward the front of the underside of the vehicle resulting in a very concentrated load on the structure ( $\approx 1000$  lbs.). Similarly, on landing a rear hook would snare a horizontal net to bring the craft to a stop (and also the forward hook was to prevent the RPV from being ejected backwards off the net in a sling-shot manner). In order to come to a stop in a reasonable distance, decelerations on the order of 5 g's were necessary resulting in a similar load being placed on the rear hook as the front hook encountered on take-off.

In flight, the loads act primarily along the RPV's vertical axis in both the positive and negative directions. To be maneuverable, the aircraft must be able to execute sharp maneuvers such as pull-ups, push-overs, and tight horizontal turns. This would allow "close in" flying (road or river following, tree-top flying, etc.) that would make the aircraft harder to detect and track and thus, to bring down. For this reason, the goal of +8 g's to -5 g's was set. This also carried over to the ability to take the large gust loads which could well be encountered in a battlefield zone.

To provide for maximum longitudinal stability throughout the flight envelope called for a well-placed c.g. as well as small c.g. travel for all mission profiles. Flexibility in locating mission equipment in the nose due to the availability of a large volume with which to work with inside the revolved NACA 0018 airfoil helped in this matter. Judicious choices in propulsion system locations, fuel tank locations, and horizontal tail location and size produced the longitudinal stability desired.

#### 5.1.2 Candidate Construction Methods

The size of this RPV (15 ft. wing span) is about half the size of a general aviation airplane and about twice the size of a radio-controlled model airplane. This would seem to indicate that construction techniques from either might be employed. For this reason, metal skin over metal ribs and spars was compared with fiber-reinforced epoxy over a foam core for the RPV construction.

The conventional construction technique (metal skin over metal ribs and spars) has been used for over four decades and has provided aircraft with a rugged though fairly expensive structure. Unfortunately,

it provides a large radar return, usually requires a protective coating (paint), has a large weight penalty and does not conform well to aerodynamic shaping. The latter problem has led to many aircraft having less efficient wing sections in order to reduce manufacturing problems and consequently, costs.

The use of fiber-reinforced epoxy (typically fiberglass) skins over foam cores was a recent addition to the construction scene for R-C modelers. This technique has drastically reduced construction time, tools and complexity while keeping the costs down and the durability and maintainability high. These advantages plus the fact that the result is a light, easily manufactured article that has no radar return makes this method quite attractive. However, this type construction will not carry the concentrated loads created by the rigors of take-off and landing the RPV nearly as well as the conventional construction. For this reason, a compromise was searched for to minimize this problem while maintaining the advantage of the epoxy-foam combination.

### 5.1.3 Wing

#### 5.1.3.1 Wing Configuration

The wing chosen was the NACA 4412 airfoil with an elliptical planform for low induced drag. This was economically feasible from a manufacturing point of view only if a fiber-reinforced epoxy skin was utilized. Many candidate fibers were reviewed (Table 5.1-1)<sup>1</sup> and the strength-to-weight ratios of the better ones compared with other materials<sup>2</sup> in Table 5.1-2. These, along with the vibrational damping characteristics<sup>3</sup> (Table 5.1-3) and excellent resistance to chemicals<sup>3</sup> (Table 5.1-4), pointed to Du Pont's Kevlar 49 aramid

Type →	Acrylics							Polyolefins		
	Polyacrylonitrile (Orlon)	Acrylonitrile Vinyl Chloride Derivatives	Acrylonitrile Vinyl Chloride (Dyne)	Modified Acrylic (Verel)	Acrylonitrile Base (Creslan)	Dinitrile <sup>a</sup> (Darvan)	Nitrile <sup>b</sup> Alloy (Zefran)	Polyethylene		Polypropylene
								Type I	Type II	
<b>NATURE OF FIBER</b>										
Form	Staple	Staple	Staple	Staple	—	—	—	Monofilament		Monofil.
Length, in.	—	—	—	—	—	—	—	—		—
Width,	14-27	15-30	—	—	—	—	—	250-1300		—
Cross Section	Dogbone	—	—	—	—	—	—	Circular		Circular
<b>PROPERTIES<sup>c</sup></b>										
Spec. grav.	1.14	1.17	1.3	1.37	1.17	1.18	1.19	0.92	0.95-0.96	0.90-0.91
Breaking Tenacity, gm/den	2.2-2.6	2.5	2.5-3.3	2.5-2.8	3.3	1.75	3.5	1.0-3.0	5.0-7.3	5.5-7.0
Wet	1.8-2.1	2.0	2.5-3.3	2.4-2.7	3.3	1.5	3.1	1.0-3.0	5.0-7.3	5.5-7.0
Ten Str, 1000 psi	32-39	37-40	40-57	42-47	41	26	53	11-35	50-90	—
Breaking Elong, %	20-28	36	30-42	33-35	32	30	33	20-80	10-40	12-25
Wet	26-34	44	30-42	32-34	32	30	33	20-80	10-40	—
Stiffness (avg), gm/den <sup>d</sup>	10	7	8.2	8.0	10.3	6	11	2-12	20-50	—
Strain Recovery <sup>e</sup>	—	99, 89 (5%)	94	88 (4%)	90 (1%)	100 (3%)	99, 72 (10%)	90-95 (5%)	Slow	—
(at 2%), %				55 (10%)	48 (5%)	75 (5%)				
Toughness (avg), gm-cm/den-cm	0.40	0.46	0.53	0.46	0.53	0.3	0.58	0.3	—	—
Moisture Regain, %	1.5	1.2	0.3-0.4	3.5-4	1.3	2-3	2.5	None	None	—
<b>CORROSION RESISTANCE</b>										
Strong Acids	Good-exc.	Good exc.	Good	Exc.	Good-exc.	Good-exc.	Exc.	Exc. to all but oxidizing acids		Sim. to polyethylene
Weak Acids	Exc.	Exc.	Exc.	Exc.	Exc.	Exc.	Exc.	Exc.	Exc.	Exc.
Strong Alkalies	Poor	Poor	Good	Discolors	Poor	Poor	Fair	Exc.	Exc.	Exc.
Weak Alkalies	Fair-good	Fair-good	Exc.		Fair-good	Fair-good	Good	Exc.	Exc.	Exc.
Heat	Soft at 455 F	5% shrinkage at 487 F	Unless HT, <sup>f</sup> shrinks 250 F	Stiffens above 300 F	Sticks at 450 F <sup>g</sup>	Sticks at 450 F <sup>g</sup>	Sticks at 490 F <sup>g</sup>	Melts 225 F	Melts 265-280 F	Melts 325-335 F

<sup>a</sup> Though not an acrylic (actually a polymer of vinylidene cyanide) it is listed here because of similar properties. <sup>b</sup> Nitrile alloy based on acrylonitrile. <sup>c</sup> 70 F, 65% RH, unless otherwise noted. <sup>d</sup> Ratio of breaking stress to breaking strain (i.e., gm/den to rupture divided by strain in cm/gage cm at breaking stress). <sup>e</sup> Recovery after 2% strain, except where specific percentage is given in parentheses. <sup>f</sup> Heat treated. <sup>g</sup> Copper block method.

Type →	Nylon							Cellulose Esters	
	6/6			6			Qiana	Cellulose Acetate	Cellulose Triacetate (Arel)
	Regular	High Tenacity	Staple	Regular	High Tenacity	Staple			
<b>NATURE OF FIBER</b>									
Form	Filament	Filament	Staple	Filament	Filament	Staple	Filament	Fil, Staple	Fil, Staple
Length, in.	Cont.	Cont.	—	Cont.	Cont.	—	Cont.	—	—
Width, $\mu$	11-43	16-43	14-43	—	—	—	19-35	11-46	—
Cross section	Round	Round	Round	Round	Round	Round	Trilobal	Clover Leaf	Clover Leaf
<b>PROPERTIES<sup>a</sup></b>									
Spec Gravity	1.14	1.14	1.14	1.14	1.14	1.14	1.03	1.32	1.3
Breaking Tenacity, gm/den	4.6-5.9	5.9-8.8	4.0-4.7	4.5-5.8	6.8-8.6	3.8-5.5	2.7-3.8	1.3-1.5	1.2-1.4
Wet	4.0-5.2	5.1-7.6	3.5-4.2	4.3-5.3	5.4-7.5	—	—	0.8-1.2	0.8-1.0
Ten Str, 1000 psi	67-86	86-128	58-69	73-84	109-125	70-80	35.5-50.0	22-28	20-26
Breaking elong, %	26-32	18-28	38-42	24-34	16-17.5	37-40	26-36	23-34	22-28 <sup>b</sup>
Wet	30-37	21-32	42-46	28-38	19-24	42-46	—	30-45	30-40
Stiffness (avg), gm/den <sup>c</sup>	—	—	—	—	—	—	7.5-15.0	5.5	5.2
Strain recovery <sup>d</sup> (at 2%), %	100, 100	100 (4%)	—	—	100, 100	100 (4%)	100	48-65 (4%)	88 (3%) 43 (10%)
Toughness (avg), gm-cm/den-cm	0.76	0.85	0.87	0.67	0.75	0.64-0.78	0.85-1.0	0.17	0.16
Moisture Regain, %	4.5	4.5	4.5	4.0	4.0	4.0	2.5	6	3.2
<b>CORROSION RESISTANCE</b>									
Strong Acids	Dissolves in cold HCl, H <sub>2</sub> SO <sub>4</sub> , and HNO <sub>3</sub>			Degraded by oxidizing agents & mineral acids			Depends on conc.	Decompose	Decompose
Weak Acids	Ult disintegration in 5% boiling HCl			Weakens on prolong. exp. to benzoic and oxalic acids			Excel.	Decompose	Decompose
Strong Alkalies	Substantially inert			Substantially inert			Excel.	Saponifies, Res (cold) similar to viscose.	
Weak Alkalies	Substantially inert			Substantially inert			Excel.	Same as strong alk.	
Heat	Yellows slightly after 5 hr at 300 F; melts at 482 F			Yellows slightly after 5 hr at 300 F; melts at 420 F			Good	Soft 350-375 F; Melts 500 F	Melts at 575 F

<sup>a</sup> 70 F, 65% RH, unless otherwise noted. <sup>b</sup> For filament; 35-400% for staple. <sup>c</sup> Ratio of breaking stress to breaking strain (i.e., gm/den to rupture divided by strain in cm/gage cm at breaking stress). <sup>d</sup> Recovery after 2% strain except where specific percentage strain is given in parentheses. <sup>e</sup> Basic flammability of untreated fiber.

Table 5.1-1

Type →	Regenerated Cellulose (rayons)				Aramids			Polyesters		
	Viscose		Saponified Acetate		Nomex <sup>a</sup>	Kevlar 29	Kevlar 49	Polyethylene Terephthalate (Dacron)		
	Reg to Med Tenacity	High Tenacity	(Fortisan)	(Fortisan 36)				Regular	High Tenacity	Staple
<b>NATURE OF FIBER</b>										
Form	Fil, staple	Filament	Filament	Filament	Fil, staple	Filament	Filament	Fil, staple	Fil, staple	Fil, staple
Length, in.	—	—	—	—	1-2.5	Cont.	Cont.	1.5-4.0	1.5-4.0	1.5-4.0
Width, μ	4.3-8.4	10-15	3-9	3-9	—	11.9	11.9	11-28	11-28	18-25
Cross section	Irreg	Irreg	Irreg	Irreg	Round	Round	Round	Circular	Circular	—
<b>PROPERTIES<sup>a</sup></b>										
Spec grav	1.46-1.52	—	1.5	1.5	1.38	1.44	1.45	1.38	1.38	1.38
Breaking Tenacity, gm/den	1.5-3.2	3.0-5.0	6.7	8	5.3	21.5	21.5	4.4-5.0	6-7	3.8-4.3
Wet	0.7-1.9	1.9-3.6	5.1-6.0	6.0-6.4	4.1	21.5	21.5	4.4-5.0	6-7	3.8-4.3
Ten Str, 1000 psi	29-65	65-105	136	155	95.5	400	400	77-88	106-123	67-76
Breaking Elong, %	15-30	9-22	6	6.2	12.2	3.4	2.25	19-25	9-11	30-36
Wet	17-40	14-30	6	6	16	4	2.25	19-25	9-11	30-36
Stiffness (avg), gm/den <sup>b</sup>	11.1-16.6	25.5-29	117	135	—	460	1000	—	—	—
Strain Recovery <sup>c</sup> (at 2%), %	30-97	70-100	100 (20%) 60 (40%)	85.7 (5%)	—	—	—	97, 80 (8%)	100, 90 (8%)	—
Toughness (avg), gm-cm/den-cm	0.19-0.21	0.22-0.30	0.21	0.26	—	—	—	0.78	0.50	1.03
Moisture Regain, %	13	13	10.7	9.6	5.0	5.0	3.5	0.4	0.4	0.4
<b>CORROSION RESISTANCE</b>										
Strong Acids	Disintegrates in hot dilute or cold concentrated acids		Similar to cotton		Str loss	Good	Good	Dissolves in H <sub>2</sub> SO <sub>4</sub>		
Weak Acids	Swell, str reduced		Similar to cotton		Mod str loss	Good	Good	Good		
Strong Alkalies	Good		Similar to cotton		Str loss	Good	Good	Disintegrates when boiled		
Weak Alkalies	—		Similar to cotton		Better than Nylon 6/6	Good	Good	Good		
Heat	—		Similar to cotton		320 F long term	320 F long term	390 F long term	Melts at 480 F		

<sup>a</sup> 70 F, 65% RH, unless otherwise noted. <sup>b</sup> Ratio of breaking stress to breaking strain (i.e., gm/den to rupture divided by strain in cm/gage cm at breaking stress). <sup>c</sup> Recovery after 2% strain except where specific percentage strain is given in parentheses. <sup>d</sup> 20 denier yarn with 3 yarns/in. of twist. <sup>e</sup> After 1000 hr at 500 F has 65% RT breaking strength; degrades above 700 F.

Type →	Organic, man-made					Organic, natural				
	Vinyl Derivatives				Polyvinyl Alcohol	Novoloid	Fluorocarbon	Cotton	Hemp	Silk
	Vinyl Chloride Acetate	Vinylidene Chloride, saran								
	Mono Filament	Filament	Staple		Kynol	TFE				
<b>NATURE OF FIBER</b>										
Form	Staple	—	—	—	Staple	Fil, staple	Filament	Staple	Staple	Fil, staple
Length, in.	—	—	—	—	—	—	—	1-1.5	—	—
Width	16-18	1300	50	—	—	14	—	16-21	18-23	10-13
Cross section	Barbell	Circular	Circular	Circular	Peanut	—	Circular	Ribbonlike	Triangular	Triangular
<b>PROPERTIES<sup>a</sup></b>										
Spec grav	1.33-1.35	1.7	1.7	1.7	1.26-1.30	1.25	2.3	1.55 <sup>d</sup>	1.48	1.25 <sup>e</sup>
Breaking Tenacity, gm/den	0.7-1.0	1.2-2.3	Up to 2	Up to 1.5	4.4-6.0	1.7	1.6	1.5-6.0	5-7	3.5-4.5
Wet	0.7-1.0	1.2-2.3	Up to 2	Up to 1.5	3.7-5.0	1.56	1.6	1.5-6.0	5-7	3-4
Ten Str, 1000 psi	12-17	15-45	44	33	—	27	47	—	—	—
Breaking Elong, %	100-120	20-30	15-25	15-25	15-17	35	13	6-9	1-3	20-25
Wet	100-120	20-30	15-25	15-25	—	37	13	7-10	1-3	25-30
Stiffness (avg), gm/den <sup>b</sup>	1.5	7-10	8-12	8-12	24-40	45	12	60-70	200	100
Strain Recovery <sup>c</sup> (at 2%), %	—	95 (10%)	95 (10%)	95 (10%)	—	95	88 (3%)	95	90 (<1%)	90 (<2%)
Toughness (avg), gm-cm/den-cm	1.3	0.17-0.27	0.125	0.125	0.79-0.92	0.5	0.12	0.15	0.04	0.44
Moisture Regain, %	up to 1.5	None	None	None	4.5-5.0	6	None	6 <sup>f</sup> , 8 <sup>g</sup>	8 <sup>h</sup>	10
<b>CORROSION RESISTANCE</b>										
Strong Acids	Excellent	Exc; fair to conc H <sub>2</sub> SO <sub>4</sub>			—	Res hot and conc non-oxidizing mineral acids	Inert	Dissolves	Dissolves	Dissolves
Weak Acids	Excellent	Excellent			—	Some instability	Inert	Stable	Stable	Fair
Strong Alkalies	Excellent	Excellent except to NH <sub>4</sub> OH			—	—	Inert	Swell	Swells	Dissolves
Weak Alkalies	Excellent	Excellent			—	—	Inert	Good	Stable	Fair
Heat	Melts 260F	Softens at 240-280 F			Melts 420 F	Good to 570F	Good to 400 F	Good	Stable	Good

<sup>a</sup> 70 F, 65% RH, unless otherwise noted. <sup>b</sup> Ratio of breaking stress to breaking strain (i.e., gm/den to rupture divided by strain in cm/gage cm at breaking stress). <sup>c</sup> Recovery after 2% strain except where specific percentage strain is given in parentheses. <sup>d</sup> Dry cotton @ 68 F. <sup>e</sup> Depends on type and growth conditions. <sup>f</sup> Scoured. <sup>g</sup> Mercerized. <sup>h</sup> Bleached. <sup>i</sup> Reummed dry @ 77 F.

Table 5.1-1 cont.

Type →	Inorganic, man-made					Inorganic, natural				
	Glass		Graphite		Boron <sup>1</sup>	Asbestos		Alumina Silica	Carbon	Zirconia
	Type E	Type S	High Mod.	High Str.		Chrysotile	Crocidolite	—	—	—
<b>NATURE OF FIBER</b>										
Form	Cont, Staple	Cont.	Cont, Chopped	Cont, Chopped	Cont	Crude	—	Staple	Cont, Fil	Can be cont
Length, in.	—	—	—	—	—	3/8-2	1/8-3	1/4-10	—	—
Width, μ	—	—	7.1-7.6	7.49-7.99	—	0.02	0.02	3-20	8-10	—
Cross section	Cyl, tub	Cyl	Circular	Circular	Circular	Tub	Cyl	—	Irreg	—
Min/Max dia, mil	0.03-0.04	0.03-0.04	0.072-0.075	0.078-0.08	2-8	—	—	—	0.03-0.04	0.039 <sup>9</sup>
<b>PROPERTIES</b>										
Spec grav	2.54	2.49	1.85-1.9	1.79-1.83	2.3-3.48	2.4-2.6	3.2-3.3	2.73	1.4-1.85	5.6-5.9
Break Tenacity										
gm/den										
70F, 65% RH	3.9-4.7	—	—	—	—	2.5-3.1	—	1.4-6.5	7.5	—
Wet	4.0-4.6	—	—	—	—	—	—	—	—	—
Tens <sup>tr</sup> (70F 65%RH)										
1000psi	300-500	500-650	340 min	410 min	400 avg	350-750	100-300	50-230	30-180	150-200
Breaking Elong, %, 70F 65%										
RH	3-4	—	0.62-0.68	1.2-1.4	—	—	None	1.4-2.7	2.5	—
Wet	2.5-3.5	—	—	—	—	—	None	—	—	—
Strain Recovery (at 2%), %	100	—	—	—	—	—	100	—	100	—
Toughness (avg), gm-cm/den-cm	0.07	—	—	—	—	—	—	—	—	—
Moisture Regain (70 F, 65 RH), %	0	—	—	—	—	—	0	—	2-14	—
Ther Cond Btu-ft/hr-sq ft-F	7.2	—	—	—	—	—	—	—	11	—
<b>CORROSION RESISTANCE</b>										
Strong Acids	Attack only by HF and hot H <sub>3</sub> PO <sub>4</sub>		Excellent		—	Poor	Good, exc. HF	Sim to borosil glass	Excel.	Fair, exc. HF, hot H <sub>2</sub> SO <sub>4</sub>
Weak Acids	Stable		Excellent		—	Poor-good	Excel.	—	Excel.	Good
Strong Alkalies	Resist most		Excellent		—	Excel.	Excel.	—	Excel.	Excel.
Weak Alkalies	Resist most		Excellent		—	Excel.	Excel.	—	Excel.	Excel.
Heat	600 F		4500 F <sup>8</sup> 750 F <sup>1</sup>	1700 F <sup>8</sup> 600 F <sup>1</sup>	—	1400-1900 F	1400 F	2300 F max 320 F melts	4500 F max, 6040 F <sup>9</sup>	—
Sunlight	Inert		Inert		Inert	Inert	Inert <sup>7</sup>	Inert	Inert	Inert

<sup>1</sup> Properties may vary widely depending on glass comp. values shown are for borosilicate. <sup>2</sup> Sometimes in inert atmosphere. <sup>3</sup> In air. <sup>4</sup> Meas. on tungsten substrate. <sup>5</sup> function of the matrix when used in composites.

Table 5.1-1 cont.



## Strength-To-Weight Ratios of Various Types of Materials

Material	Strength-to-Weight Ratio* x 10 <sup>-3</sup>
Polycarbonate	210
Polystyrene	230
Nylon	260
Styrene-Acrylonitrile Copolymers	310
Brass (Yellow Cast)	320
Zinc Alloys (Cast)	350
Glass/Polystyrene	360
Glass/Polycarbonate	370
Glass/Styrene-Acrylonitrile Copolymers	410
Magnesium	460
Aluminum	530
Glass/Nylon	550
Orlon	850
Nylon 6/6	1322
Boron	3833
Type E Glass	4861
High Strength Graphite	6170
Type S Glass	6395
Kevlar 49	7639

\* Tensile strength in psi divided by weight in pounds per cubic inch.

Table 5.1-2

DECAY OF FREE VIBRATIONS

	<u>Loss Factor x 10<sup>-4</sup></u>
1020 Steel	<20
Ductile Cast Iron	30
Graphite/Epoxy	30
Fiberglass/Epoxy	47
Kevlar 49/Epoxy	160
Cured Polyester Resin	400

$$\text{Loss Factor} \approx \frac{A_n}{A_n + 1}$$

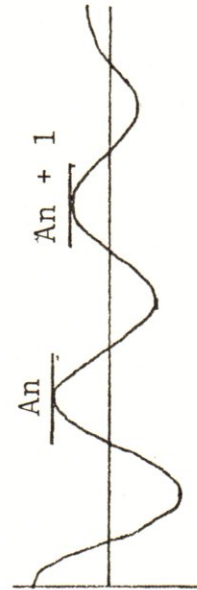


Table 5.1-3

ENVIRONMENTAL STABILITY OF "KEVLAR" 49  
 UNIDIRECTIONAL TAPE REINFORCED 3M SP-306  
 EPOXY RESIN COMPOSITES

Environment	Interlaminar Shear Strength, psi*
Control	10,520
Water Boil (2 hours)	9,290
Salt Water Room Temp. 100 hours	9,770
Texaco "Abjet K-40" Jet Fuel Room Temp. 100 hours	10,480
"Skydrol" Lubricating Oil Room Temp. 100 hours	10,460

\* Short Beam Shear, 4/1 span/depth ratio

Table 5.1-4

fiber. The Kevlar was found to be available as woven fabric in several styles<sup>4</sup> (Table 5.1-5) and style 285 was chosen for its conformability and lower costs<sup>5</sup>. Typical properties of the various fabric styles in an epoxy composite<sup>4</sup> (usually 50-50 by volume) are given in Table 5.1-6. As a point of comparison, the yarn and composite properties<sup>6</sup> are shown in Table 5.1-7.

Research showed Kevlar to be in use in several applications including the skin of the Lockheed Quila RPV<sup>7</sup>. Use as hulls for boats<sup>8</sup> has demonstrated its resistance to sharp inward blows in that the composite does not crack but can be "popped" back out without structural failure. Repair has proven comparatively easy requiring only a simple fabric and epoxy patch as with fiberglass followed by sanding to smooth contours. Painting is unnecessary for the Kevlar but camouflage might still be required. For best results, the fabric is pre-impregnated with XCE epoxy resin ("pre-peg"), cut, vacuum molded, cured and joined section-to-section with epoxy. Unfortunately, the Kevlar fabric costs about \$14.00 per square yard at present and this is much higher than that for a similar weave of fiberglass (about \$1.00 per square yard). This, plus the increased tooling costs of Kevlar (cutters, drills, sanders, etc.) drive up the manufacturing costs on a per unit area basis over fiberglass. Fortunately, the total area involved (less than 40 square yards per RPV) is not large so the increased costs incurred are not overly burdensome.

In order to provide structural mounting and stress distribution, aluminum main and rear spars were placed at basically the 30% and 75% chord locations, respectively, and run parallel to each other

FABRICS OF KEVLAR® 49 ARAMID

<u>Style</u>	<u>Basis Weight (oz./yd.<sup>2</sup>)</u>	<u>Fabric Construction (Ends/Inch)</u>	<u>Yarn Denier*</u>	<u>Weave</u>	<u>Fabric Thickness (mils)</u>
120	1.8	34 x 34	195	Plain	4.5
143	5.6	100 x 20	380/195	Crowfoot	10
181	5.0	50 x 50	380	8-harness satin	9
243	6.7	38 x 18	1140/380	Crowfoot	13
281	5.0	17 x 17	1140	Plain	10
285	5.0	17 x 17	1140	Crowfoot	10
328	6.8	17 x 17	1420	Plain	13

\*Denier: Weight in grams of 9000 meters of yarn.

Table 5.1-5

TYPICAL COMPOSITE PROPERTIES  
(Vacuum Bag, Autoclave Molded Epoxy)\*

<u>Style</u>	<u>Fabric v/o</u>	<u>Tensile Strength (10<sup>3</sup> lb/in<sup>2</sup>)</u>	<u>Tensile Modulus (10<sup>6</sup> lb/in<sup>2</sup>)</u>	<u>Flex Strength (10<sup>3</sup> lb/in<sup>2</sup>)</u>	<u>Flex Modulus (10<sup>6</sup> lb/in<sup>2</sup>)</u>	<u>Shear Strength (lb/in<sup>2</sup>)</u>
120	45	65/65	4.3/4.3	50/50	4.0/4.0	7000
181	40	60/60	4.0/3.2	50/50	3.8/3.2	6300
281	40	55/55	3.8/3.8	50/50	3.3/3.3	6000
285	40	55/55	4.0/3.8	50/50	3.6/3.1	6000
328	45	55/55	3.8/3.8	45/45	3.3/3.3	6000
143	40	110/13	6.3/1.1	65/18	5.8/1.0	7500/2500
243	40	115/20	6.8/1.7	65/25	6.1/1.2	7000/4500

\*350°F (177°C) service temperature

Table 5.1-6

**"KEVLAR" 49: YARN PROPERTIES**

DENSITY 1.44 g/cc • 40% lower than glass.  
(C.052 lb/in.<sup>3</sup>)

FILAMENT DIAMETER 0.00047 in. • About the same as glass.

FIBER ELONGATION\* 2.8% • Significantly lower than other organic fibers.

TENSILE STRENGTH\* 525,000 psi • Substantially above conventional organic fibers, equivalent to S-glass, and higher than graphite.

SPECIFIC TENSILE\* 10x10<sup>6</sup> in. • Highest of any commercially available fiber.

MODULUS 19x10<sup>6</sup> psi • Twice that of E-glass.

SPECIFIC MODULUS 3.5x10<sup>8</sup> in. • Between that of glass fibers and the high modulus graphites.

CHEMICAL RESISTANCE Good • Highly resistant to organic solvents, fuels and lubricants.

TEXTILE PROCESSIBILITY Excellent • Can be readily woven on conventional fabric looms.

FLAMMABILITY CHARACTERISTICS Excellent • Yarns retain 90% of their tensile strength after weaving.

TEMPERATURE RESISTANCE Excellent • Knot strength is 35% of straight tensile strength.

• Can be easily handled on filament winding and pultrusion equipment.

• Inherently flame resistant. Self-extinguishing when flame is removed. Does not melt.

• No degradation of yarn properties in short term exposures up to temperatures of 500°F.

**"KEVLAR" 49: GENERAL COMPOSITE\* PROPERTIES**

DENSITY • 25-30% lower than that of glass composites.

SPECIFIC TENSILE • Superior to all other composites reinforced with commercially available fibers.

SPECIFIC MODULUS • About two times that of S-glass composites.

PROCESSIBILITY • Can be readily handled using conventional reinforced plastics fabrication techniques.

ELECTRICAL PROPERTIES • Machining techniques for drilling, routing, cutting and milling have been developed.

ENVIRONMENTAL STABILITY • Superior to glass composites and equivalent to quartz fiber composites in dielectric constant and loss tangent.

FLAMMABILITY • Useful long term temperature range: -320° to +320°F.

IMPACT STRENGTH • No degradation in jet fuel, lubricating oils, water, salt water, or high humidity.

• Good UV stability.

• Meets all FAA flammability and smoke requirements in flame resistant, low smoke resins.

• Far exceeds impact strengths of graphite and boron and better than glass in some tests.

• About half that of glass composites.

• Equivalent to glass and graphite in some resins.

• Far superior to glass.

• Superior to glass.

**TEST DATA FOR "KEVLAR" 49 PLASTIC COMPOSITES**

**MECHANICAL PROPERTIES**

DENSITY .050 lbs/cu. in. UNIDIRECTIONAL\* FABRIC\*\* 0.048 lbs/cu. in.

TENSILE STRENGTH 200,000 psi 75,000 psi

TENSILE MODULUS 11.0x10<sup>6</sup> psi 4.5x10<sup>6</sup> psi

COMPRESSIVE STRENGTH 40,000 psi 25,000 psi

COMPRESSIVE MODULUS 11.0x10<sup>6</sup> psi 4.5x10<sup>6</sup> psi

INTERLAMINAR SHEAR STRENGTH 9,000 psi 7,500 psi

IMPACT STRENGTH (Charpy Unnotched) 150 ft. lbs./in.<sup>2</sup> 75 ft. lbs./in.<sup>2</sup>

**ELECTRICAL PROPERTIES**

DIELECTRIC CONSTANT (10<sup>6</sup>Hz) 3.3 4.1

LOSS TANGENT (10<sup>6</sup>Hz) 0.023 0.024

VOLUME RESISTIVITY 5x10<sup>15</sup> ohms-cm.

DIELECTRIC STRENGTH (125 mil) 960 V/mil

\*ASTM D2343-67

\*Composite made with 8-harness satin weave fabric (~5 oz/yd<sup>2</sup>), epoxy resin, v/o = ~55 (autoclave cured)

\*Filament wound, continuous aligned fiber reinforced epoxy resin, v/o = 65. (Autoclave cured)

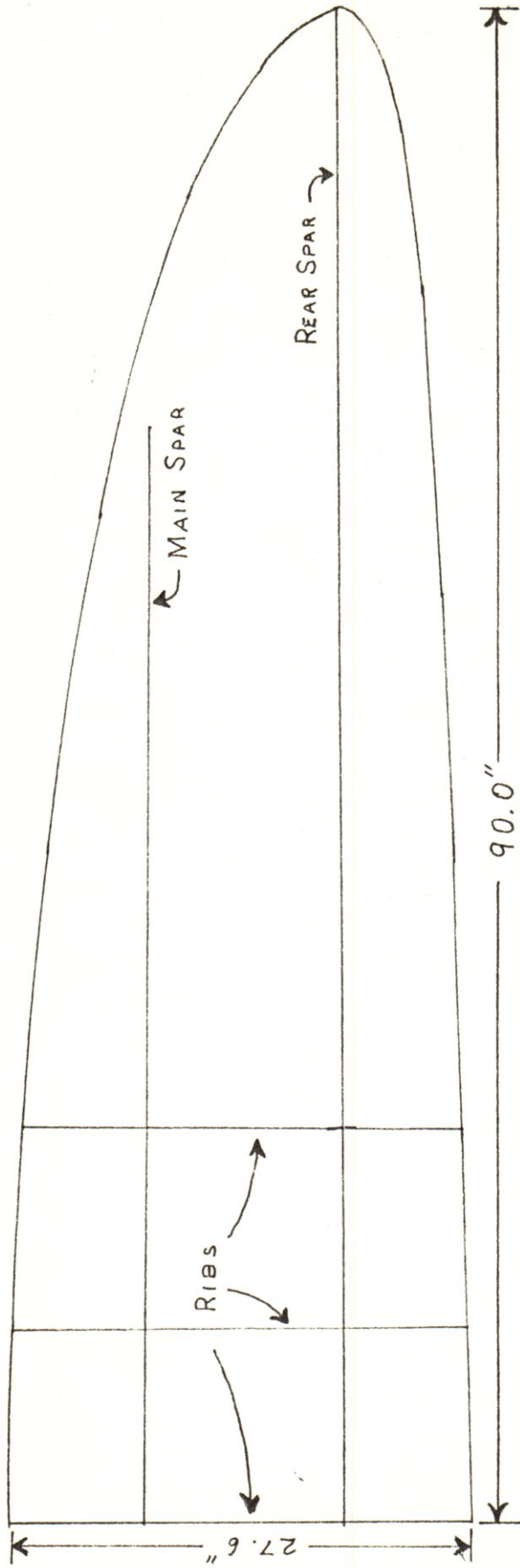
\*\*8-Harness satin weave fabric (~5 oz yd<sup>2</sup>), epoxy resin, v/o = ~55. (Autoclave cured)

(Figure 5.1-1). Due to the elliptic nature of the planform, it was possible to locate only the rear spar on a constant chord line and maintain a meaningful structure. Therefore, the main spar was positioned parallel to the rear spar but its length was limited by the planform to approximately 73% of the full span. Its chord-wise location was expected to be roughly that of the wing elastic axis thus minimizing the torsional loads encountered by the I-beam cross-section of the main spar. The rear spar (a hollow tube) was located to act as a hinge point for the full span flaps as well as to provide additional torsional rigidity in the wing. The cross-sectional properties of the spars are shown in Figure 5.1-2. Both the main and rear spars were of extruded 2024-T6 aluminum for strength and low manufacturing costs. The two different sized sections of the rear spar were welded together via a machined joint.

Five aluminum ribs, spaced 12" apart, were used to provide additional support of the wing structure in and around the area of the wing-fuselage mounting and wing fuel tanks (four plastic tanks sandwiched between the five ribs and positioned fore and aft by the main and rear spars). The ribs were stamped .050" 2024-T6 aluminum. The servo motors (2) for the flaps were each mounted to the outboard ribs and the flaps were driven simultaneously through a universal joint at the wing root. This provided redundancy in the flap deflection system while insuring equal flap deflections for both wings. Also, the spoiler servos (one each) were braced to the main spar and skin.

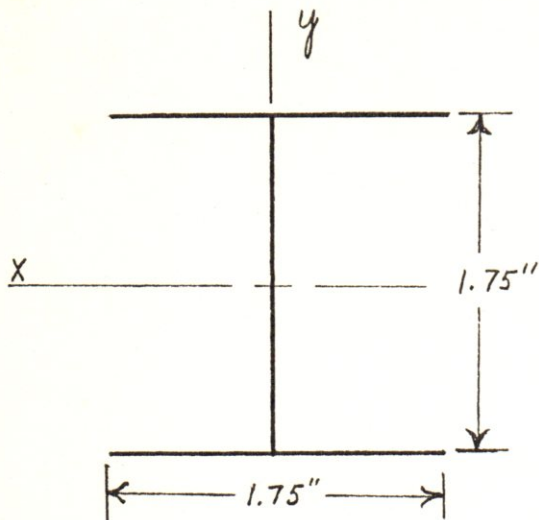
Foam was used to fill spaces remaining such as those forward of the main spar, outboard of the ribbed section and the interior of the flaps. The foam contributed little strength and an insig-





WING SEMI-SPAN PLANFORM

FIGURE 5.1-1



MAIN SPAR

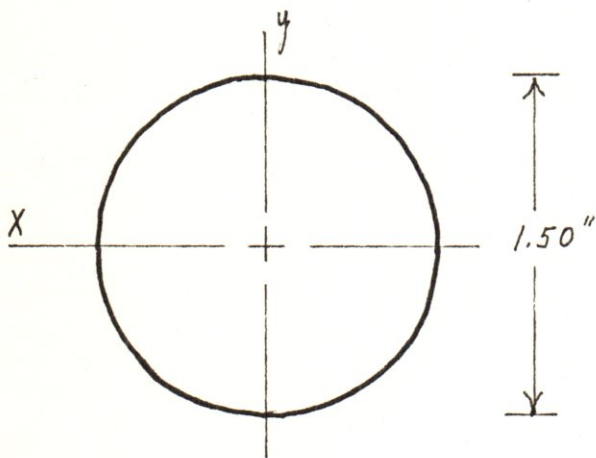
Thickness = 0.04"

Area = 0.20680 sq. in.

$I_x = 0.11789 \text{ in.}^4$

$I_y = 0.08571 \text{ in.}^4$

$J = 0.20360 \text{ in.}^4$



INBOARD REAR SPAR

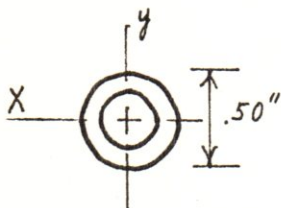
Thickness = 0.01 "

Area = 0.04681 sq. in.

$I_x = 0.01299 \text{ in.}^4$

$I_y = 0.01299 \text{ in.}^4$

$J = 0.02598 \text{ in.}^4$



OUTBOARD REAR SPAR

Thickness = 0.10"

Area = 0.12566 sq. in.

$I_x = I_y = 0.00267 \text{ in.}^4$

$J = 0.00534 \text{ in.}^4$

Wing Spars' Cross-Sectional Properties

Figure 5.1-2

nificant weight but eliminated volumes for water condensation and created a rigid containment for wires and tubing. Additional wing stiffness was obtained (but not used in the calculations) by assuming a slight "overfill" of the foam thereby pre-stressing the skin a small amount. Finally, in order to have the fuel tanks tightly located but cushioned slightly, foam was used to fill all the spaces around them.

#### 5.1.3.2 Wing Construction

A construction technique similar to the Aquila was envisioned for the wing. The wing upper and lower surface shells and flaps would be formed of a single layer of prepreg Kevlar and the rib and spar structure would be assembled. The rear spars would be joined at the root by a universal joint, as mentioned above, and the main spar would have to be cut and welded to account for the  $7.50^\circ$  anhedral. The metal and skin structures would be joined with epoxy with the upper wing surface shell used first to allow checking the operation of the control surfaces. All tanks, wiring, and tubing would be positioned, as would the flaps, prior to mating the lower wing surface shell. Again all surfaces would be joined with epoxy. Finally, all cavities would be filled by injecting structural foam.

#### 5.1.4 Fuselage

##### 5.1.4.1 Fuselage Configuration

There were many factors affecting the fuselage configuration, the major ones of which are:

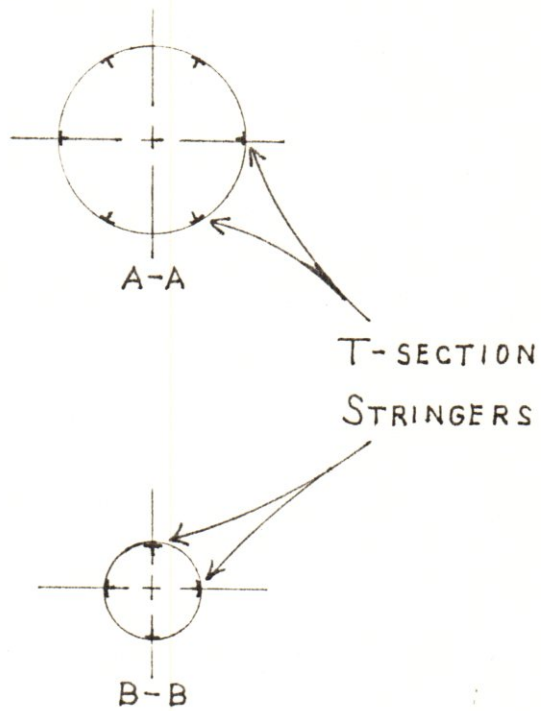
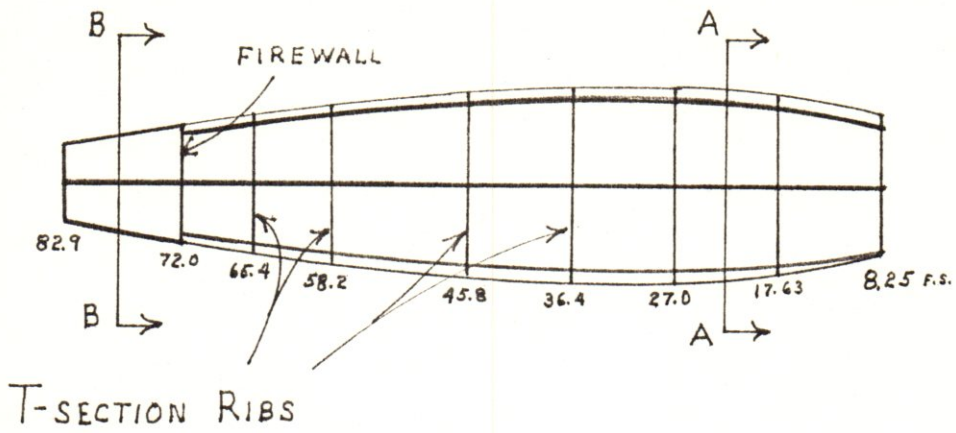
- 1.) low drag,
- 2.) large forward volume for missions equipment,
- 3.) adequate structure for rear-mount propulsion system and tail boom,

- 4.) adequate volume for fuel, propulsion and electronics,
- 5.) large, localized take-off and landing loads,
- 6.) light weight,
- 7.) minimize radar cross-section, and
- 8.) ease in manufacture and maintenance.

All these were well satisfied by the configuration arrived at. The revolved NACA 0018 airfoil provided the necessary volume for the missions equipment, fuel, propulsion and control electronics while keeping the drag respectably low. The Kevlar skin over aluminum bulkheads and stringers was chosen for the high strength-to-weight ratio possible (and necessary), low radar return and comparative ease in manufacture and maintenance.

The internal structure (Figure 5.1-3) consisted basically of nine (9) bulkheads spaced out along the approximately 90 inch length of the fuselage braced by six (6) stringers running longitudinally from the first bulkhead at the 8.25 F.S. (fuselage station in inches) to the eighth bulkhead (also the engine firewall) at the 72.0 F.S. Two stringers were located on either side of the fuselage centerline (in the horizontal plane) with the others spaced out in 60° increments. This arrangement allowed maximum visibility downward for cameras, laser target designators, etc. The two horizontal stringers were run all the way to the ninth bulkhead with only two additional stringers, spaced at 90° intervals, between them to brace the last two bulkheads. This was considered more than adequate for this section since very little weight and thus small loads were involved.

Due to the fact that the wing rode imbedded in the fuselage, small changes had to be made in the locations of the bulkheads and



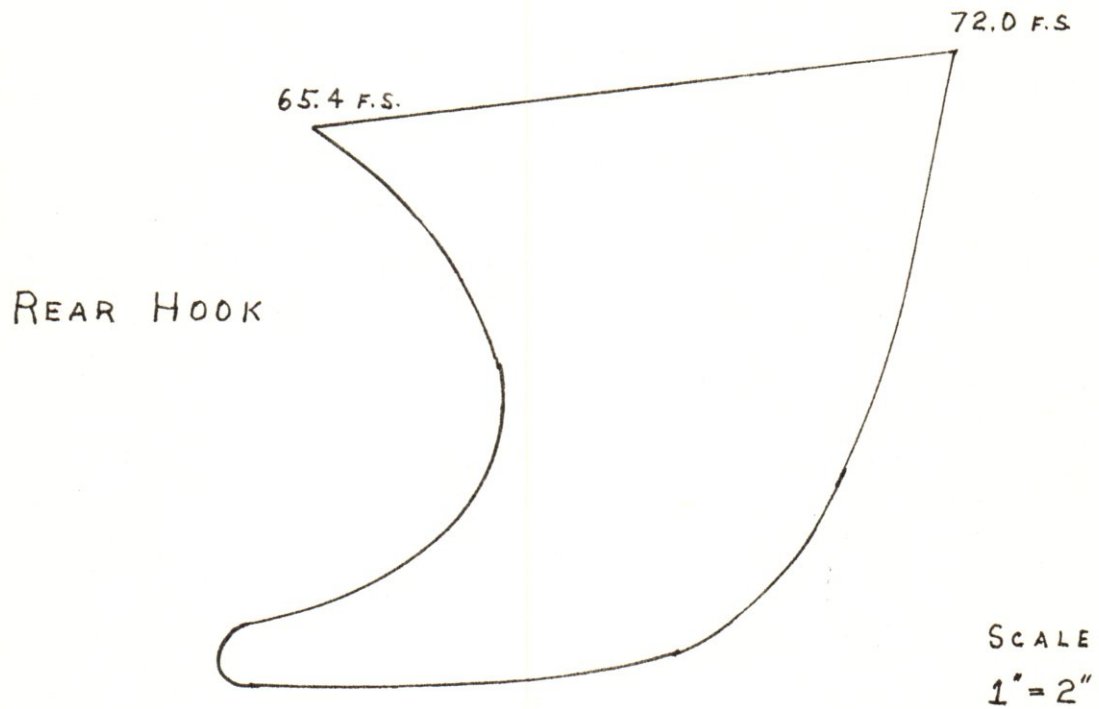
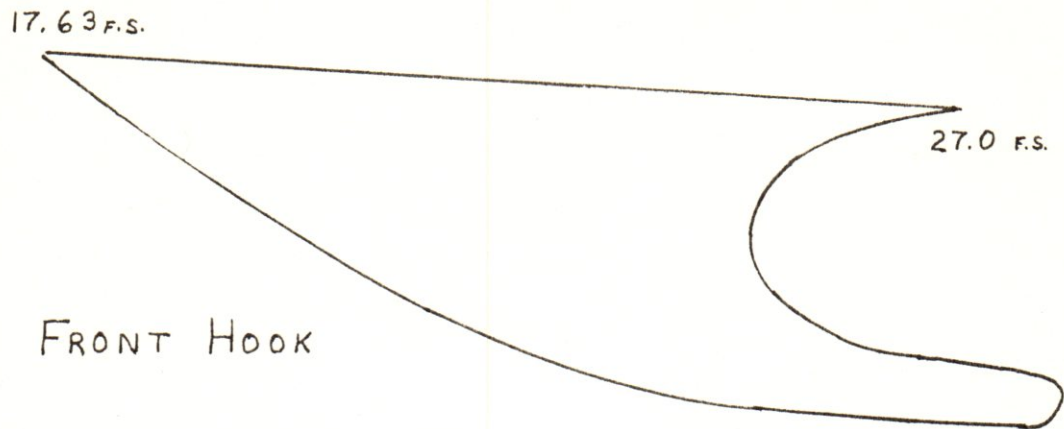
Fuselage Basic Internal Structure

Figure 5.1-3

stringers in the affected area. Two bulkheads were located at the positions of the wing main and rear spars to facilitate load carry-through. Stringers maintained their angular locations with respect to the fuselage centerline, however, and these provided extra support of the wing. Because of the imbedded nature of the wing and to keep the flow as undisturbed as possible, a wing-cap was added to smooth the change of contours between the fuselage and the top of the wing. This, too, was of Kevlar.

To absorb take-off and landing loads, two hooks (Figure 5.1-4) were attached to the underside of the fuselage. The one in front (27.0 F.S.) took the take-off loads from the rocket sled or hydraulic catapult of 1000 lbs. or so. The rear hook (65.4 F.S.) was designed to snag a horizontal net and decelerate the aircraft with an initial force of about 1000 lbs. Additionally, when landing, the front hook was to snag the net after the RPV was slowed before it could be shot backwards after stretching the net but, this load was considered small compared to that encountered at take-off. These hooks were designed as Kevlar structures supported internally by two 1.2" O.D. aluminum rods 0.10" thick.

The nose was configured as a plexiglass or acrylic hemisphere that would be replaceable and mount to the first bulkhead. Portions of the underside were available, if needed, to be replaced by optical glass for cameras in the areas forward and aft of the front hook. For accessibility to the missions equipment, the top third of the fuselage between the first and fourth bulkheads was hinged. This allowed quick replacement of equipment and easy refueling access without necessitating wing removal. For the most part, the missions



Profile of Recovery Hooks

Figure 5.1-4

equipment was mounted on racks which attached to the stringers. Access to the engine compartment was provided by several removable skin panels. The tail boom was located immediately behind the wing and bolted to two bulkheads thus allowing for removal-replacement.

#### 5.1.4.2 Fuselage Construction

The fuselage construction was envisioned to be similar to that of the wing. The aluminum frame would be assembled with the fuel tank, muffler, intake cooling air ducting, tubing and wiring in place. The Kevlar skin (5 layers thick) would be epoxied to the metal frame and all joints sealed. Note that the loop-type dipole communications antenna would be laid-up in the fuselage skin and thus be protected. The engine and shroud assembly would be added separately.

#### 5.1.5 Tail

##### 5.1.5.1 Tail Configuration

A conventional tail was decided upon -- it would be supported by a single boom affixed to the fuselage immediately behind the wing. The boom had a  $31.2^{\circ}$  incline from the top of the fuselage in order to clear the propeller shroud. Once the shroud was cleared (7.5 inches above the fuselage centerline) the boom extended horizontally for a distance of 68 inches at which point the tail was attached.

The boom was configured as a tube of Kevlar wrapped spirally with a thickness of 0.20 inches (20 ply) and an outside diameter of 3.00 inches. This insured the tail would not deflect vertically more than 4.0 inches under the maximum download of 250 lbs. The



circular cross-section yields the best torsional stiffness and thus minimize twisting of the tail about the boom. The hollow interior of the boom afforded space for wires and cables running between the fuselage and the servos in the tail as well as possible additional antennas in the tail.

The horizontal tail consisted of a symmetrical (NACA 0009) airfoil with 25% of the area of the wing. An elliptical planform was also used here with an axis of symmetry about the 50% chord line. A single spar was placed here and provided the pivot point for movement of this all-moving horizontal tail. The spars from both halves of the horizontal tail were extended into the boom where they were geared to the servo.

The vertical tail was designed to be identical to one-half of the horizontal tail so as to cut manufacturing costs and reduce the numbers of different spare parts required on hand. Each airfoil section had four ribs spaced every ten inches and braced by the main spar. Foam filled all remaining spaces and pre-stressed the skin.

#### 5.1.5.2 Tail Construction

Tail construction would consist of three basic steps: 1) boom construction, 2) airfoil construction (3 per vehicle), and 3) integration of the parts.

The boom would be laid up with various orientations of the multiple plies to insure no directional properties. The airfoil sections would be constructed identically to the wing (minus fuel tanks and control surfaces). Finally, servos, gears, and control linkage would be mounted in the boom as a single assembly and the

tail surfaces added. Completion of the basic RPV would only require bolting the tail boom and wing to the fuselage and mating electrical and fuel line connectors.

## 5.2. WEIGHT AND BALANCE

### 5.2.1 Basic RPV

The RPV in its basic form, i.e. no payload and no fuel, was determined to have, at 93 lbs., a weight of less than half its design maximum take-off gross weight of 210 lbs. This weight and its moment arm(s) was obtained from a NASTRAN model of the RPV (section 5.3). The weights and moments of the various components were approximated and compared with the total obtained from NASTRAN (Table 5.2-1). The light weight of the structure allowed great flexibility in the carrying of fuel and equipment with the c.g. location and length of travel becoming the limiting factors. Thus, the missions equipment was positioned so as to produce favorable center of gravity locations throughout the mission and the fuel tanks were positioned to reduce c.g. travel during the mission. The fuselage fuel tank was positioned so that its center of gravity coincides with that of the wing tanks. This caused the c.g. shift to be a straight line with no "jumps" as the wing tanks empty.

### 5.2.2 Mission A

The surveillance-reconnaissance mission (Chapter 2) was equipped with a television camera in the nose for flight control and real-time surveillance and three TA-8M2 motorized photo-reconnaissance cameras mounted in tandem. Together with full fuel (5 gallons in wing tanks + 8 gallons in fuselage), the take-off gross weight (T.O.G.W.) comes to 221 lbs. which amounts to only 5% over the design T.O.G.W. This small increase in weight came while increasing the fuel capacity by 30% (to 13 gallons) and adding the third still camera to the structure that was originally estimated. Even so,

Component	Weight	Arm	Moment
Fuselage	18.0 lbs	45.8"	824.4 in-lbs
Wing	10.0	47.5	475.0
Tail	2.50	147.3	368.75
Boom	7.5	110.0	830.8
Engine	10.0	74.75	747.5
Alternator	7.0	70.00	490.0
Drive Shaft	0.5	82.90	41.5
Fan and Shroud	1.5	88.00	132.0
Batteries	10.0	65.4	654.0
Muffler	6.0	65.4	212.4
Flap Servos	4.0	58.2	232.9
Tail Servos	2.0	147.3	294.6
Autopilot, Radios, Etc.	10.0	43.0	430.0
Fuselage Fuel Tank	1.0	52.0	52.0
Wiring, Tubing, Etc.	3.0	52.0	156.0
Fuel	78.0	52.0	4056.0

Totals

Basic RPV/DRY	93.0 lbs	63.9"	5941.85 in-lbs
NASTRAN	93.04	63.75"	5931.0
Basic RPV/WET	171.0 lbs	58.5"	9997.9 in-lbs
NASTRAN	171.04 lbs	58.4"	9987.0

Basic RPV Component Weights and Moments

Table 5.2-1

a sizeable fraction of the available payload volume remained unused.

The weights and moments used for this mission appear in Table 5.2-2. The relative change in c.g. is shown in Figures 5.2-1 and 2. Note the extremely small change in c.g. throughout this mission (0.45") which would indicate that the maneuverability (static margin) does not change appreciably.

### 5.2.3 Mission B

The laser target designator-damage reporting mission as described in Chapter 2 consists of the basic RPV equipped with the Honeywell laser target designator with infrared sensor in the nose and one TA-8M2 mounted behind the front hook. Its T.O.G.W. came to 229 lbs which was about 9% over the design T.O.G.W.. But here, too, endurance was increased by over 35% over the original design estimation.

Table 5.2-3 lists the weights and moments of the components of this mission and the relative locations and changes are illustrated in Figures 5.2-3 and 4. Due to the heavy laser target designator being located at the very nose, the c.g. was shifted forward several inches from Mission A. Even with the c.g. travel five times that of Mission A (2.21"), the location and travel were well within the limits allowed due to the large tail moments available.

Component	Weight	Arm	Moment
Basic RPV/Dry	93.0 lbs	63.8 "	5931.0 in-lbs
TV Camera	10.0	10.0	100.0
2 Photo Cameras	27.0	27.0	729.0
1 Photo Camera	13.2	38.0	501.6
Fuel	78.0	52.0	4056.0

Totals

Mission A/DRY	143.2 lbs	50.71"	7261.6 in-lbs
Mission A/WET	221.2	51.16	11317.6

Mission A Weights and Moments

Table 5.2-2

Component	Weight	Arm	Moment
Basic RPV/Dry	93.0 lbs	63.8 "	5931.0 in-lbs
Laser Target Designator	45.0	10.0	450.0
1 Photo Camera	13.2	38.0	501.6
Fuel	78.0	52.0	4056.0

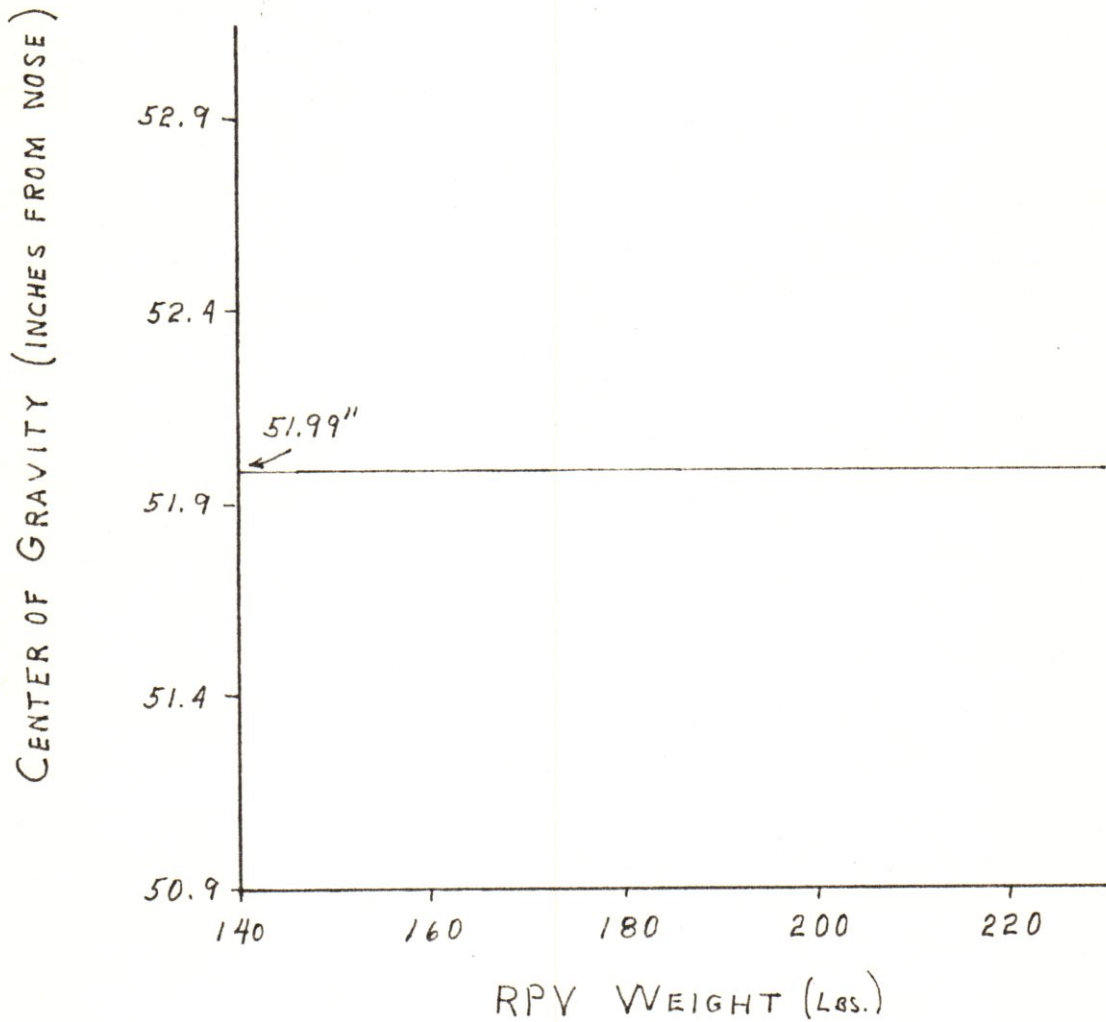
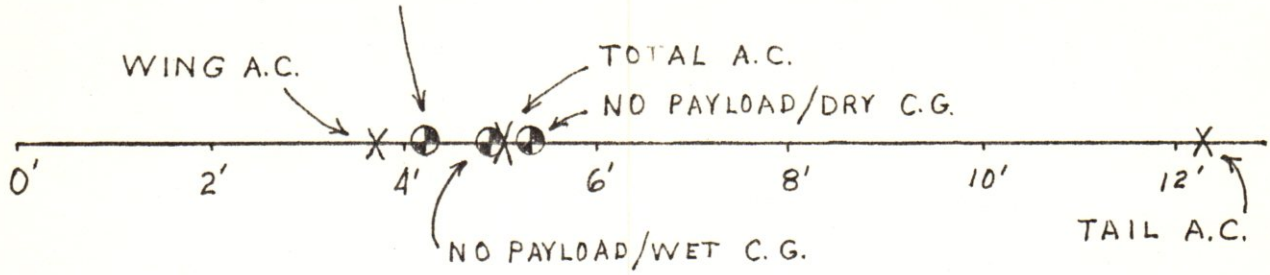
Totals

Mission B/DRY	151.2 lbs	45.52"	6882.6 in-lbs
Mission B/WET	229.2	47.73"	10938.6

Mission B Weights and Moments

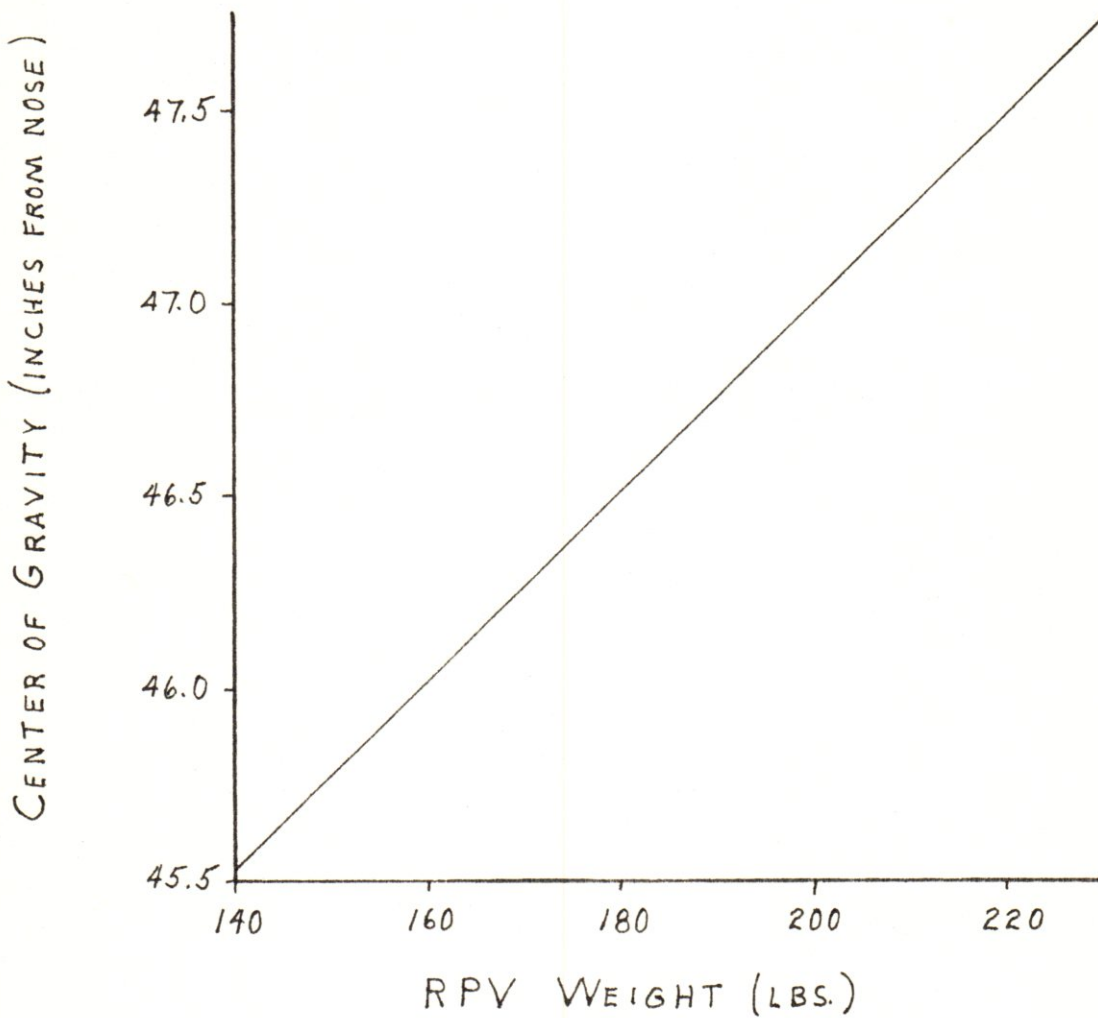
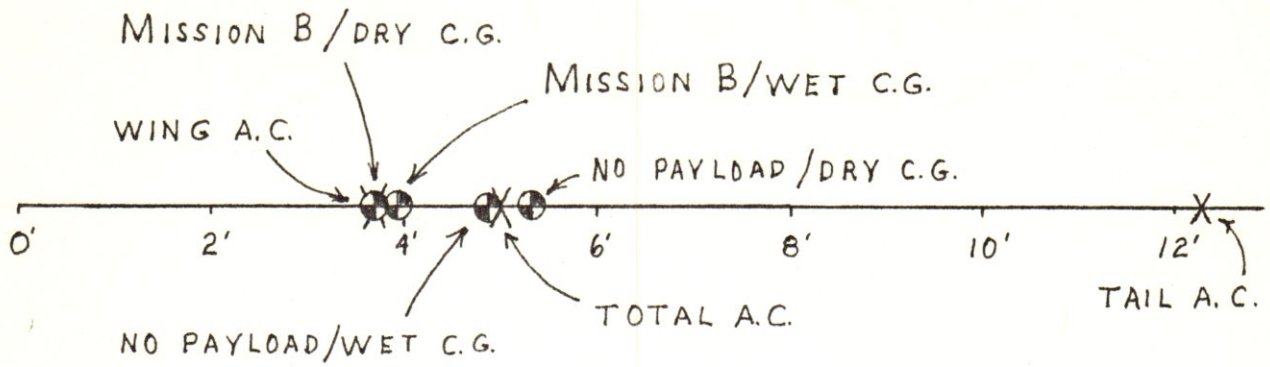
Table 5.2-3

MISSION A WET & DRY C.G.



Mission A C.G. Location and Travel

Figures 5.2-1 and 2



Mission B C.G. Location and Travel

Figures 5.2-3 and 4



## 5.3. NASTRAN MODEL

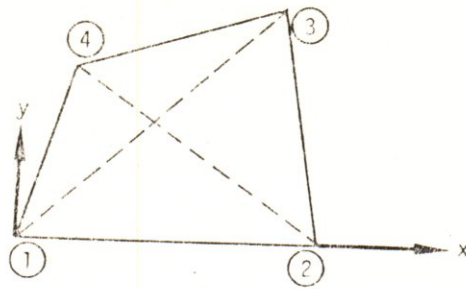
### 5.3.1 NASTRAN Modeling

NASTRAN (NAsa STRuctural ANalysis Program) is a general purpose digital computer program designed to solve (among other things) static and dynamic loading problems, buckling analysis and normal modes analysis using a finite element approach. It assumes "the distributed physical properties of a structure are represented by a model consisting of a finite number of idealized elements that are interconnected at a finite number of grid points, to which loads are applied"<sup>9</sup>. Everything is then referenced to these grid points throughout the problem. The structural elements provide the means of specifying the properties of the structure including material properties and mass distribution. Finally, constraints are applied to specify boundary conditions.

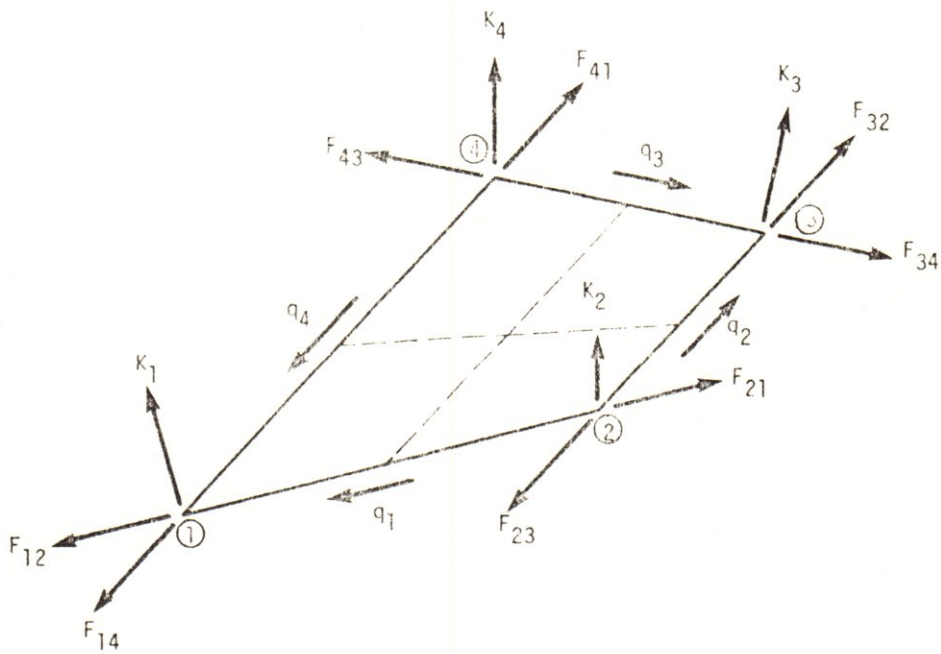
#### 5.3.1.1 Grid Points

The structure was modeled using 263 grid points located in three-dimensional space with the origin being the tip of the fuselage airfoil (the point defined by the nose of the NACA 0018 airfoil coordinates before being modified by the hemispherical glass nose). The coordinate axes used coincide with the stability axes system (Figure 5.1-3). Furthermore, symmetry about the XZ-plane was assumed so only one-half (right side) was modeled.

A FORTRAN program was written to generate the locations of the grid points defining the fuselage (Appendix A.5.2) as well as the structural elements involved and punch cards for input to NASTRAN. Each grid point was initially given all six degrees-of-freedom (DOF) available -- 3 translational and 3 rotational.



(a) Coordinate System.

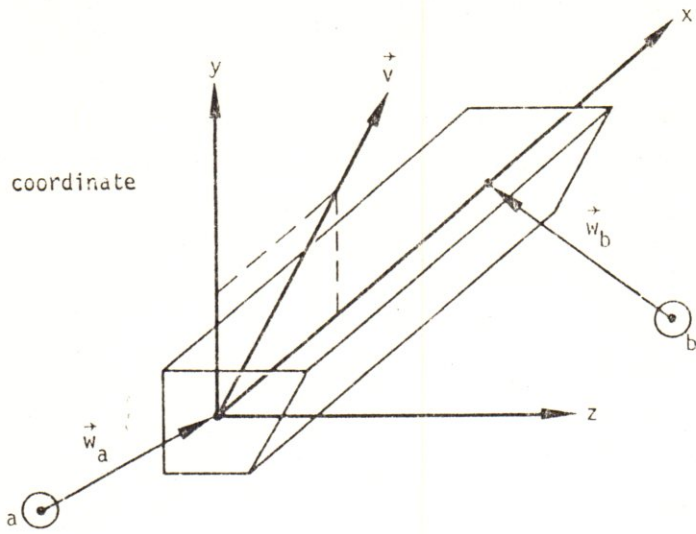


(b) Corner forces and shear flows.

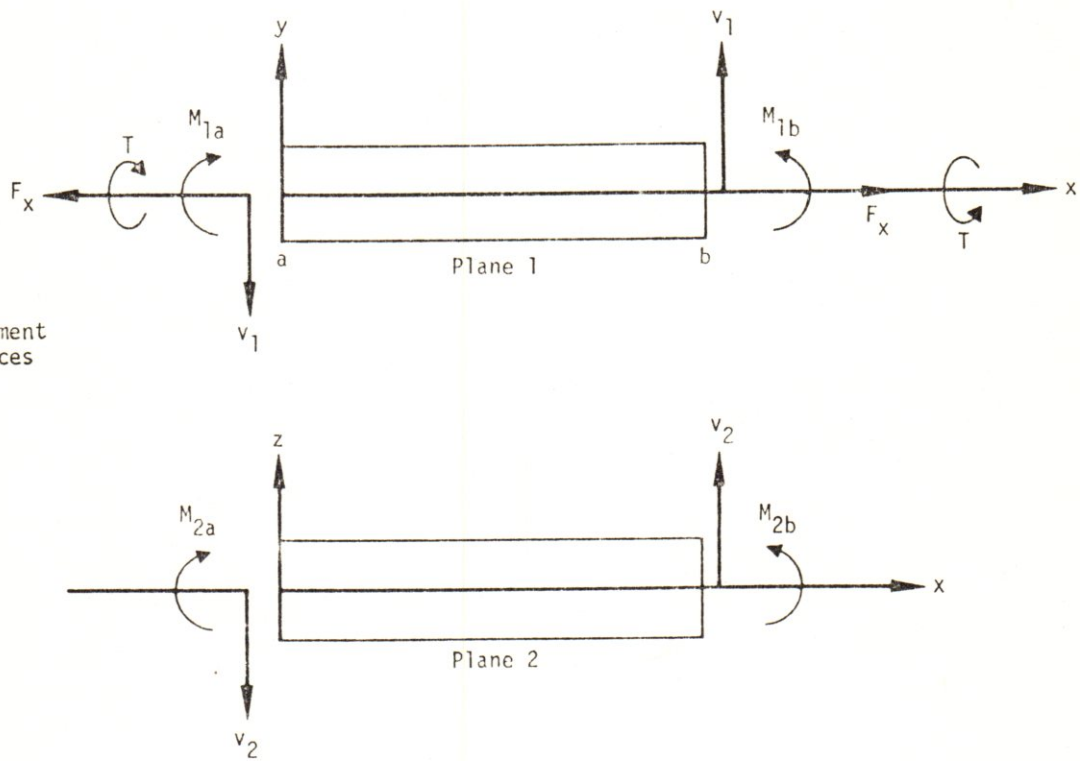
Coordinate System and Element Forces for CQDMEM2 Elements

Figure 5.3-1

(a) Element coordinate system

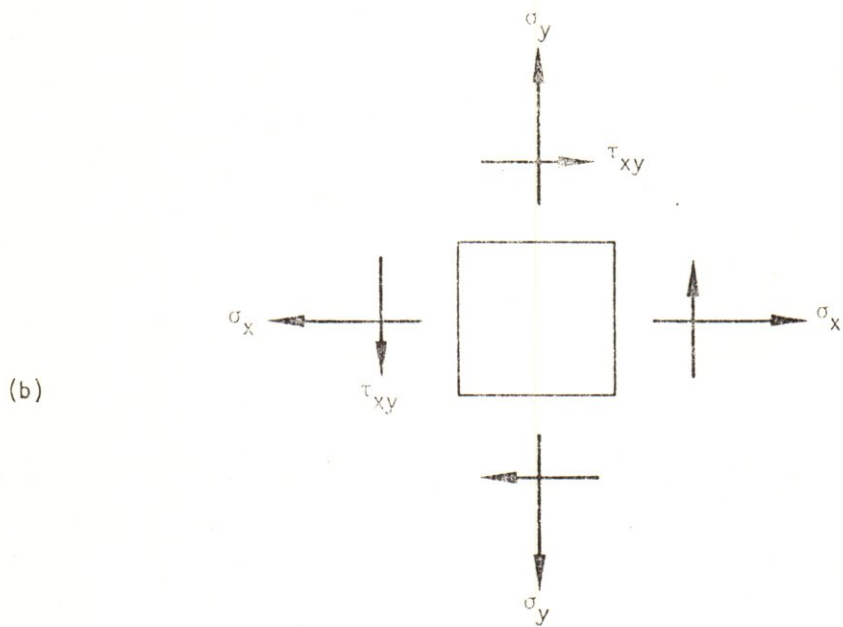
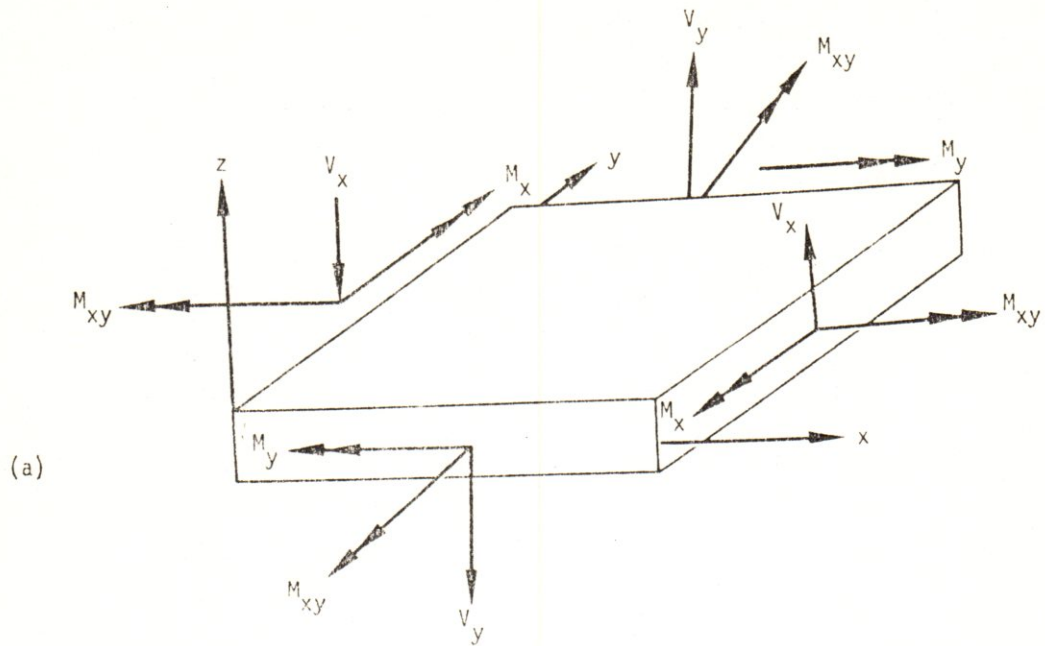


(b) Element forces



Bar Element Coordinate System and Element Forces

Figure 5.3-2



Forces and Stresses in CQUAD2 Elements

Figure 5.3-3

Similarly, the wing was modeled using its own program (Appendix A.5.3) but its coordinate axes were located at the leading edge of the wing root. A coordinate transformation card was then used to properly position the wing on the fuselage.

The same wing modeling program was used to model the tail surfaces and coordinate transformations were applied to these structures to locate them properly with respect to the fuselage. Finally, the grid point locations of the hooks, tail boom, propulsion system and missions equipment were entered by hand.

#### 5.3.1.2 Elements

There were three basic elements used in the NASTRAN model of the RPV structure: 1) membrane element, 2) bar element and 3) plate element. A quadrilateral membrane element (Figure 5.3-1) was used to model the Kevlar skin. This element (CQDMEM2) assumes finite inplane stiffness and zero bending stiffness<sup>10</sup>. This says that the Kevlar skin absorbs its share of the load through tension and compression only which is standard procedure for modeling aircraft skins. The bar element (CBAR) was used to model all the aluminum spars, and ribs and stringers. It can include all six DOF at each end (Figure 5.3-2) which are extension, torsion, bending in two perpendicular planes and the associated shears. All the aluminum wing ribs were modeled with a plate element (CQUAD2) which included both inplane and bending stiffness for a solid homogeneous cross section (Figure 5.3-3).

All the elements were positioned by using them to connect the appropriate grid points. Properties (mass and inertia) were assigned through "property" cards. For the skin and plate (CQDMEM2 &

CQUAD2) elements this consisted of only material properties (Young's modulus, shear modulus, Poisson's ratio, and mass density) and element thicknesses (Table 5.3-1). Bar elements required, in addition, moments of inertia in bending and the torsional moment of inertia and the cross-sectional area. The values of these used and the cross-section involved are listed in Figure 5.3-4 as calculated in Appendix A.5.4.

In addition to the basic RPV structure, the masses of various system components had to be included in the final model. The use of CONM2 cards enabled the components to be modeled as concentrated masses located at specified grid points within the interior of the structure. The components involved include the engine, fan and shroud assembly, muffler, batteries, autopilot and radios, servos, alternator, fuel tanks, fuel, and missions equipment.

#### 5.3.1.3 Constraints

Two types of constraint are available to the user of NASTRAN -- single-point constraints (SPC's) and multipoint constraints (MPC's). The SPC's constrain designated degrees-of-freedom to zero thus enforcing zero motion of the specified grid point(s) in the direction of the degrees(s)-of-freedom indicated. Throughout, SPC's were used to eliminate degrees-of-freedom either where the elements used provided no stiffness for that motion or where the effects of those degrees-of-freedom were considered negligible. For example, they were used to eliminate the inplane bending D.O.F. in the membrane elements since they provided no stiffness for that motion.

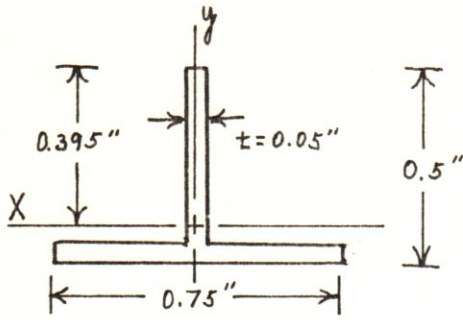
Multipoint constraints are used to specify a linear relationship among selected degrees of freedom. This allows one to define, in effect, infinitely rigid, zero mass elements. One way they were

	Young's Modulus	Shear Modulus	Poisson's Ratio*	Density (lbm/in <sup>3</sup> )
Aluminum	10.6 x 10 <sup>6</sup> PSI	4.0 x 10 <sup>6</sup> PSI	0.33	0.100
Kevlar	4.5 x 10 <sup>6</sup> PSI	2.0 x 10 <sup>6</sup> PSI	0.13	0.48

$$* \mu = \frac{E}{2G} - 1$$

Materials Properties

Table 5.3-1



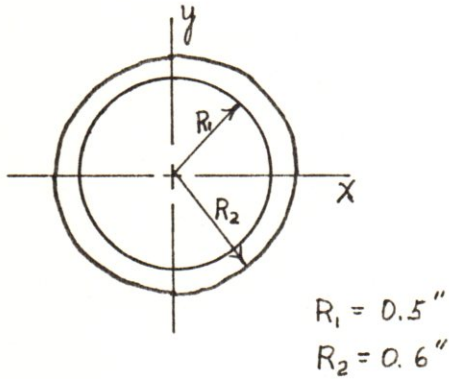
Fuselage Ribs & Stringers

Area = .0625 inches<sup>2</sup>

$I_x = 0.00128 \text{ inches}^4$

$I_y = 0.00176 \text{ inches}^4$

$J = 0.00304 \text{ inches}^4$



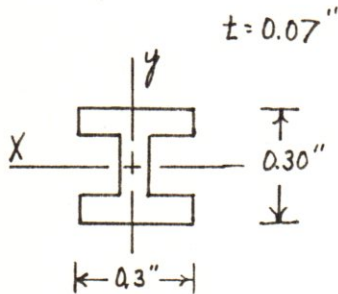
Hook Reinforcement Tube

Area = 0.350 inches<sup>2</sup>

$I_x = 0.0527 \text{ inches}^4$

$I_y = 0.0527 \text{ inches}^4$

$J = 0.1054 \text{ inches}^4$



Tail Spars

Area = 0.05356 inches<sup>2</sup>

$I_x = 5.5 \times 10^{-4} \text{ inches}^4$

$I_y = 3.0 \times 10^{-4} \text{ inches}^4$

$J = 8.5 \times 10^{-4} \text{ inches}^4$

Component Cross-Sectional Properties

Figure 5.3-4



used was in constraining points along the centerline of the fuselage to always remain "centered" within the fuselage structure during deformation of the structure due to the applied loads.

### 5.3.2 NASTRAN Results

#### 5.3.2.1 Weights and Moments Inertia

NASTRAN computed total weights, moments of inertia and center of gravities using the mass densities and element volumes input. This feature was of great convenience in that weights and balances did not have to be recalculated by hand each time the structure was modified or for different missions.

A portion of one such output is shown in Figure 5.3-5. Due to the locations of the fuel tanks and missions equipment, the moments of inertia stayed within the same order of magnitude during changes in missions and fuel quantities. The values obtained are small enough to provide the RPV with excellent maneuverability dynamics but also indicates the RPV would be susceptible to gusts.

#### 5.3.2.2 Displacements

Loadings were applied to the structure and the deformation noted. Since the RPV was designed to have an operational load range of +8 g's to -5 g's, the analysis was run to 150% of these values. To simulate these loading conditions, a gravitational load was applied in the appropriate direction and pressure loads applied to the lifting surfaces to simulate the lift produced. For take-off and landing, concentrated loads were applied at the hooks in the appropriate directions.

The displacements obtained due to these loadings were compared with those expected or allowed. Especially important were

C U T P U T F R O M G R I D P C I N T W E I G H T G E N E R A T O R

---

REFERENCE PCINT = 1

---

```

***
** 1.1303C2E C2 0.0
** 0.0 1.130302E C2 -1.795339E-07 0.0 1.133727E 02 -2.133727E 02 -4.770828E 02
** C.0 -1.795339E-07 1.130302E C2 4.770828E 02 2.133727E 02 -1.299748E-05 -5.785832E 03 -5.785832E 03
** 0.0 2.133727E C2 4.770828E 02 1.130302E C2 4.770828E 02 3.039556E-07 -1.557912E 04 -1.557912E 04
** -2.133727E 02 -1.299748E-07 3.039556E-07 -1.557912E 04 2.133727E 02 2.600242E 04 3.665844E 05 -1.973034E 03
** -4.770828E 02 -5.785832E 03 3.039556E-07 -1.557912E 04 -2.973034E 03 3.665844E 05 3.784057E 05
**

```

S

```

***
** 1.000000E 00 0.0 0.0
** 0.0 1.000000E 00 0.0
** C.0 0.0 1.000000E 00
***

```

DIRECTICN	MASS	X-C.G.	Y-C.G.	Z-C.G.
MASS AXIS SYSTEM (S)	1.130302E 02	0.0	4.220843E-07	-1.887750E-09
X	1.130302E 02	-5.118837E 01	-1.149912E-07	-1.887750E-09
Y	1.130302E 02	-5.118837E 01	4.220843E-07	-1.887750E-09
Z	1.130302E 02			

I (S)

```

***
** 1.372053E 04 -1.581352E 03 4.656926E 03
** -1.581352E 03 7.001450E 04 -2.072422E 03
** 4.656926E 03 -2.072422E 03 8.022494E 04
***

```

- (1) Rigid body mass matrix [MO] relative to the reference point in the basic coordinate system.
- (2) Transformation matrix [S] from basic coordinate system to principal mass axes.
- (3) Principal masses and associated centers of gravity.
- (4) Inertia matrix I(S) about the center of gravity relative to the principal mass axes.

Figure 5.3-5

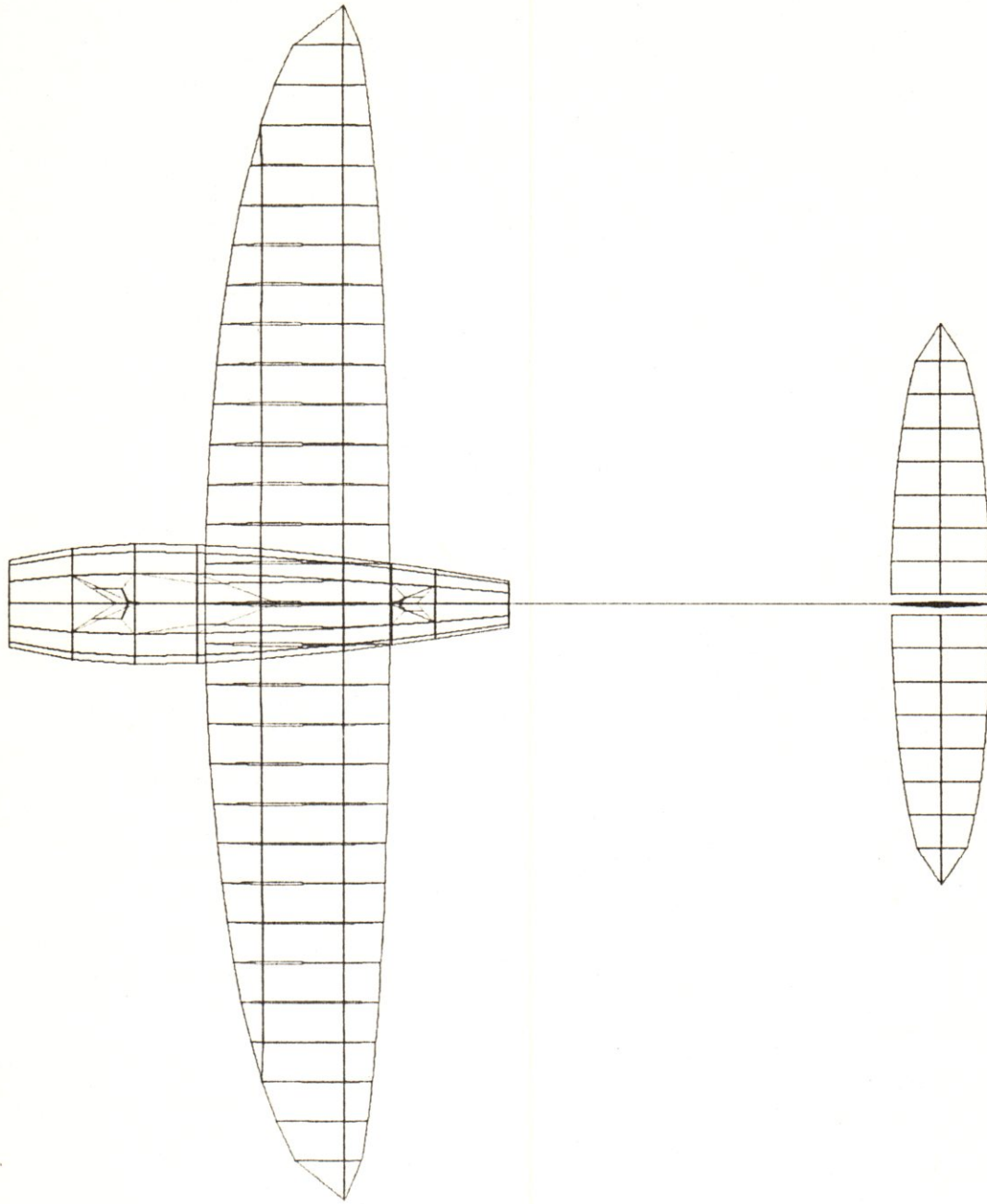
those of the wing-tips and the tail. These results were then used to improve the model through structural modifications.

#### 5.3.2.3 Stresses

For the most part, the limiting factor for the structural loads was the stresses encountered. For each loading condition, the stresses in all the members was compared with the materials' limitations to determine margin of safety. If the structural limits were exceeded, that portion of the structure was strengthened. The final structure was able to carry all the design loads without failure in any part of the structure and stayed within the weight limitations.

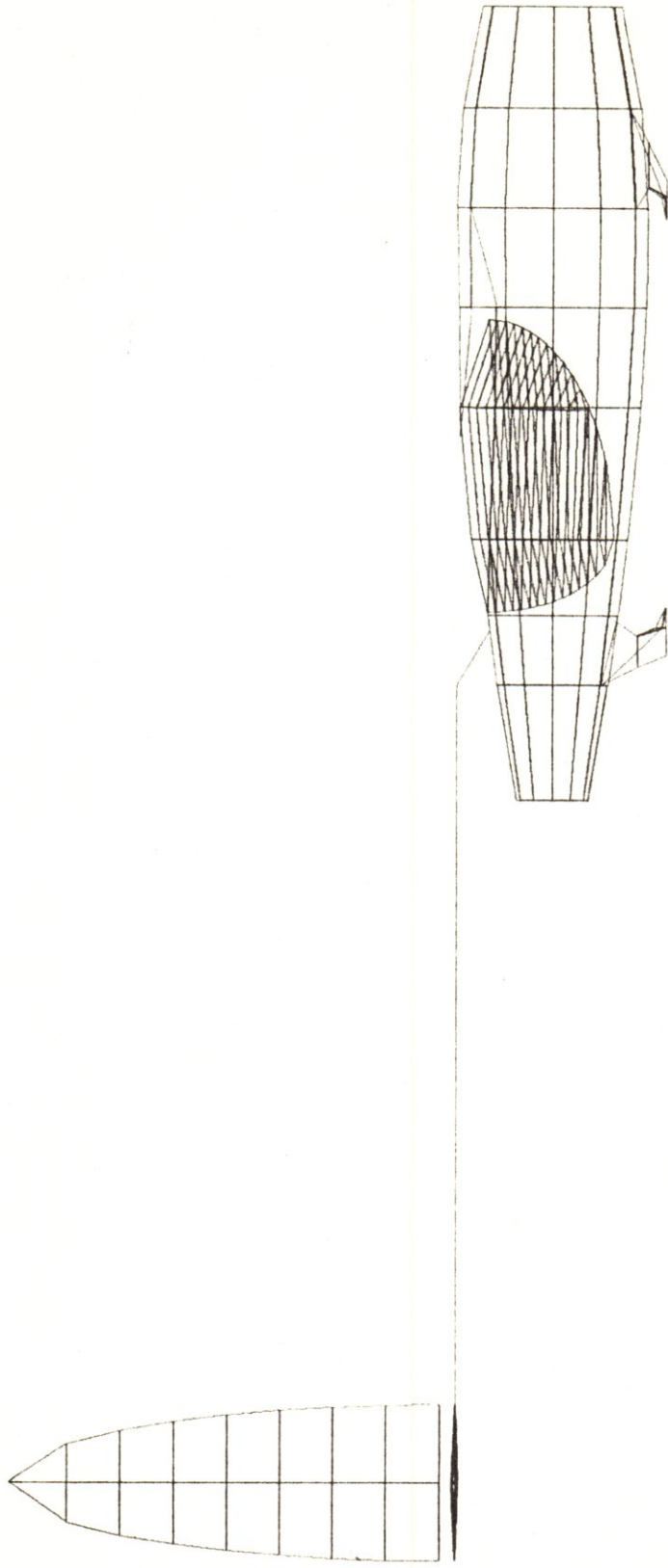
#### 5.3.2.4 Final Structure

NASTRAN provides structured plots as a standard feature. This feature was used to insure all the grid points were located properly. Another convenience feature is the ability to have the plotter show the structure as reflected about a plane of symmetry. This enabled the final plots to show the entire structure as reflected about the XZ-plane. The final 3-view plots are shown in Figures 5.3-6, 7, and 8.



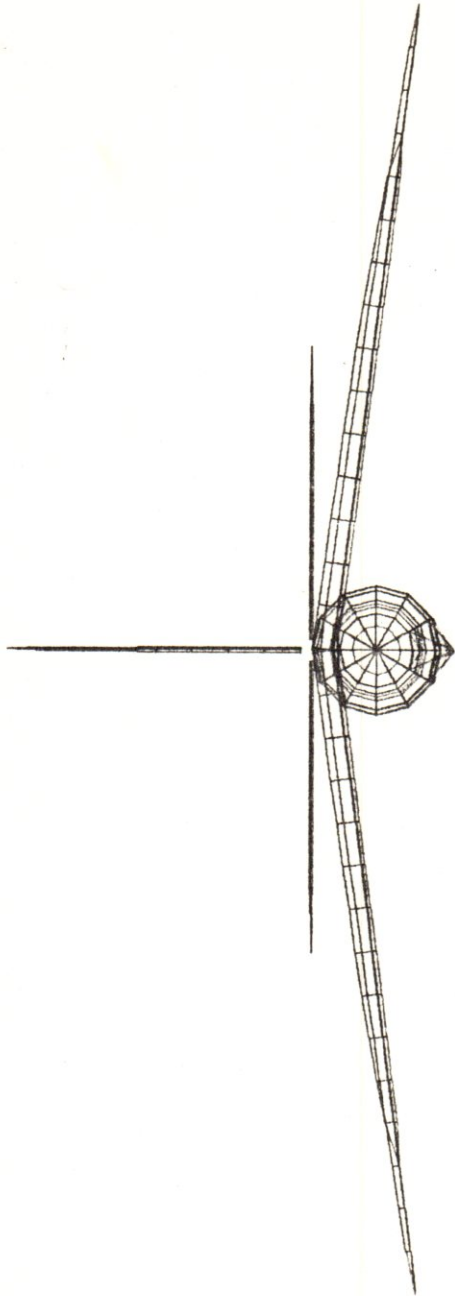
PPV FUSELAGE-WING STRUCTURE ANALYSIS  
AIRFOIL - NACA 4412 FUSELAGE - REVOLVED NACA 0015  
KEVLAR SKIN WITH ALUMINUM BRACING  
UNDEFORMED SHAPE

Figure 5.3-6



SPV FUSELAGE-WING STRUCTURE ANALYSIS  
AIRFOIL - NACA 4412 FUSELAGE - REVOLVED NACA 0013  
KEVLAR SKIN WITH ALUMINUM SPACING  
UNDEFORMED SHAPE

Figure 5.3-7



RPV FUSELAGE-WING STRUCTURE ANALYSIS  
 AIRFOIL- NACA 4412 FUSELAGE- REVOLVED NACA 0019  
 KEVLAR SKIN WITH ALUMINUM BRACING  
 UNDEFORMED SHAPE

Figure 5.3-8

## 5.5 REFERENCES

1. "1978 Materials Selector", Materials Engineering, Mid-November, 1977, pp. 224-226.
2. "Reinforced Thermoplastic", Encyclopedia of Polymer Science and Technology, Vol. 12, John Wiley & Sons, New York, 1970, pp. 31-41.
3. "Characteristics and Uses of Kevlar 49 Aramid High Modulus Organic Fiber", E.I. DuPont De Nemours & Co., Inc., 1975.
4. "Properties of Kevlar 49 Aramid Fabrics and Fabric Reinforced Epoxy and Polyester Composites", E.I. DuPont De Nemours & Co., Inc., Dec. 1975.
5. Personal Correspondence, Textile Fibers Dept. -- Kevlar Special Products, E.I. DuPont De Nemours, & Co. Inc., March 13, 1978.
6. "Properties and Characteristics of Kevlar 49 Yarn and Composites", E.I. DuPont De Nemours & Co., Inc., 1975.
7. "Remotely Pilot Vehicles and Target Drones", Aviation Week and Space Technology, March 13, 1978, pp. 122-123.
8. Hand, A.J., "Kevlar Boats -- Say Goodbye to Fiberglass?" Popular Science, Feb. 1977, pp. 99-101.
9. NASTRAN User's Manual -- Level 15.5
10. NASTRAN Theoretical Manual -- Level 15.5

APPENDICES



A 2.2-1

The thrust and final velocity for take-off and kinetic energy for landing were found from the following basic equations:

$$\text{Force (F)} = M a$$

$$\text{Kinetic (K)} = 1/2 M V^2$$

and

$$\text{distance (s)} = V_0 t + \frac{1}{2} a t^2$$

where M = mass of RPV  
a = acceleration  
V = velocity

Knowing the weight of the RPVs and acceleration of the Aquila system, the thrust was found to be

$$F = (146 \text{ lbm}) (6 \text{ gs}) = 876 \text{ lbs.}$$

With this information and knowing the Aquila landing speed the following table was made.

	Aquila	RPV
Weight	146 lb	230 lb
Take-Off Velocity	83 ft/sec	70 ft/sec
Take-Off Distance	20 ft	20 ft
Acceleration	6 gs	3.8 gs
Landing Velocity	98 ft/sec	70 ft/sec
Kinetic Energy Landing	21773 ft-lbs	17500 ft-lbs

A.3.1

Let  $S \equiv$  Wing Area

$b \equiv$  Wing Span

$c_r \equiv$  Wing Root Chord.

For elliptic wing

$$c = c_r \sqrt{1 - \frac{4x^2}{b^2}}$$

where the  $x$  axis lies along the span.

Let  $a_1 + a_2 = 1$

then  $c_r = c_r (a_1 + a_2)$

or,  $c_1 = c_r a_1 \sqrt{1 - \frac{4x^2}{b^2}}$

$$c_2 = c_r a_2 \sqrt{1 - \frac{4x^2}{b^2}}$$

and  $c = c_1 + c_2$

### A.3.2.

The following program assumes an elliptic untwisted planform. The input consists of the dimensions of the wing root chord and span along with Oswald efficiency factor,  $e$ , and the airfoil section data. Lift coefficient is assumed to be that of the section. Drag coefficient is calculated on the basis of the following equation,

$$C_D = C_{D_0} + \frac{C_L^2}{\pi AR e}$$

where  $e$  was assumed safely to be 0.95. The induced angle of attack is also given from;

$$\alpha_i = - \frac{C_L}{\pi AR} .$$

```

1  $JCB          ,NOEXT,T=99,P=5000
2  DIMENSION CLS(35),CDS(35),CMS(35),ALPHA(80),X(100),CL(80),CD(80)
3  DIMENSION CM(80),CLALF(80),CDALF(80),CMALF(80),RANGE(80),ENDUR(80)
4  DIMENSION ALPHI(80)
5  COMMON CLS,CDS,CMS
6  COMMON K
7  1000 FORMAT(1X,10(2X,F8.3))
8  1100 FORMAT(1X,'      ALPHA      CL      CLALPHA      CD      CDALPHA
9  *CM      CMALPHA      RANGE      ENDUR      IALPHA')
10 1200 FORMAT('1')
11 WRITE(6,1200)
12 READ,NCL,NSEC,K,E
13 DO 100 I=1,NCL
14 100 READ,CLS(I),CDS(I),CMS(I)
15 READ,CR,B
16 S=.785398*CR*B
17 CBAR=S/B
18 XBAR=(B/2.)*(1.-(CBAR/CR)**2)**.5
19 AR=B*B/S
20 WRITE(6,1000)S,CBAR,AR,XBAR
21 PRINT,'      '
22 PRINT,'      '
23 PRINT,'      '
24 DX=B/(2.*NSEC);X(1)=0.0;NNNN=NSEC+1
25 DO 110 I=2,NNNN
26 110 X(I)=X(I-1)+DX
27 NCLCL=NCL*2.
28 DO 120 J=1,NCLCL
29 S=0.0
30 ALPHA(J)=J/2.-K
31 CLF=0.0;CDF=0.0;CMF=0.0
32 CALL SECLDM(ALPHA(J),CLALPH,CDALPH,CMALPH,CLOCAL,CDOCAL,CMOCAL)
33 DO 125 I=1,NNNN
34 C=1.-X(I)**2*4./((B*B)
35 IF(C.LT.0.)C=0.
36 C=CR*(SQRT(C))
37 S=S+C*DX
38 CLF=CLF+CLCCAL*C*DX
39 CDF=CDF+CDOCAL*C*DX
40 CMF=CMF+CMOCAL*C*C*DX
41 125 CONTINUE
42 S=S*2.
43 CL(J)=2.*CLF/S
44 CD(J)=2.*CDF/S+(CL(J)**2)/(3.1417*AR*E)
45 CM(J)=2.*CMF/S/CBAR
46 RANGE(J)=CL(J)/CD(J)
47 IF(CL(J).GE.0.)GO TO 10
48 ENDUR(J)=0.
49 GO TO 120
50 10 ENDUR(J)=(CL(J)**1.5)/CD(J)
51 120 CONTINUE
52 CLALF(1)=0.;CDALF(1)=0.;CMALF(1)=0.;ALPHI(1)=0.
53 DO 130 J=2,NCLCL
54 CLALF(J)=(CL(J)-CL(J-1))/(ALPHA(J)-ALPHA(J-1))
55 CDALF(J)=(CD(J)-CD(J-1))/(ALPHA(J)-ALPHA(J-1))
56 CMALF(J)=(CM(J)-CM(J-1))/(ALPHA(J)-ALPHA(J-1))
57 GAMA=.5*CL(J)*CR
58 W=-GAMA/2./B
59 ALPHI(J)=ATAN(W)*57.2958
60 130 CONTINUE

```

```

66      WRITE(6,1100)
67      DO 140 J=1,NCLCL
68      WRITE(6,1000)ALPHA(J),CL(J),CLALF(J),CD(J),CDALF(J),CM(J),CMALF(J)
        *,RANGE(J),ENDUR(J),ALPHI(J)
69      140 CONTINUE
70      WRITE(6,1200)
71      150 CONTINUE
72      STOP;END

```

```

74      SUBROUTINE SECLCM(XXX,XX,XY,YX,YY,ZZ,ZY)
75      DIMENSION CLS(35),CDS(35),CMS(35)
76      COMMON CLS,CDS,CMS
77      COMMON K
78      II=XXX
79      I=II+K
80      IF(I.GT.1)CC TC 5
81      XX=CLS(I+1)-CLS(I)
82      XY=CDS(I+1)-CDS(I)
83      YX=CMS(I+1)-CMS(I)
84      GO TO 10
85      5 CONTINUE
86      XX=CLS(I)-CLS(I-1)
87      XY=CDS(I)-CDS(I-1)
88      YX=CMS(I)-CMS(I-1)
89      10 CONTINUE
90      YY=XX*(XXX+K-I)+CLS(I)
91      ZZ=XY*(XXX+K-I)+CDS(I)
92      ZY=YX*(XXX+K-I)+CMS(I)
93      RETURN;END

```

\$ENTRY

## A.3.3.

The changes in the airfoil section characteristics as the result of flap deflection were calculated using the methods suggested by McCormick. The governing equations were the following:

$$\Delta C_L = 2\pi\eta\tau\delta_f$$

$$\Delta C_D = \delta_1\delta_2\delta_f$$

$$\Delta C_m = -\mu_1\Delta C_L$$

where

$$\eta = f_1(\delta_f)$$

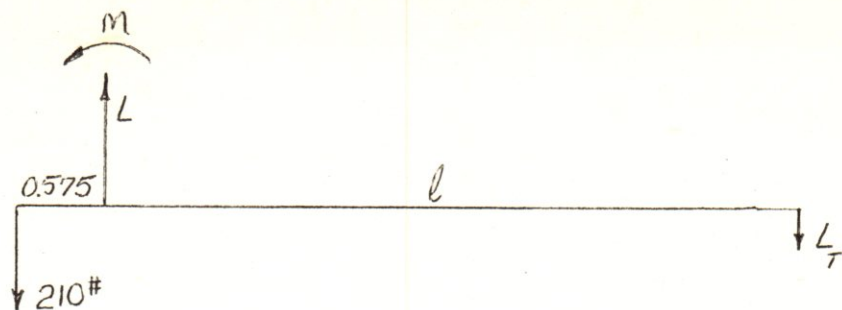
$$\tau = f_2\left(\frac{c_f}{c}\right)$$

$$\delta_1 = f_3\left(\frac{c_f}{c}\right)$$

$$\delta_2 = f_4\left(\frac{b_f}{b}\right)$$

$$\mu_1 = f_5\left(\frac{C_f}{C}\right).$$

A.3.4.



$$L = L_T + 210 = \frac{1}{2} \rho V^2 C_L S_w$$

$$M = \frac{1}{2} V^2 \bar{c} S_w C_m$$

$$S_w = 25.92 \text{ ft}^2$$

$$\rho = 0.002378 \text{ slugs/ft}^3$$

$$\bar{c} = 1.788 \text{ ft}$$

$$V = \text{from } 56.6 \text{ fps to } 54.4 \text{ fps.}$$

$l$	$L_T$	$S_{h.T.}$
5.2	36.72	11.27
6.2	30.51	9.61
7.2	26.10	8.37
8.2	22.8	7.40
9.2	20.24	6.66
10.2	18.20	6.04

After the tail airfoil was chosen,  $S_{h.T.}$  was reduced to 6.5 ft with  $l = 8.4$  ft. without degrading the performance.

### A.3.5

This program is capable of calculating the force and moment coefficients of the RPV in six degrees of freedom. The input consists of the following;

- 1  $T, \delta_s$
- 2-53  $\alpha_w, \alpha_w, C_{L_w}, C_{L_{\alpha_w}}, C_{D_w}, C_{D_{\alpha_w}}, C_{m_w}, C_{m_{\alpha_w}}$
- 54-113  $\delta_F, \Delta C_{L_{\delta_F}}, \Delta C_{D_{\delta_F}}, \Delta C_{m_{\delta_F}}$
- 114-142  $\alpha_{H.T.}, C_{L_T}, C_{L_{\alpha_T}}, C_{D_T}, C_{D_{\alpha_T}}$
- 143  $b_w, C_{r_w}, \eta_{H.T.}$ , tail boom angle with respect to fuselage chord line, shroud area.
- 144  $b_{H.T.}, C_{r_{H.T.}}$ , H.T. to W. distance, tail boom diameter.
- 145-170 fuselage normalized  $C_D$
- 171 attitude, density, weight,  $\delta_F)_{max.}$ ,  $x_{cg}$  from nose.

Also are calculated the horizontal velocity for level flight, power required,  $\bar{x}_{a.c.}$ ,  $\bar{x}_{a.c.}$ ,  $\alpha_{H.T.}$ ,  $C_L/C_D$ , and  $C_L^{3/2}/C_D$ . For glide condition line number 69 must be deleted. The following appendices show the methods by which different parameters of this program were calculated.



\$JOB

,T=99,P=15000

C(I,1)=ABSOLUTE ANGLE OF ATTACK  
C(I,2)=WING CL  
C(I,3)=WING CL-ALPHA  
C(I,4)=WING CD  
C(I,5)=WING CD-ALPHA  
C(I,6)=WING CM  
C(I,7)=WING CM-ALPHA  
C(I,8)=WING DOWNWASH ANGLE AT H.TAIL  
C(I,9)=C(DOWNWASH ANGLE)/C(ALPHA)  
C(I,10)=GEOMETRIC ANGLE OF ATTACK OF H.TAIL  
C(I,11)=H.TAIL CL  
C(I,12)=H.TAIL CL-ALPHA  
C(I,13)=H.TAIL CD  
C(I,14)=H.TAIL CD-ALPHA  
C(I,15)=FUSELAGE NORMALIZED CD  
C(I,16)=FLAP DEFLECTION ANGLE  
C(I,17)=CHANGE OF CL DUE TO THE FLAPS  
C(I,18)=CHANGE OF CD DUE TO THE FLAPS  
C(I,19)=CHANGE OF CM DUE TO THE FLAPS  
C(I,20)=GEOMETRIC ANGLE OF ATTACK  
C(I,21)=ROLLING MOMENT COEFFICIENT DUE TO SIDE-SLIP  
C(I,22)=ROLLING MOMENT COEFFICIENT DUE TO RUDDER DEFLECTION  
C(I,23)=ROLLING MOMENT COEFFICIENT DUE TO SPOILER DEFLECTION  
C(I,24)=SIDE FORCE COEFFICIENT DUE TO SIDE-SLIP  
C(I,25)=SIDE FORCE COEFFICIENT DUE TO RUDDER DEFLECTION  
C(I,26)=YAWING MOMENT COEFFICIENT DUE TO SIDE-SLIP  
C(I,27)=YAWING MOMENT COEFFICIENT DUE TO RUDDER DEFLECTION  
C(I,28)=SIDE FORCE COEFFICIENT DUE TO YAW RATE  
C(I,29)=ROLLING MOMENT COEFFICIENT DUE TO YAW RATE  
C(I,30)=YAWING MOMENT COEFFICIENT DUE TO YAW RATE

```

1 DIMENSION C(61,50)
2 FORMAT('1')
3 100 FORMAT('0',1X,I2,18(1X,F6.2))
4 NNNN=1
5 MMMM=2
6 READ(5,*)SIDE,DELS
7 DO 1 I=1,25
8 READ(5,*)C(I,20)
9 1 READ(5,*)(C(I,J),J=1,7)
10 DO 5 I=1,61
11 5 READ(5,*)(C(I,J),J=16,19)
12 DO 3 I=1,29
13 3 READ(5,*)(C(I,J),J=10,14)
14 CLAVEW=0.0
15 CLAVEH=0.0
16 DO 13 I=1,12
17 CLAVEW=CLAVEW+C(I,3)/12.
18 J=I+8
19 CLAVEH=CLAVEH+C(J,12)/12.
20 13 CONTINUE
21 READ(5,*)BW,CRW,GAMA,SHROWD
22 READ(5,*)BHT,CRHT,ETHAHT,XL,DB
23 DO 4 I=1,25
24 4 READ(5,*)C(I,15)
25 DO 11 IW=1,16
26 READ(5,*)ALTITU,RHO,WI,DELFI,XCGI
27 WRITE(6,100)
28 PRINT,' ALTITUDE=',ALTITU,' DENSITY=',RHO
29 PRINT,'
30 W=WI
31 XCG=XCGI
32 DO 11 IDELF=1,13,2
33 DELF=DELFI-(IDELF-1)*5
34 PRINT,'
35 PRINT,' WEIGHT=',W,' XCG=',XCG,' DELF=',DELF
36 PRINT,'
37 K=DELF+1
38 E=6.78195/(XL)**0.25
39 DO 2 I=1,25
40 C(I,8)=(C(I,2)+C(K,17))*E
41 2 C(I,9)=C(I,3)*E
42 XD=3.568-XCG
43 SW=.785398*BW*CRW
44 CBARW=SW/BW
45 ARW=BW/CBARW
46 SHT=.785398*BHT*CRHT
47 CBARHT=SHT/BHT
48 ARHT=BHT/CBARHT
49 DO 11 I=1,25
50 STALL=C(25,1)-4.*C(K,16)/60.
51 IF(C(I,1).GT.STALL)GO TO 8
52 CLW=C(I,2)+C(K,17)
53 CMW=-C(I,6)-C(K,19)+.0689*C(I,2)
54 CLH=-SW*(XD*CLW+CBARW*CMW)/(XC*ETHAHT*SHT*(1.+XL/XC))
55 Q=W*XD/(-XL*SHT*ETHAHT*CLH-CBARW*SW*CMW)
56 IF(Q.LE.0.0)GO TO 12
57 V=(Q*2./RHO)**0.5
58 J=0
59 6 J=J+1
60 IF(J.GT.29)GO TO 9

```

```

61      7 DIFFER=CLH-C(J,11)
62      IF(ABS(DIFFER).GT.0.15)GO TO 6
63      DELTAH=DIFFER/C(J,12)+C(J,10)+C(I,8)
64      CDHT=(DIFFER/C(J,12))*C(J,14)+C(J,13)
65      A=(GAMA-C(I,1))/57.2958
66      CDBN=0.05*DB*(XL-1.725)*(TAN(A))/(12.*SW)
67      CDFTN=CDFT*SHT/SW
68      CDSHRD=0.2*SHRCWD/SW
69      CDSHRD=0.
70      CDFN=C(I,15)
71      CDVN=C(15,13)*SHT*0.5/SW
72      CDTOT=C(I,4)+CDFN+CDBN+CDHTN+CDVN+CDSHRD+C(K,18)+(C(K,17)*C(K,17)+
*2.*C(K,17)*C(I,2))/(2.9845*ARW)
73      ENDURE=0.0
74      IF(CLW.LE.0.0)GO TO 10
75      ENDURE=CLW**1.5/CDTOT
76      10 RANGE=CLW/CDTOT
77      XCGP=(XCG-3.125)/1.788
78      STATIC=CLAVEH*ETHAHT*SHT*(1.-C(I,9))/(SW*CLAVEH)
79      XACP=(0.24800+STATIC*4.71300)/(1.+STATIC)
80      CLP=CLW+CLT*ETHAHT*SHT/SW
81      CLAP=C(I,3)+C(J,12)*ETHAHT*SHT*(1.-C(I,9))/SW
82      CMAP=CLAP*(XCGP-XACP)
83      CMP=C(11,6)+CMAP*C(I,1)
84      PI=CLP*CCS(C(I,20)/57.296)+CDTOT*SIN(C(I,20)/57.296)
85      POWER=h*V*CDTOT/PI/550.
86      C(I,21)=-.2215*CLAVEH*SIDE-.0089*CLW-.00265*CLH-.0089*CLAVEH*(2.31
**CCS(C(I,20)/57.296)-(8.84-XCGP*CBARW)*SIN(C(I,20)/57.296))
87      C(I,22)=-.0089*CLAVEH*(2.31*COS(C(I,20)/57.296)-(8.84-XCGP*CBARW)*
*SIN(C(I,20)/57.296))
88      C(I,23)=.898*CLAVEH*SIN(DELS/57.296)
89      C(I,24)=-.134*CLAVEH
90      C(I,24)=C(I,24)*57.296
91      C(I,25)=-C(I,24)
92      C(I,26)=.0089*CLAVEH*((8.84-XCGP*CBARW)*COS(C(I,20)/57.296))
93      C(I,26)=C(I,26)*57.296-.0279*XCG+.0973
94      C(I,27)=-C(I,26)
95      C(I,28)=CLAVEH*.01588*(8.84-XCGP*CBARW)*COS(C(I,20)/57.296)
96      C(I,29)=C(I,28)*(-SIN(C(I,20)/57.296)*(8.84-XCGP*CBARW)+1.43)/15.
97      C(I,30)=-C(I,28)*(8.84-XCGP*CBARW)*COS(C(I,20)/57.296)/15.
98      C(I,21)=C(I,21)*57.296
99      C(I,22)=C(I,22)*57.296
100     C(I,28)=C(I,28)*57.296
101     C(I,29)=C(I,29)*57.296+1.96*CLW/V
102     C(I,30)=C(I,30)*57.296
103     WRITE(6,105)NNNN,C(I,1),C(I,20),CLW,ENDURE,RANGE,V,DELTAH,C(I,8),P
*OWER,XACP,XCGP,CMAP
104     WRITE(6,105)MMM,CLP,CDTOT,CMP,(C(I,J),J=21,30)
105     GO TO 11
106     12 PRINT,0,' ...TOO LOW AN ANGLE OF ATTACK..DOWNWARD LIFT.... '
107     GO TO 11
108     8 PRINT,' ...TOO HIGH AN ANGLE OF ATTACK...WING STALL... '
109     GO TO 11
110     9 PRINT,' ...IMPOSSIBLE CCONFIGURATION...H.TAIL STALL... '
111     11 CONTINUE
112     WRITE(6,100)
113     STOP;END

```

\$ENTRY

A.3.6

$$\left. \frac{dM}{d\alpha} \right|_B = \frac{\rho}{36.5} \int_0^l w_f^2(x) \left. \frac{d\bar{e}}{d\alpha} \right|_x dx$$

$$\left. \frac{dM}{d\alpha} \right|_B = \frac{\rho}{36.5} \sum_{i=1}^{i=n} w_f^2(x_i) \left. \frac{d\bar{e}}{d\alpha} \right|_i \Delta x_i$$

Ahead of the wing

$$\left. \frac{d\bar{e}}{d\alpha} \right|_{C_{L\alpha}} = \frac{C_{L\alpha}}{0.08} \cdot \left. \frac{d\bar{e}}{d\alpha} \right|_{0.08}$$

where  $\left. \frac{d\bar{e}}{d\alpha} \right|_{0.08}$  is given by the author.

Behind the wing

$$\frac{d\bar{e}}{d\alpha} = 18 \frac{C_{L\alpha}}{\alpha} \cdot \frac{\lambda^{0.3}}{AR^{0.725}} \left( \frac{3c\bar{c}}{l_H} \right)^{0.25}$$

where then

$$\left. \frac{d\bar{e}}{d\alpha} \right|_{x_i} = \frac{x_i}{l_H} \left( 1 - \frac{d\bar{e}}{d\alpha} \right)$$

Thus

$$\Delta \bar{X}_{a.c.}_B = - \frac{dM/d\alpha}{\bar{\rho} S \bar{c} C_{L\alpha w}}$$

$$\frac{dM}{d\alpha} = \frac{\rho}{36.5} \cdot \frac{1}{1728} \cdot \frac{C_{L\alpha}}{0.08} (16106.647)$$

$$\Delta \bar{X}_{a.c.}_B = - 0.0689$$

and

$$C_{m_f} = C_{\frac{L}{w}} (0.0689)$$

Wing a.c. is given by:

$$X_{a.c.} = \frac{\int_0^b C_{l_2} \alpha x d(y/b/2)}{\int_0^b C_{l_2} \alpha d(y/b/2)}$$

$$\alpha = 2.3 \sqrt{1 - (y/b/2)^2}$$

$$X_{a.c.} = 1.725 \frac{\int_0^{\pi/2} \cos^2 \theta (1 - \cos \theta) d\theta}{\int_0^{\pi/2} \cos^2 \theta d\theta}$$

$$X_{a.c.} = 0.2608$$

A.3.7.

$$C_L = C_{L_0} + C_{L_\alpha} \alpha + C_{L_{i_H}} i_H + C_{L_{\delta_E}} \delta_E$$

For all moving symmetrical tail and wing flaps

$$C_L = C_{L_w} + C_{L_{\delta_F}} \delta_F + \frac{S_H}{S_w} \eta_H C_{L_H} \alpha_H$$

where

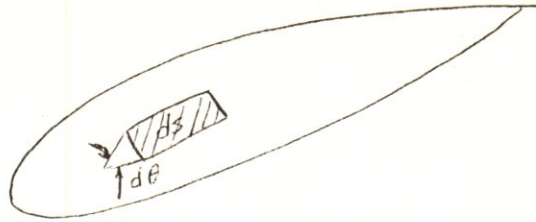
$$\alpha_H = \alpha - \epsilon$$

and

$$\epsilon = 18 C_{L_w} \frac{\lambda^{0.3}}{AR^{0.725}} \left( \frac{3 \bar{c}}{l_H} \right)^{0.25}$$

Throughout the stability calculations  $\eta_H$  was safely assumed to be 0.95.

A.3.8.



$$ds = r d\theta dx$$

$$S = \int_0^c \int_0^\pi r d\theta dx$$

$$C_{D_F} = \frac{1}{S_w} \int_0^c \int_0^\pi C_D R(x) dx d\theta + C_{D_i}$$

$$C_D = C_{D_0} + C_{D_\alpha}$$

$$\alpha = \alpha_i \sin \theta$$

$$C_{D_F} = \frac{1}{S_w} \int_0^c \int_0^\pi [C_{D_0} + C_{D_\alpha} (\alpha \sin \theta)] R(x) dx d\theta + C_{D_i}$$

The same method results in

$$C_{L_F} \approx \frac{1}{S_w} \int_0^c \int_0^\pi C_{L_\alpha} \alpha^2 \sin^2 \theta R(x) dx d\theta$$

$$C_{L_F} \approx \frac{\pi}{2S_w} \int_0^c C_{L_\alpha} \alpha R(x) dx$$

then

$$C_{D_F} = \frac{1}{S_w} \left\{ [(\pi - 2) C_{D_0} + 2 C_{D_0}] \int_0^c R(x) dx + \frac{C_{L_F}^2}{\pi A R E} \right\}$$

A.3.9.

$$C_D = C_{D_0} + C_{D_\alpha} \alpha + C_{D_{i_H}} i_H + C_{D_{\delta_E}} \delta_E$$

$$C_D = C_{D_w} + C_{D_{fuselage}} + C_{D_{Flaps}} + \frac{(\Delta C_{p_{Flaps}}^2 + C_{L_w} \cdot \Delta C_{p_{flap}})}{\pi A R e}$$

$$+ \frac{S_{boom}}{S_w} C_{D_{boom}} + \frac{S_H}{S_w} \eta_H C_{D_H} + C_{D_{shroud}}$$

For the case of power-on  $C_{D_{shroud}} = 0$ .



A.3.10

$$C_m = C_{m_0} + C_{m_\alpha} \alpha + C_{m_{i_H}} i_H + C_{m_{\delta_E}} \delta_E$$

Considering the special structure on hand;

$$C_m = \left( C_{L_0} + C_{L_\alpha} \alpha \right) \left( \bar{X}_{c.g.} - \bar{X}_{a.c.} \right) + C_{m_{a.c.}} + C_{L_{\alpha_H}} \eta_H \frac{S_H}{S_w} \left( \bar{X}_{a.c.} - \bar{X}_{c.g.} \right) (\alpha - \epsilon)$$

It was assumed in this part that

$$C_{L_{wB}} = C_{L_w}$$

A.3.11.

To find  $\bar{x}_{a.c.}$   $C_{m\alpha} = 0$

then

$$\bar{x}_{a.c. \text{ plane}} = \frac{\bar{x}_{a.c. \text{ WB}} + \frac{C_{L\alpha H}}{C_{L\alpha \text{ WB}}} \eta_H \frac{S_H}{S_W} \bar{x}_{a.c. H} \left(1 - \frac{d\epsilon}{d\alpha}\right)}{1 + \frac{C_{L\alpha H}}{C_{L\alpha \text{ WB}}} \eta_H \frac{S_H}{S_W} \left(1 - \frac{d\epsilon}{d\alpha}\right)}$$

For the specific structure on hand  $\bar{x}_{a.c. \text{ plane}}$  stays constant whether the power is on or off due to passing of the thrust line through c.g.

A.3.12.

$$\tan \Lambda_n = \tan \Lambda_m - \frac{4}{AR_w} \left[ (n-m) \frac{(1-\lambda)}{(1+\lambda)} \right]$$

where  $n, m \equiv$  fractions of chord

$$\lambda \equiv \text{taper ratio} = \frac{2}{3}$$

For this structure  $m = \frac{3}{4} \Rightarrow \tan \Lambda_{c/4} = 0$

then

$$\tan \Lambda_n = \frac{4}{AR_w} \left[ \left( \frac{3}{4} - n \right) \frac{\left( 1 - \frac{2}{3} \right)}{\left( 1 + \frac{2}{3} \right)} \right]$$

therefore at leading edge  $\Lambda_0 \cong 4.23^\circ$

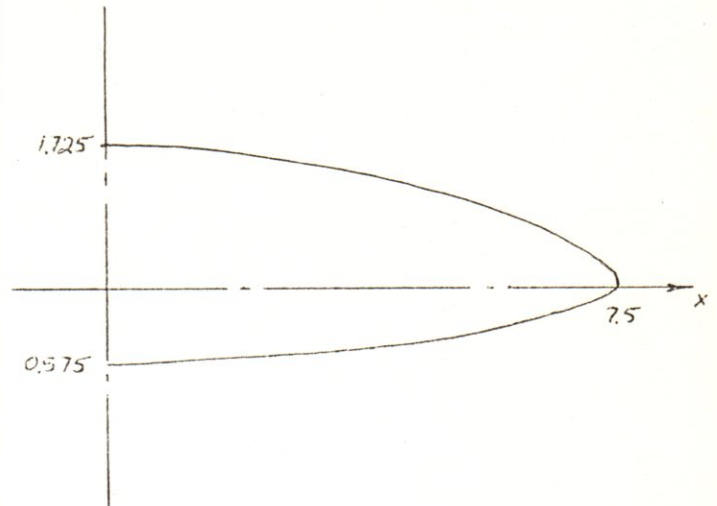
at  $c/4$   $\Lambda_{c/4} \cong 2.82^\circ$

at trailing edge  $\Lambda_c \cong -1.41^\circ$

For horizontal tail  $m = 0.5 \Rightarrow \tan \Lambda_{c/2} = 0$

therefore  $\Lambda_{L.E.} \cong 3.23^\circ$

A.3.13



$$C_l = C_{l_0} + C_{L_\beta} \beta + C_{L_{\delta_s}} \delta_s + C_{L_{\delta_R}} \delta_R$$

$C_{l_0} :$

$$C_{l_0} = 0.0$$

$C_{L_\beta} :$

$$C_{L_\beta} = C_{L_\beta_{WB}} + C_{L_\beta_H} + C_{L_\beta_V}$$

$$C_{L_\beta_{WB}} = C_{L_\beta_T} + C_{L_\beta_\Lambda} + C_{L_\beta_{wing\ location}}$$

Dihedral Effect.

$$c = 2.3 \sqrt{1 - \frac{x^2}{(7.5)^2}}$$

$$dL_\beta = -2 \int x c dx C_{L_\alpha} d\alpha$$

$$dL_\beta = - \int_{x=0.25}^{7.5} 4.6 x \sqrt{1 - \frac{x^2}{(7.5)^2}} C_{L_\alpha} d\alpha dx$$

$$d\alpha = \beta T$$

and

$$C_{L_\beta} = \frac{L_\beta}{Sb}$$

Sweep Effect (Wing)  $C_{L_{\beta}}^{\text{dihedral}} = -0.2215 C_{L_{\alpha}} \pi$

$$dL_{\beta_{\Lambda}} \cong -x C_{L_{\alpha}} c dx (2\beta \sin 2\Lambda)$$

$$C_{L_{\beta}}^{\text{sweep}} = -0.00887 C_L$$

Sweep Effect (H. Tail)

$$dL_{\beta_{\Lambda_H}} = -x C_{L_{\alpha_H}} \eta_H [\beta \sin 2\Lambda] (2.452)(3.375)/3.$$

$$C_{L_{\beta_{\Lambda_H}}} = -0.00265 C_{L_H}$$

Vertical Tail and Body

$$\bar{z} = \frac{\int_0^{3.375} x \sqrt{1 - \frac{x^2}{(3.375)^2}} dx}{\int_0^{3.375} \sqrt{1 - \frac{x^2}{(3.375)^2}} dx} = \frac{4b_v}{3\pi}$$

then

$$\bar{z}_v = \frac{4b_v}{3\pi} + 0.75$$

$$AR_{\text{eff}_v} = \frac{A_v(B)}{A_v} A_v \left\{ 1 + K_H \left[ \frac{A_{v_{HB}}}{A_{v_B}} - 1 \right] \right\}$$

$$S_v = 3.25 \text{ ft}^2$$

$$b_v = 3.375 \text{ ft} \Rightarrow A_v = 3.5$$

$$\lambda = 2/3 \Rightarrow \frac{A_{vB}}{A_v} = 1.0, \frac{A_{vHB}}{A_{vB}} = 0.9, K_H = 0.97$$

then

$$AR_{\text{eff. } v} = 3.16$$

For side wash effect:

$$\left(1 + \frac{2\sigma}{2\beta}\right) \eta_v = 0.724 + 3.06 \frac{S_v/S_w}{1 + \cos \lambda \cdot c/w} + 0.4 \frac{z_w}{d} + 0.009 AR_w$$

therefore

$$\left(1 + \frac{2\sigma}{2\beta}\right) \eta_v = 1.069$$

$$C_{Y_{\beta}} = -k C_{L_{\alpha_v}} \left(1 + \frac{2\sigma}{2\beta}\right) \eta_v \frac{S_v}{S_w}$$

where

$$k = 1.0$$

then

$$C_{Y_{\beta}} = -0.134 C_{L_{\alpha_v}}$$

therefore since

$$C_{Y_{\beta}} = C_{Y_{\beta}} \frac{\bar{z}_v \cos \alpha - b_v \sin \alpha}{b_w}$$

$$\text{Thus } C_{Y_{\beta}} = -0.02215 C_{L_{\alpha_w}} \bar{P} - 0.0337 C_{L_{\alpha_w}} - 0.00265 C_{L_{\alpha_H}} \\ - 0.0089 C_{L_{\alpha_v}} \left[ 2.31 \cos \alpha - (8.84 - \bar{x}_{cg} \cdot \bar{c}) \sin \alpha \right]$$

$C_{L_{\delta_s}}$ :

$$C_{L_{\delta_s}} = \frac{C_{L_{\alpha}} \Delta \alpha'_s}{2}$$

$$\Delta \alpha'_s = 1.167 \frac{h_s}{c} - 0.05835$$

$$h_s = (\text{spoiler width}) \sin \delta_s + 0.05$$

$$\beta = \sqrt{1 - M^2} \cong 1$$

$$\beta R \cong 8 > 2$$

$$\mu_{\beta} = \tan^{-1} (\tan 2.86 / \beta) = 2.876 < 60$$

therefore the above method is applicable and,

$$b = 0.25'$$

$$\left. \begin{array}{l} y_i = 5.0 \Rightarrow \eta_i = 0.667 \\ y_o = 6.0 \Rightarrow \eta_o = 0.8 \end{array} \right\} \Rightarrow \eta_{ave.} = 0.7335$$

$$C_{L_{\delta_s}} \beta / \kappa = 0.675$$

$$\kappa = C_{L_{\alpha}} / 2\pi$$

then

$$C_{L_{\delta_s}} \cong \frac{0.675}{2\pi} C_{L_{\alpha}}$$

therefore

$$C_{L_{\delta_s}} = \frac{0.675}{4\pi} C_{L_{\alpha}} [1.167 (0.25 \sin \delta_s + 0.05) - 0.5835]$$

thus

$$C_{L_{\delta_s}} = 0.898 C_{L_{\alpha}} \sin \delta_s$$

$C_{L\delta R}$ 

For all moving vertical tail

$$C_{L\delta R} = C_{L\beta V}$$

therefore:

$$C_{L\delta R} = -0.0089 C_{L\alpha V} [2.31 \cos \alpha - (8.84 - \bar{x}_{cg} \bar{c}) \sin \alpha]$$

Magnitudes and Comments

derivative	accepted	available	comments
$C_{L\beta}$	+0.1 - -0.4	0. - -0.63	Resistance to side-slip is desirable during landing
$C_{L\delta A}$	0.0 - 0.4	0.08	Spoiler has twice as much range of deflection
$C_{L\delta R}$	-0.04 - +0.04	-0.13 - -0.05	Vertical tail has one fourth the freedom of motion of rudder.



A.3. 14.

$$C_Y = C_{Y_0} + C_{Y_\beta} \beta + C_{Y_{\delta_R}} \delta_R + C_{Y_{\delta_S}} \delta_S$$

$$C_{Y_0} = 0$$

$$C_{Y_{\delta_S}} \approx 0$$

$C_{Y_\beta}$  was calculated in the previous part. For all moving V. tail

$$C_{Y_\beta} = -C_{Y_{\delta_R}}$$

therefore

$$C_{Y_\beta} = -0.134 C_{L_{\delta_v}} \beta$$

and

$$C_{Y_{\delta_R}} = 0.134 C_{L_{\delta_v}} \delta_R$$

Magnitudes and Comments.

derivative	accepted	available	Comments
$C_{Y_\beta}$	-0.1 - -2.0	-0.78	acceptable
$C_{Y_{\delta_R}}$	0. - 0.5	0.78	V. tail has one forth the freedom of motion of rudder.

A.3.15.

$$C_n = C_{n_0} + C_{n_\beta} \beta + C_{n_{\delta_S}} \delta_S + C_{n_{\delta_R}} \delta_R$$

$$C_{n_0} = 0 \quad \text{and} \quad C_{n_{\delta_S}} \approx 0.$$

For all moving vertical tail;

$$C_{n_\beta} = -C_{n_{\delta_R}}$$

$$C_{n_\beta} = -C_{n_{\delta_R}} = -C_{Y_v} \cdot l_v + f(c.g.)$$

or,

$$C_{n_\beta} = 0.0089 C_{C_{\alpha_v}} (8.84 - \bar{x}_{c.g.} \bar{c}) \cos \alpha - 0.0279 X_{c.g.} + 0.0973$$

Magnitudes and Comments.

derivative	accepted	available	comments
$C_{n_\beta}$	0 - 0.4	0.38	acceptable
$C_{n_{\delta_R}}$	0 - -0.15	-0.38	v.tail has one fourth the freedom of motion of rudder

A. 3. 16

$$C_{Y_r} = C_{Y_r}^{WBH} + C_{Y_{r_v}}$$

Due to the small size of the body and length,

$$C_{Y_r}^{WBH} \approx 0$$

$$C_{Y_{r_v}} = C_{L_{\alpha_v}} \frac{2 \cdot l_v}{b} \eta_v \frac{S_v}{S}$$

Assuming

$$\eta_v = 0.95$$

then

$$C_{Y_r} = C_{Y_{r_v}} = C_{L_{\alpha_v}} (0.01588) (8.84 - \bar{x}_{cg} \cdot \bar{c}) \cos \alpha$$

Magnitudes and Comments.

derivative	accepted	available	Comments
$C_{Y_r}$	0 - 1.2	0.65 - 0.74	acceptable.

A.3.17.

$$C_{D_r} = C_{L_{r_w}} + C_{L_{r_B}} + C_{L_{r_H}} + C_{L_{r_V}}$$

$$C_{L_{r_B}} \approx 0 \quad \text{and} \quad C_{L_{r_H}} \approx 0.$$

$$C_{L_{r_w}} = \frac{1}{9.5b} \int_{-7.5}^{7.5} y w C_{L_w} (0.5 \rho \Delta \bar{w}^2 + \rho V \Delta \bar{w}) dy$$

$$w = 2.3 \sqrt{1 - \frac{y^2}{(7.5)^2}}$$

$$\Delta \bar{w} = r y$$

therefore

$$C_{D_{r_w}} = 1.96 \frac{C_{L_w}}{V}$$

$$C_{D_{r_V}} = C_{L_{\alpha_V}} \frac{2 \cdot l_V \cdot z_V}{b^2} \eta_V \frac{S_V}{S}$$

Magnitudes and Comments.

derivative	accepted	available	Comments
$C_{D_r}$	0. - 0.6	0.05 - 0.09	acceptable

A.3.18

$$C_{n_r} = C_{n_r}_{WB} + C_{n_r}_V$$

Due to the small sizes of the body;

$$C_{n_r}_{WB} \cong 0$$

therefore

$$C_{n_r} = C_{n_r}_V$$

$$C_{n_r}_V = - C_{y_r}_V \frac{2 \cdot l_v^2}{b^2} \eta_v \frac{S_v}{S}$$

or

$$C_{n_r} = - C_{y_r}_V \cdot \frac{l_v}{b}$$

Magnitudes and Comments.

derivative	accepted	available	Comments
$C_{n_r}$	0 - -1.0	-0.36 - -0.39	acceptable.

A.3.19

Landing can be performed in any direction. The following are suggested for load and weather conditions.

Weather	Load	Flaps (DEG.)	Stall Speed (Nauts)	Air Speed (Nauts)	Approach Angle (deg.)	max. R.C. Available (fpm)	Descend Rate (fpm)
Turbulent	empty 143.2 #	20	27	33	less than 4	310	Any
	full 229.24 #	20	35	42	less than 0.5	50	Any
Calm	empty 143.2 #	60	24	29	1.2	—	80
	full 229.24 #	40	32	39	2.4	—	165

For other flap settings refer to Figures A.3.19.a and A.3.19.b.

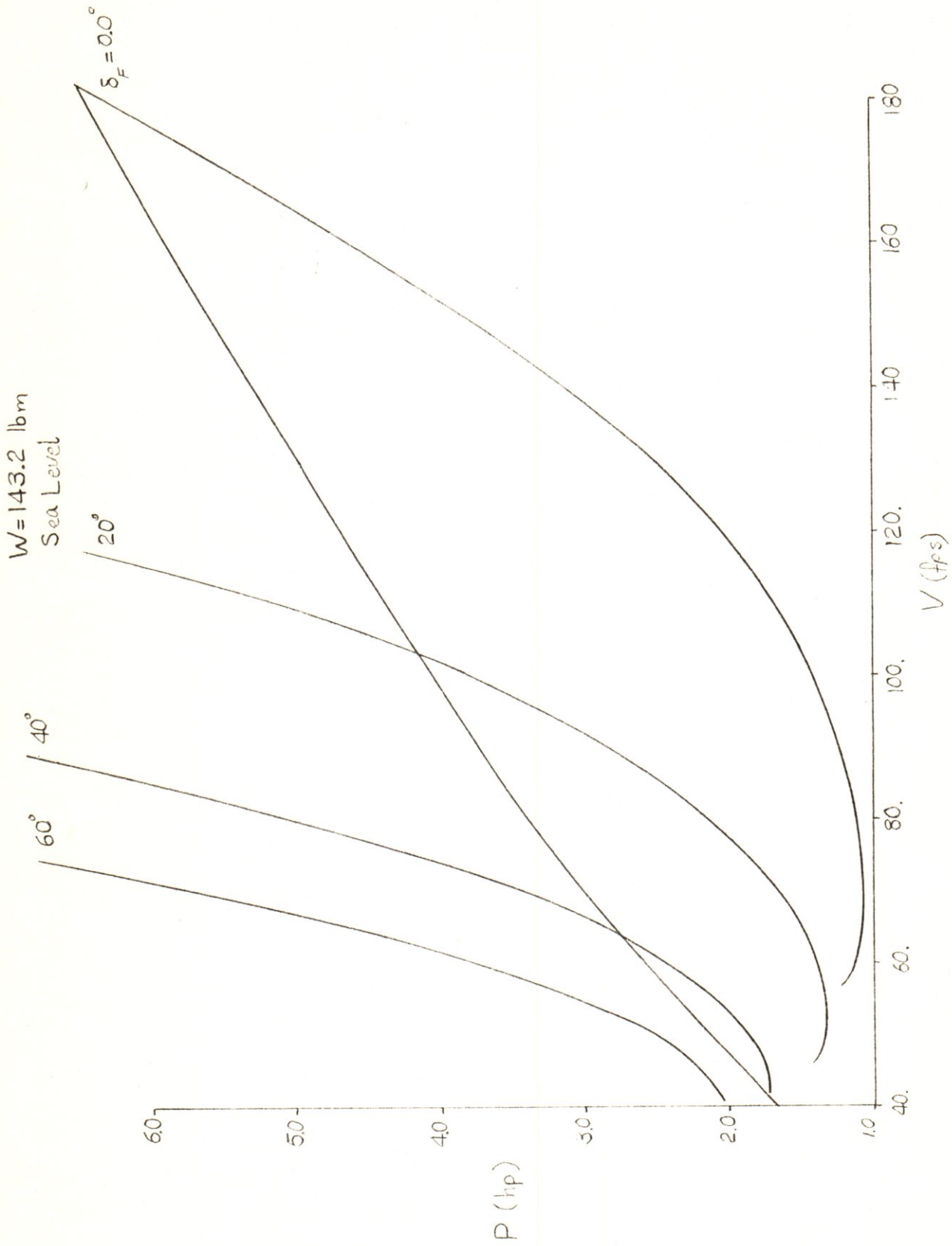


Fig A.3.19.a

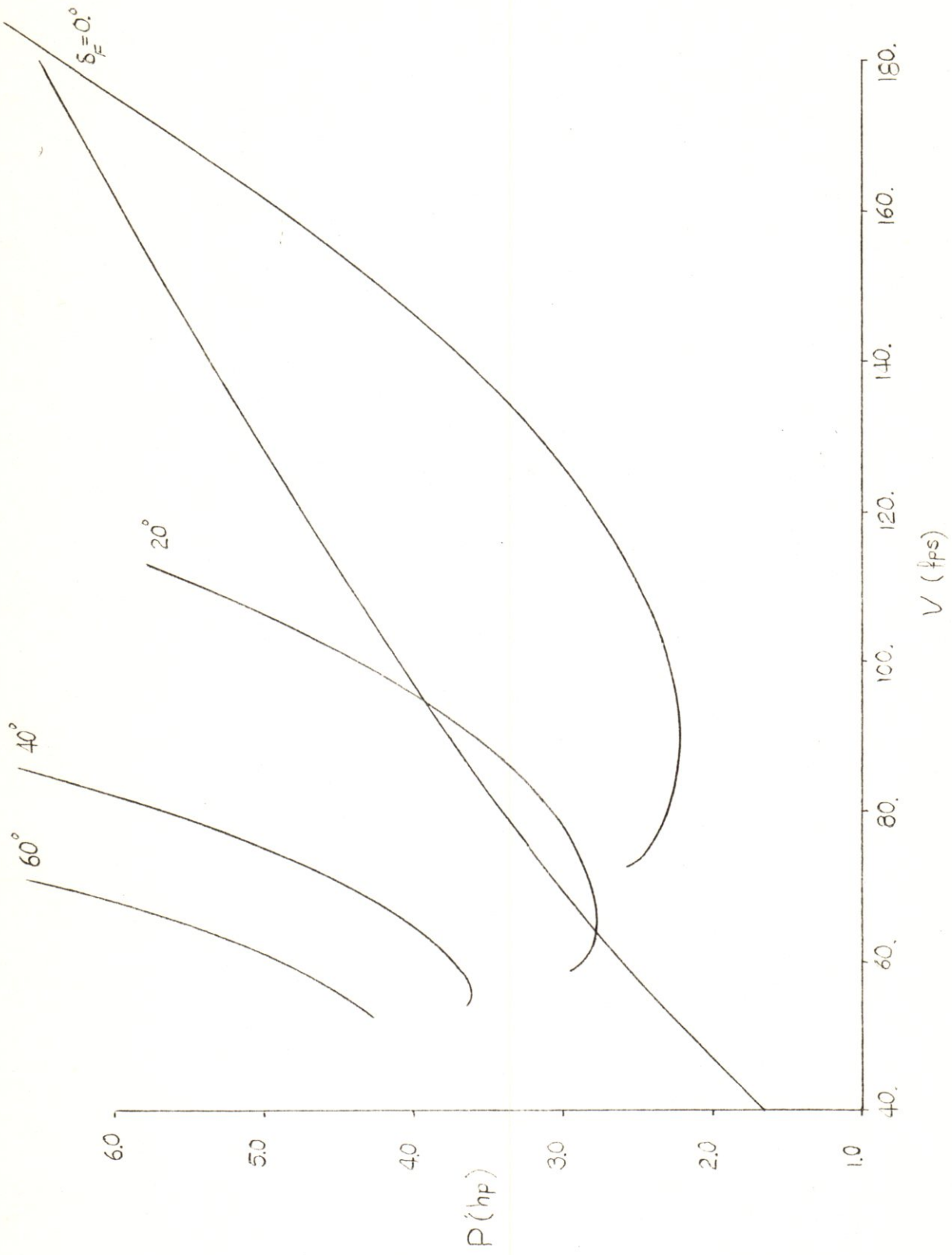


Fig A.3.19.b



# Appendix 4

## A.2.2.2

$$A. \quad \Delta H_p = 6130 \frac{\text{BTU}}{\text{lb}_{\text{mfuel}}} \quad 2g_c \Delta H_p = 3.065 \times 10^8 \frac{\text{ft}}{\text{s}^2}$$

ideal  $V_j = \sqrt{2g_c \Delta H_p} = 17,500 \text{ fps}$

Propulsive efficiency,  $\eta_p$

$$\eta_p = \frac{2r}{1+r^2}, \quad r = \frac{U}{V_j}$$

$U$  - forward vel.  $V_j$  - jet velocity

For  $\text{H}_2$  &  $\text{O}_2$

$$r = \frac{110}{17500} = 0.006286 \quad \eta_p = \frac{2(0.006286)}{1+(0.006286)^2}$$

$$\eta_p = 0.0126$$

Power required is  $1650 \frac{\text{ft-lbf}}{\text{s}}$

$$1 \text{ BTU} = 777 \text{ ft-lbf}$$

$$\text{at } \eta_p = 0.022 = \frac{\text{Power out}}{\text{Power in}} = \frac{1243 \frac{\text{ft-lbf}}{\text{s}}}{P_{\text{in}}}$$

$$P_{\text{in}} = 75000 \frac{\text{ft-lbf}}{\text{s}} \quad \Delta H_p = 6130 \frac{\text{BTU}}{\text{lb}_{\text{mf}}}$$

$$\Delta H_p = (6130 \frac{\text{BTU}}{\text{lb}_{\text{mf}}}) (777 \frac{\text{ft-lbf}}{\text{BTU}})$$

$$\Delta H_p = 4763010 \frac{\text{ft-lbf}}{\text{lb}_{\text{mf}}}$$

$$\dot{m}_f = \frac{P}{\Delta H_p} = \frac{75000 \frac{\text{ft-lbf}}{\text{s}}}{4763010 \frac{\text{ft-lbf}}{\text{lb}_{\text{mf}}}} = 0.01575 \frac{\text{lb}_{\text{mfuel}}}{\text{s}}$$

$$\dot{m}_f = (0.01575 \frac{\text{lb}_{\text{mf}}}{\text{s}}) (3600 \frac{\text{s}}{\text{hr}}) = 56.687 \frac{\text{lb}_{\text{mf}}}{\text{hr}}$$

over 20 hours for  $V_i = 10000 \frac{ft}{s}$

$$m_f = 1133.74 \text{ lb}_{mf}$$

B.  $m_f = (15 \text{ lb}_f)(0.6 \frac{\text{lb}_{mf}}{\text{lb}_f\text{-hr}})(20 \text{ hr}) = 180 \text{ lb}_{mf}$

C.  $m_f = \frac{180 \text{ lb}_{mf}}{2} = 90 \text{ lb}_{mf}$

D.  $m_f = (3 \text{ hp})(0.48 \frac{\text{lb}_{mf}}{\text{hp-hr}})(20 \text{ hr}) = 28.8 \text{ lb}_{mf}$

E.  $shp = \frac{hp_{req}}{\eta} = \frac{3 \text{ hp}}{0.85} = 3.53 \text{ hp}$

$$m_f = (3.53 \text{ hp})(0.6 \frac{\text{lb}_{mf}}{\text{hp-hr}})(20 \text{ hr}) = 42.36 \text{ lb}_{mf}$$

F.  $shp = \frac{hp_{req}}{\eta} = \frac{3 \text{ hp}}{0.5} = 6 \text{ hp}$

$$m_f = (6 \text{ hp})(0.6 \frac{\text{lb}_{mf}}{\text{hp-hr}})(20 \text{ hr}) = 72 \text{ lb}_{mf}$$

G.  $m_f = (15 \text{ lb}_f)(2 \frac{\text{lb}_{mf}}{\text{lb}_f\text{-hr}})(20 \text{ hr}) = 600 \text{ lb}_{mf}$

4.2.2.3

Preliminary estimates of  $P_{req}$

Dash  $C_D = 0.015$  37.5 ft<sup>2</sup> wing

10.75 hp req. at 220 fps  
or 150 mph

$$\textcircled{a} \quad \eta_{\text{prop}} = 0.65 \quad \text{shp}_{\text{req}} = \frac{10.75 \text{ hp}}{0.65} = 16.54 \text{ hp}$$

4.2.2.4

fuel heating value  $\approx 18000 \frac{\text{BTU}}{\text{lbm}}$

$$C_{\text{pair}} = 0.24 \frac{\text{BTU}}{\text{lbm} \cdot \text{R}} \quad 1 \text{ hp} = 0.70733 \frac{\text{BTU}}{\text{s}}$$

for 10 hp and  $\text{SFC} = 0.9 \frac{\text{lbm}}{\text{hp} \cdot \text{hr}}$

fuel flow of  $9 \frac{\text{lbm}}{\text{hr}}$  is required

$$\dot{m}_f = \frac{9 \frac{\text{lbm}}{\text{hr}}}{3600 \frac{\text{s}}{\text{hr}}} = 0.0025 \frac{\text{lbm}}{\text{s}}$$

$$\text{heat flow} = (18000 \frac{\text{BTU}}{\text{lbm}}) (0.0025 \frac{\text{lbm}}{\text{s}})$$

$$\dot{Q}_{\text{gen}} = 45 \frac{\text{BTU}}{\text{s}}$$

9 hp gets outside the fuselage to the fan

$$\dot{Q}_{\text{fan}} = (9 \text{ hp}) (0.70733 \frac{\text{BTU}}{\text{hp} \cdot \text{s}}) = 6.366 \frac{\text{BTU}}{\text{s}}$$

Assume 50% of  $\dot{Q}_{\text{gen}}$  goes out the tailpipe (accounts for unburnt fuel, too)

$$\begin{aligned} \dot{Q}_{\text{excess}} &= 0.5 (45 \frac{\text{BTU}}{\text{s}}) - 6.366 \text{ BTU} \\ &= 16.134 \frac{\text{BTU}}{\text{s}} \end{aligned}$$

at ~~80 ft~~ sea level  $\rho = 0.076572 \frac{\text{lbm}}{\text{ft}^3}$

if surroundings 90°F allow air temp. out of cooling system to be 150°F.  $\Delta T = 60^\circ R$

$$\text{air flow} = \frac{16,134 \frac{\text{BTU}}{\text{s}}}{(0.24 \frac{\text{BTU}}{\text{lbm} \cdot ^\circ R})(60^\circ R)} = \dot{m}_a = 1.1204 \frac{\text{lbm}}{\text{s}}$$

$$\text{at } V = 80 \frac{\text{ft}}{\text{s}} \quad A = \frac{1.1204 \frac{\text{lbm}}{\text{s}}}{(0.076572 \frac{\text{lbm}}{\text{ft}^3})(80 \frac{\text{ft}}{\text{s}})} = 0.1829 \text{ ft}^2$$

$$A = 26.34 \text{ in}^2$$

allowing for a 2" diam. hub and 6" id. for duct end.

$$A = \pi (3''^2 - 0.5''^2) \doteq 27.5''^2$$

~~4.2.2.2~~

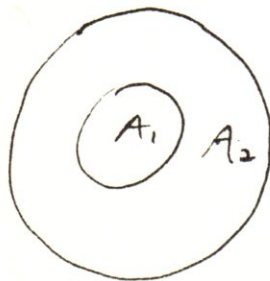
4.2.2.3

Fan sizing estimation

Assume 1.02 pressure ratio at 5006 ft. Assume Pressure =  $P = 14.5 \text{ psia}$

$$\text{Thrust Loading} = \frac{(14.5)(0.2)}{(14.5 \frac{\text{lb}_f}{\text{in}^2})(0.2)} = 0.29 \frac{\text{lb}_f}{\text{in}^2}$$

$$A_{\text{req}} = \frac{12.1 \text{ lb}_f}{0.29 \frac{\text{lb}_f}{\text{in}^2}} = 41.72 \text{ in}^2$$

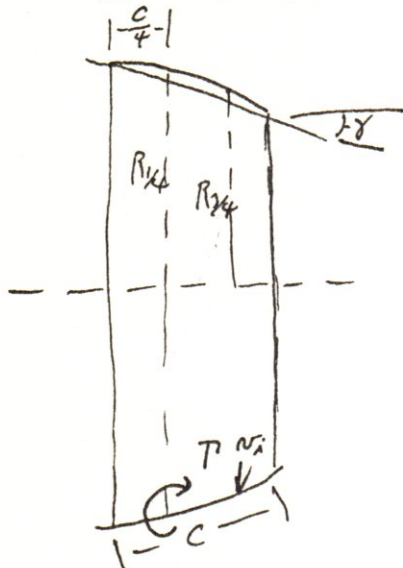


$$A_2 = \pi r_2^2 - \pi r_1^2 \quad r_2 = \sqrt{\frac{A_2 + \pi r_1^2}{\pi}}$$

$$r_2 = \sqrt{\frac{41.72 + \pi (3'')^2}{\pi}} = 4.72''$$

$$r_1 = r_{\text{hub}} = 3''$$

## Shroud Design



Approximation to a ring airfoil by Mc Cormick

$$v_i = \frac{T}{\pi D_{3/4}} f\left(\frac{c}{D_{1/4}}, \frac{D_{3/4}}{D_{1/4}}\right)$$

$v_i$  is radial (outward) velocity induced by the ring lift at  $c_{3/4}$ .

From the boundary condition at  $c_{3/4}$  is that radial velocity in total is zero, finding the radial  $v_i$  induced by the rotor must be equal and opposite. The free-stream condition of the rotor under the same shroud internal axial velocity solves for  $T$ .

$$v_{iR} = -\frac{1}{2} \frac{R R^2 \omega_0}{(Z^2 + R R^2)^{3/2}}$$

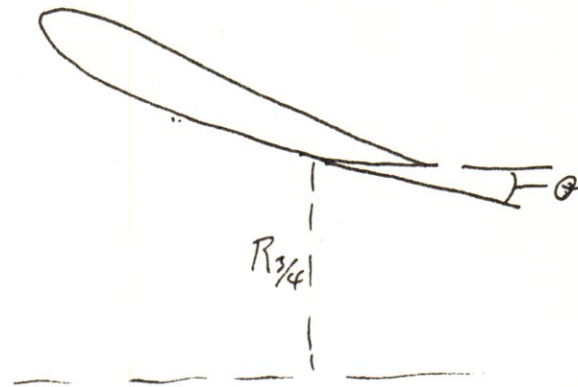
$$\omega_0 = \frac{1}{2} \left\{ -V + \left[ V^2 + \frac{T R}{\left(\frac{R}{2}\right) \pi R R^2} \right]^{1/2} \right\}$$

Continuity  $(V + w_a) \pi R^2 = (V + \omega_0) \pi R^2$

$$w_a = \frac{R R^2}{R^2} (V + \omega_0) - V$$

The resultant flow should be tangent to the shroud.

Therefore for a shroud inner surface angle of  $\theta$  at  $c_{3/4}$



$$\theta = \frac{-N_i R_{3/4} - V_i}{V + W a_{3/4}}$$

$$\text{or } N_i = -N_i R_{3/4} - \theta (V + W a_{3/4})$$

$$\text{giving } T = \frac{\pi D_{3/4}}{f\left(\frac{c}{D_{3/4}}, \frac{D_{3/4}}{D_{3/4}}\right)} [-N_i R_{3/4} - \theta (V + W a_{3/4})]$$

From the Kutta - Joukowski law the force on the shroud is

$$T_s = -\rho N_i R_{3/4} T \pi D_{3/4}$$

$$T_s = \frac{-\rho (\pi D_{3/4})^2 [-N_i R_{3/4} - \theta (V + W a_{3/4})] N_i R_{3/4}}{f\left(\frac{c}{D_{3/4}}, \frac{D_{3/4}}{D_{3/4}}\right)}$$

Defining a thrust coefficient

$$\cancel{C_T} \quad C_T = \frac{T}{\frac{1}{2} \rho A V^2}$$

Solve for  $C_T$  in terms of  $f, w_0, N_{iR^{1/4}}, N_{iR^{3/4}}, C_{TR}$  (rotor)

$$T_s = \rho N_{iR^{3/4}} T \pi D^{1/4}$$

$$P = N_{iR^{3/4}} \pi D^{1/4} \frac{1}{f \left( \frac{c}{D^{1/4}}, \frac{D^{3/4}}{D^{1/4}} \right)}$$

$$N_{\lambda^{3/4}} = -N_{iR^{3/4}} - \theta (V + w_{a^{3/4}})$$

$$w_{a^{3/4}} = \frac{R R^2}{R^{3/4}} (V + w_0) - V$$

$$N_{i^{3/4}} = -N_{\lambda^{3/4}} - \theta \left( V + \frac{R R^2}{R^{3/4}} (V + w_0) - V \right)$$

$$w_0 = \frac{V}{2} \left\{ -1 + [1 + C_{TR}]^{1/2} \right\}$$

$$N_{i^{3/4}} = -N_{iR^{3/4}} - \theta \frac{R R^2}{R^{3/4}} \frac{V}{2} \left\{ -1 + [1 + C_{TR}]^{1/2} \right\}$$

~~$$P = \dots$$~~

$$T = \frac{N_{i^{3/4}}}{f} \pi D^{1/4}$$

$$T_s = \frac{\rho \pi^2 D^{1/4}^2}{f} N_{iR^{3/4}} \left( N_{iR^{3/4}} + \theta \frac{R R^2}{R^{3/4}} \frac{V}{2} \left\{ -1 + [1 + C_{TR}]^{1/2} \right\} \right)$$

$$C_{T_s} = \frac{2 \pi D^{1/4}^2}{f R R^2 V^2} \left[ N_{iR^{3/4}} N_{iR^{3/4}} + N_{iR^{3/4}} \theta \frac{R R^2}{R^{3/4}} \frac{V}{2} \left\{ -1 + [1 + C_{TR}]^{1/2} \right\} \right]$$

$$N_{iR^{3/4}} = \frac{1}{2} \frac{R^{1/4} R^2 w_0}{(z^2 + R R^2)^{1/2}} \quad \text{define } L = \frac{c}{R}$$

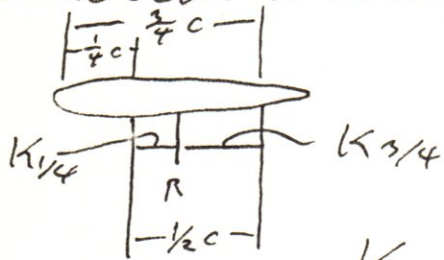
$$z = K \frac{c}{R_R} R_R \text{ where } K \text{ is a function of } c$$

$$\Rightarrow z^2 = K^2 L^2 R_R^2$$

$$\text{so } v_{iR_{1/4}} = \frac{1}{2} \frac{R_{1/4}}{R_R} \frac{W_0}{(K_{1/4}^2 L^2 + 1)^{3/2}}$$

$$\text{similarly } v_{iR_{3/4}} = \frac{1}{2} \frac{R_{3/4}}{R_R} \frac{W_0}{[K_{3/4}^2 L^2 + 1]^{3/2}}$$

relation between  $K_{1/4}$  &  $K_{3/4}$



$$K_{1/4} + K_{3/4} = \frac{1}{2}$$

$$K_{1/4} = \frac{1}{2} - K_{3/4}$$

$$K_{1/4}^2 = \frac{1}{4} - 2K_{3/4} + K_{3/4}^2$$

$$K_{3/4}^2 = \frac{1}{4} - 2K_{1/4} + K_{1/4}^2$$

giving, in the end

$$C_{TS} = \frac{R_{1/4} 2\pi D_{1/4}^2}{f R}$$

$$C_{TS} = \frac{\pi R_{1/4}^3 \{-1 + [1 + C_{TR}]^{1/2}\}}{f R_R^2} \left\{ \frac{1}{2} \frac{R_{3/4}}{R_R} \frac{1}{(K_{1/4}^2 L^2 + 1)} \right\}$$

$$\left\{ \frac{1}{2} \frac{R_{3/4}}{R_R^2} \frac{1}{(K_{1/4}^2 L^2 + 1) [(1/2 - K_{1/4})^2 L^2 + 1]^{3/2}} \right. \\ \left. + \theta \frac{R_R}{R_{3/4}^2} \frac{1}{(K_{1/4}^2 L^2 + 1)^{3/2}} \right\}$$



Drag of the shroud

$$C_{Ds} = C_f \frac{S}{A} = 8 \frac{C}{D} C_f$$

where  $S$  is the surface area of the shroud,  $A$  is the rotor area reference.  $C_f$  is the skin friction coefficient.

$$C_T = C_{TR} + C_{Ts} - C_{Ds}$$

But  $C_{Ts} = f(C_{TR})$  so we wish to optimise  $C_{Ts}$  for the design point.

Model shroud with a conical inner surface. Vary the major parameters  $D_{1/4}/D_{1/4}$ , radius, chord, and rotor location for the loiter condition. ~~Then~~ solve for the shroud Coefficient of Thrust factor  $F$  and solve for required  $C_{TR}$ .

Program follows:

```

C      PROGRAM SHROUD OPTIMIZE,
C      OPTIMIZATION OF A SHROUDED PROPELLER SHROUD
      DIMENSION F(11,4)
      REAL L
      INTEGER H
      COMMON F
      WRITE(6,70)
      DO 10 I=1,11
10     READ(5,11)F(I,1),F(I,2),F(I,3),F(I,4)
      DO 50 H=1,21,2
      R=(0.4+0.01*FLOAT(H-1))*12.0
      D=0.6
      DO 50 J=2,3
      D=D+0.2
      DO 50 J1=11,28
      C=FLCAT(J1)/2.0
      L=C/R
      CD=0.0096*C/R
      DO 50 J2=5,55,5
      CK1=(FLOAT(J2)-5.0)/100.0
      ST=(R*(1.0-D))/(C*(CK1*(D-1.0)+0.5))
      IF(ST.GT.1.0) GO TO 50
      T=ARCSIN(ST)
      R1=R+CK1*C*ST
      R3=R-(0.5-CK1)*C*ST
      CD1=C/(2.0*R1)
      IF(CD1.LT.0.4) GO TO 50
      CALL TABLE(J,CD1,FF)
      Z=R3/(2.0*(R**2.0)*(((CK1*L)**2.0+1.0)*((0.5-CK1)*L)*2.0+1.0)**1
a.5)
      Q=T*R/((R3**2.0)*((CK1*L)**2.0+1.0)**1.5)
      FFF=(R1**3.0)*ATAN(1.0)*4.0*(Z+Q)/((R*R)*FF)
      S3=0.0
      S=10000.0
      DO 20 J3=75,250
      S2=FLCAT(J3)/100.0
      S1=ABS(2.0-2.0*SQRT(1.0+S2)+(1.0+(R*R)/(FFF*ATAN(1.0)*4.0))*S2-((R
a*R)/(FFF*ATAN(1.0)*4.0))*(38.55057/((R*R)-9.0)+CD))
      IF (S1.GT.S) GO TO 20
      S=S1
      S3=S2
20     CONTINUE
50     WRITE(6,60)S3,FFF,CD,C,R1,R3,CK1,R
      STOP
11     FORMAT(4(2X,F4.2))
60     FORMAT(8(4X,F9.6))
70     FORMAT(1X,'ROTOR THRUST',1X,'SHROUD THRUST',2X,'SHROUD DRAG',8X,'C
aHORD',1X,'1/4 C RADIUS',1X,'3/4 C RADIUS',3X,'ROTOR LOC.')
      END

```

### 4.2.2.3 Fan Performance Relative to the Shroud

It is necessary to correct the fan performance for to conditions outside the duct (especially the free-stream velocity). Since the two parts of the propulsor, the duct and the fan, are highly dependent on each other, a program was written to take the geometric properties of shrouds and their performance properties (the thrust coefficient factor  $K$ ) and arrive at the necessary correction factors. The program follows:

```
$JOB
C   SHROUD PERFORMANCE
1   5 READ,R1,F,B,C1
2   IF (R1.EQ.0) GO TO 20
3   R0=3.0
4   D=0.0096*C1/(R1-R0)
5   Z=3.14159*F/B
6   Y=3.14159*F/(R1*R1-R0*R0)
7   PRINT 100, R1
8   DO 10 I=1,1000
9   C=FLOAT(I)/20.0
10  A=-1.0+SQRT(1.0+C)
11  Q=1.0+Z*A
12  S=Y*A
13  R=C/Q
14  V=SQRT(1.0+Z*A)
15  T=S+C-D
16  T1=C/T
17  10 PRINT 200,C,Q,S,R,V,T,T1
18  GO TO 5
19  20 STOP
20  100 FORMAT('1',4X,'PERFORMANCE FOR RADIUS OF ',F5.3,' INCHES'//5X,'CT
    @ (R)',5X,'CQ RATIO',3X,'CT (S)',3X,'CT (R,P)',3X,'V RATIO',2X,'TOTA
    @ L CT',3X,'ROTOR THRUST %')
21  200 FORMAT(2X,7(3X,F7.3))
22  END
```

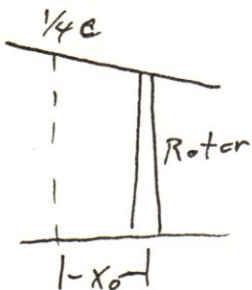
The main variables are:

$C_{TR}'$  - rotor thrust coefficient inside the duct

$\frac{V_R}{V_\infty}$  - shroud induced velocity at rotor over free-stream velocity

$\frac{C_Q'}{C_Q}$  - rotor torque coefficient inside the duct under rotor torque coefficient outside the duct

$C_{TS}$  - shroud thrust coefficient



$$A = \{ 1 + [ 1 + C_{TR}' ]^{1/2} \}$$

$$B = 2(R_R^2 - R_0^2) [ 1 + (\frac{x_0}{R_R})^2 ]^{3/2}$$

$$C_{TR}' = \left\{ 1 + \frac{\pi(F)A}{B} \right\} C_{TR}$$

$$\frac{V_R}{V_\infty} = \left\{ 1 + \frac{\pi F(A)}{B} \right\}^{1/2}$$

$$p_v = \left( \frac{C_Q'}{C_Q} \right) p_R$$

$$\frac{C_Q}{C_Q'} = \frac{1}{\left\{ 1 + \frac{\pi(F)A}{B} \right\}}$$

$$C_{TS} = \frac{\pi F}{R_R^2 - R_0^2} (A)$$

where  $R_0$  is the hub radius

$$\text{also } C_Q = \frac{Q}{\frac{1}{2} \rho V_\infty^2 R_R (R_R^2 - R_0^2)}$$

$$C_P = \frac{P}{\pi \rho V_\infty^3 R_R (R_R^2 - R_0^2)}$$

$p_v$  is the virtual pitch of the fan referenced to the free-stream condition.

### Effects of Reynolds Number

A good approximation for maximum performance of fans at the blade-element level is that, the higher the  $\frac{L}{D}$ , the better the efficiency. In this Reynolds number regime data for only four airfoils could be found:

Type	$C_L$	$C_D$	$(\frac{L}{D})_{max}$
N-60	1.0	0.025	40
NACA 4412	0.95	0.02	47.5
NACA 2412	0.8	0.014	57.14
NACA 0012	0.6	0.016	37.15

A very secondary parameter is the maximum lift coefficient

Type	$C_{Lmax}$
N-60	1.34
NACA 4412	1.21
NACA 2412	1.0
NACA 0012	0.82

The 2412, with the best  $\frac{L}{D}$ , appears to have an adequate stall margin for fan design.

## Fan Design

A computer program was written for interactive design of fans using the NACA 2412. The program uses the vortex theory presented by Dowmarch and modified by Townsbery. Linear variation of solidity in the fan, plus some control of fan loading, results in the most efficient fan possible ~~under~~ inside the shroud conditions. The program and the final fan design for the 7.2" radius duct ~~is~~ follow. The program contains data for the 2412 over a range of Reynolds numbers and finds the performance of each section according to a linear interpolation of characteristics.

Under no condition was the fan performance found to differ more than 3% from the design point (Lover), so that the lover performance was used for all projections of ~~the~~ total propulsion performance.

```

10 DIM F(6,33),G(4,51)
20 FOR I=1 TO 33
30 READ F(1,I),F(2,I),F(3,I),F(4,I),F(5,I),F(6,I)
40 NEXT I
50 DATA -0.48, 0.0304, -0.48, 0.0184, -0.48, 0.016
60 DATA -0.42, 0.0284, -0.42, 0.0172, -0.42, 0.0152
70 DATA -0.032, 0.026, -0.32, 0.016, -0.32, 0.0142
80 DATA -0.24, 0.024, -0.24, 0.0144, -0.24, 0.0132
90 DATA -0.14, 0.0224, -0.14, 0.014, -0.14, 0.0126
100 DATA -0.04, 0.0212, -0.04, 0.0136, -0.04, 0.0124
110 DATA 0.06, 0.02, 0.06, 0.0126, 0.06, 0.012
120 DATA 0.14, 0.0196, 0.14, 0.0124, 0.14, 0.0118
130 DATA 0.22, 0.0192, 0.22, 0.0124, 0.22, 0.0116
140 DATA 0.312, 0.019, 0.312, 0.0124, 0.312, 0.0116
150 DATA 0.4, 0.0192, 0.4, 0.0124, 0.4, 0.012
160 DATA 0.48, 0.02, 0.48, 0.0128, 0.48, 0.0124
170 DATA 0.56, 0.0202, 0.56, 0.013, 0.56, 0.0132
180 DATA 0.64, 0.021, 0.64, 0.0132, 0.64, 0.0142
190 DATA 0.72, 0.022, 0.72, 0.0132, 0.72, 0.0154
200 DATA 0.784, 0.0248, 0.784, 0.014, 0.784, 0.0162
210 DATA 0.84, 0.028, 0.84, 0.017, 0.84, 0.0178
220 DATA 0.9,0.031, 0.9, 0.019, 0.92, 0.0194
230 DATA 0.952, 0.036, 0.952, 0.022, 0.968, 0.0214
240 DATA 0.98, 0.046, 0.98, 0.03, 1.02, 0.024
250 DATA 1.0, 0.06, 1.0, 0.05, 1.06, 0.028
260 DATA 1.0, 0.061, 1.0, 0.055, 1.092, 0.032
270 DATA 1.0, 0.062, 1.0, 0.06, 1.1, 0.036
280 DATA 0.996, 0.063, 0.996, 0.061, 1.092, 0.04
290 DATA 0.972, 0.064, 0.972, 0.062, 1.064, 0.044
300 DATA 0.952, 0.065, 0.952, 0.063, 1.04, 0.048
310 DATA 0.928, 0.066, 0.928, 0.064, 1.0, 0.052
320 DATA 0.92, 0.067, 0.92, 0.065, 0.98, 0.056
330 DATA 0.9, 0.068, 0.9, 0.066, 0.96, 0.06
340 DATA 0.88, 0.069, 0.88, 0.067, 0.944, 0.064
350 DATA 0.872, 0.07, 0.872, 0.068, 0.928, 0.068
360 DATA 0.86, 0.071, 0.86, 0.069, 0.912, 0.07
365 DATA 0.84, 0.072, 0.84, 0.07, 0.9, 0.071
380 PRINT 'HUB SOLIDITY, 0.75 FOOT RADIUS SOLIDITY?'
390 INPUT S2,S3
394 PRINT 'BLADES?'
396 INPUT B
400 PRINT 'VELOCITY? (FT/SEC)'
410 INPUT V
420 PRINT 'RPM?'
430 INPUT W
440 W=W/60.0
450 PRINT 'AIR DENSITY? (SLUG/(FT CUBED))'
460 INPUT R5
462 PRINT 'MINIMUM ALPHA ZERO IS A MULTIPLE OF .2'

```

```

464 PRINT 'MINIMUM ALPHA ZERO?'
466 INPUT X9
470 P=V/W
472 T=0.0
474 Q=0.0
476 X=1
480 FOR R=0.25 TO 0.6 STEP 0.01
490 S0=ATN(P/(2*&PI*R))
500 S1=((S3-S2)/0.5)*(R-0.25)+S2
510 C=S1*2*&PI*R/B
520 R9=C*V/(SIN(S0)*1.5757E-4)
530 GOSUB 1520
540 J=(2*&PI*R)**2.0+P**2.0
550 K=R5*&PI*R*S1*(W*W)
560 D1=K*H*J
570 D2=K*R*I*J
580 G(1,X)=S1
590 C(2,X)=C
600 G(3,X)=B1
610 G(4,X)=B1*180.0/&PI
620 T=T+0.005*D1
630 Q=Q+0.005*D2
640 IF R<0.35 THEN 690
650 N=(T*P)/(2*&PI*Q)
660 C5=(2*T)/(R5*&PI*R*R*V*V)
670 CC=(2.0*Q)/(R5*&PI*(R**3.0)*V*V)
680 PRINT R,T,Q,N
690 T=T+0.005*D1
700 Q=Q+0.005*D2
705 X=X+1
710 NEXT R
720 PRINT
730 PRINT
740 PRINT 'BLADE GEOMETRY FOR ';B;' BLADES'
750 PRINT 'SOLIDITY OF ';S2;' AT ROOT, ';S3;' AT TIP'
760 PRINT 'VELOCITY= ';V;' PITCH= ';P
770 PRINT
780 FOR X=1 TO 30
785 R=0.24+X*0.01
790 PRINT R,G(2,X),G(4,X)
800 NEXT X
810 PRINT
820 PRINT
822 PRINT 'CHANGE ALPHA ZERO MINIMUM? 1=Y'
824 INPUT X8
826 IF X8=1 THEN 402
830 PRINT 'TIP RADIUS?'
840 INPUT R1
850 IF R1=0 THEN 380
860 IF R1<0 THEN 1800
870 PRINT 'VELOCITY?'

```



```

880 INPUT V
890 FOR P=0.2 TO 4.0 STEP 0.04
900 X=1
902 T=0.0
904 Q=0.0
910 FOR R=0.25 TO R1 STEP 0.01
920 S0=ATN(P/(2.0*&PI*R)) → S1 = G(1,X)
930 C=S1*2.0*&PI*R/B
940 R9=C*V/(SIN(S0)*1.5757E-4)
950 B1=G(3,X)
960 GOSUB 1270
970 J=(2.0*&PI*R)**2.0+P**2.0
980 W=V/P
990 K=R5*&PI*R*S1*W*W
1000 D1=K*H*J
1010 D2=K*R*I*J
1020 T=T+0.01*D1
1030 Q=Q+0.01*D2
1040 IF R<>R1 THEN 1070
1050 T=T-0.005*D1
1060 Q=Q-0.005*D2
1070 NEXT R
1080 N=(T*P)/(2*&PI*Q)
1090 C5=(2.0*T)/(R5*&PI*R1*R1*V*V)
1100 C6=(2.0*Q)/(R5*&PI*(R1**3.0)*V*V)
1110 PRINT P,C5,C6,N
1120 NEXT P
1130 PRINT
1140 PRINT 'VELOCITY= ';V
1150 PRINT
1160 PRINT 'CHANGE V? 1=Y'
1170 INPUT Z
1180 IF Z=1 THEN 870
1190 PRINT 'CHANGE RADIUS?'
1200 INPUT Z
1210 IF Z=1 THEN 830
1220 PRINT 'CHANGE DESIGN?'
1230 INPUT Z
1240 IF Z=1 THEN 380
1250 STOP
1270 REM INDUCED FLOW SOLUTION
1280 A0=P1-S0
1290 C7=4.0*SIN(S0)/S1
1300 A0=180.0*A0/&PI
1302 IF A0>=-4.4 THEN 1304
1303 A0=-4.4
1304 IF A0<=19.2 THEN 1310
1305 A0=19.2
1310 Z1=INT(INT(10.0*A0+0.001)/8+9.001)
1320 IF R9>82800 THEN 1340
1330 R9=82800

```

```

1340 IF R9<=333000 THEN 1360
1350 R9=332000
1360 IF R9<166000 THEN 1390
1370 Z2=1
1375 Z9=83200
1376 Z7=82800
1380 GO TO 1400
1390 Z2=3
1395 Z9=167000
1396 Z7=166000
1400 GOSUB 1730
1410 A0=A0*&PI/180.0
1420 T0=C0/(C0/A0+C7)
1430 A=A0-T0
1435 A1=A0
1436 A0=A*180.0/&PI
1438 Z1=INT(INT(10.0*A0+0.001)/8+9.001)
1440 GOSUB 1730
1450 Z2=Z2+1
1455 C1=C0
1460 GOSUB 1730
1465 A0=A1
1470 C2=C0
1480 S=S0+T0
1490 H=C1*COS(S)-C2*SIN(S)
1500 I=C1*SIN(S)+C2*COS(S)
1510 RETURN
1520 REM OPTIMIZED BLADE
1525 N1=0.0
1530 FOR X5=X9 TO 12.0 STEP 0.2
1540 A0=X5*&PI/180.0
1550 GOSUB 1290
1560 N=H/(I*R)
1570 IF N<=N1 THEN 1650
1580 N1=N
1590 A5=A0
1600 B1=S0+A0
1610 H1=H
1620 I1=I
1630 T1=T0
1640 A1=S0+T0
1650 NEXT X5
1660 N=N1
1670 A0=A5
1680 P=H1
1690 I=I1
1700 T0=T1
1710 A=A1
1720 RETURN
1730 REM TABLE INTERPOLATION
1740 IF Z1=33 THEN 1820

```

```
1750 Z8=((Z1-9)*8)/10.0
1755 Z8=A0-Z8
1760 Z3=(F(Z2,Z1+1)-F(Z2,Z1))/0.8
1770 Z4=Z3*Z8+F(Z2,Z1)
1780 Z3=(F(Z2+2,Z1+1)-F(Z2+2,Z1))/0.8
1790 Z5=Z3*Z8+F(Z2+2,Z1)
1800 C0=(R9-Z7)*(Z5-Z4)/Z9+Z4
1810 GO TO 1850
1820 Z4=F(Z2,Z1)
1830 Z5=F(Z2+2,Z1)
1840 C0=(R9-Z7)*(Z5-Z4)/Z9+Z4
1850 RETURN
1860 END
```

BLADE GEOMETRY FOR 4 BLADES  
 SOLIDITY OF .6 AT ROOT, .6 AT TIP  
 VELOCITY= 121.619 PITCH= 1.263136  
~~At~~ Radius (ft). Blade chord (ft). Blade Angle (Degrees)

.25	.2356194	42.20404
.26	.2450442	41.1115
.27	.2544689	40.07031
.28	.2638936	39.07756
.29	.2733183	38.13052
.3	.2827432	37.22659
.31	.2921679	36.3633
.32	.3015926	35.53836
.33	.3110175	34.74956
.34	.3204422	33.99486
.35	.3298669	33.27235
.36	.3392918	32.58023
.37	.3487165	31.91682
.38	.3581412	31.28052
.39	.3675661	30.66985
"	.3769908	30.08344

---

## Propulsor Performance

Propulsive efficiency at 5000 ft  
cruise

$$hp_{out} = C_T \left( \frac{1}{2} \rho V_\infty^2 A_R \right) \frac{1}{550 \frac{ft-lb}{hp-s}}$$

$$hp_o = C_T (282,811) \frac{1}{550} \rightarrow$$

$$C_T = \frac{2T}{\rho V^2 A} = \frac{2(1516_f)}{(0.002048 \frac{lb-ft}{s^3}) (110 \frac{ft}{s})^2 (0.2975 ft^2)}$$

$$C_T = 4.0693$$

$$hp_o = 2.092$$

Looking up  $C_T = 4.029$  in the  
propulsor performance table,  
we have

$$C_a = 1.0883 \quad p_v = 0.8474 \quad C_p = 1.2843$$
$$C_{TR} = 2.138$$

$$\text{at } 110 \frac{ft}{s} \quad C_p = (0.2771)(hp)$$

$$hp = 4.635 \quad hp_o = 2.092$$

$$\eta = \frac{hp_o}{hp} = 0.4513 \quad SFC = 0.7$$

### 4.2.3.3 BLC Estimations

Take boundary layer at 80" from the nose (placement of BLC slots)

$$80" = 6.67'$$

Multiplying by 1.2 to correct for curvature, length is 8'

$$\delta = \frac{0.37x}{Re_x^{0.2}} \text{ from Kuethe and Schetzler, } \underline{\text{Foundations of Aerodynamics}}, \text{ John Wiley \& Sons, Inc., New York, 1959}$$

at a flow velocity of  $110 \frac{ft}{s}$

$$Re_x = \frac{Vx}{\nu} \quad \nu = 0.0001567 \frac{ft^2}{s} @ 5000 ft$$

$$Re_x = \frac{(110 \frac{ft}{s})(8 ft)}{(0.0001567 \frac{ft^2}{s})} = 5.6158 \times 10^6$$

boundary layer thickness -  $\delta$

$$\delta = \frac{0.37(8 ft)}{(5.6158 \times 10^6)^{0.2}} = 0.1322 ft = 1.59 \text{ in.}$$

Displacement thickness

$$\delta^* = 0.27 \delta = 0.43 \text{ in.}$$

Area of air to be removed. Fuselage diameter at the slots is 5". Area of air to be removed would be:

$$A = \pi (2.93^2 - 2.5^2) = 7.33 \text{ in}^2$$

If this is removed at flight velocity, an overestimation results since the displacement thickness is equivalent to the thickness of stagnated air. Therefore, at  $110 \frac{\text{ft}}{\text{s}}$ , the required area for cooling and BLC air is

$$A = \frac{(1.1204 \frac{\text{lbm}}{\text{s}}) (144 \frac{\text{in}^2}{\text{ft}^2})}{(0.076572 \frac{\text{lbm}}{\text{ft}^3}) (110 \frac{\text{ft}}{\text{s}})} + 7.33 \text{ in}^2$$

$$A = 26.48 \text{ in}^2$$

To provide adequate suction of about  $\Delta p$  psia, the area would change by

$$\frac{A}{A_1} = \frac{P}{P_1} = \frac{13.7}{14.7} = 0.932$$

So that the actual area required through the fan is

$$A = 0.932 (26.48 \text{ in}^2) = 24.68 \text{ in}^2$$

McCormick states that the slots should be no wider than the

displacement thickness for stability of the remaining boundary layer.  
 Two rows of 0.2" wide slots provide the correct intake area and slot width.

4.2.3.4

$$f_{\max} = 1.3 \frac{V}{x} \quad x = 0.11 \frac{S}{b}$$

$$S = 25.95 \text{ ft} = 2.411 \text{ meters}$$

$$b = 15 \text{ feet} = 4.572 \text{ meters}$$

$$x = 0.058$$

$$\overline{f_{\max}} = V = 110 \frac{\text{ft}}{\text{s}} = 33.528 \frac{\text{meter}}{\text{s}}$$

$$f_{\max} = 1.3 \left( \frac{33.528}{0.058} \right) = 779.86 \text{ Hz}$$

$$OASPL = 10 \log \left[ \left( \frac{\sin \theta}{r} \right)^2 \left( \frac{V^6 S}{AR^4} \right) \right] + 23.0$$

$$AR = 8 \quad \overline{S} = 25 \quad S = 2.411 \text{ meters}$$

$$V = 33.528 \frac{\text{meter}}{\text{s}} \quad r = 1000 \text{ ft} = 304.8 \text{ meters}$$

$$OASPL = 9.38 + 23.0 = 32.38 \text{ dB re } 2 \times 10^{-5} \frac{\text{N}}{\text{m}^2}$$

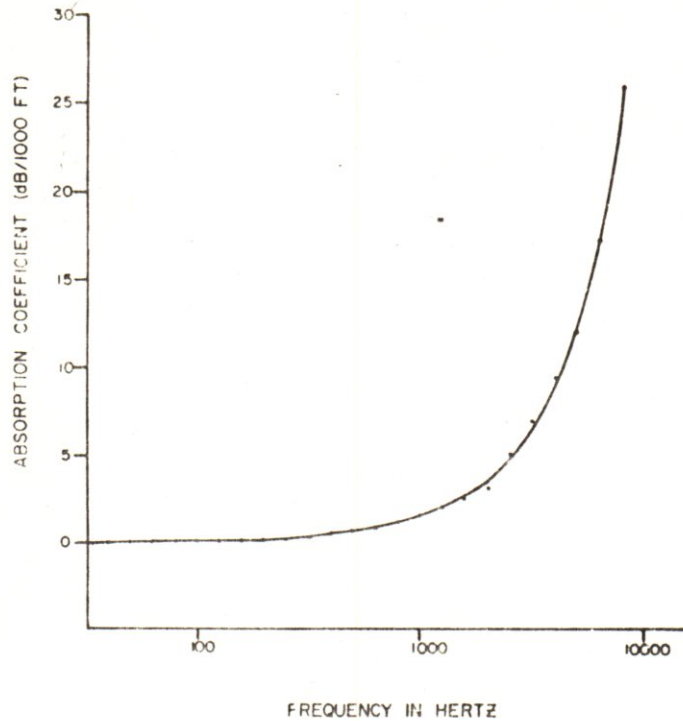
$$L_p = L_w - 20 \log R - 0.5$$

$$L_w = 32.38 + 20 \log (1000 \text{ ft}) + 0.5$$

$$L_w = 92.88 \text{ dB re } 2 \times 10^{-5} \frac{\text{W}}{\text{m}^2}$$



# 4.2.3.5 Detectability



ATMOSPHERIC ABSORPTION COEFFICIENT

$$\Delta L = 20 \log R + K (R/1000)$$

at 5000 ft

Hz	SPL (Watts x 10 <sup>-5</sup> )	SPL Ground	dB A Corr	Corr. SPL
100	76	1.32	<del>24</del> <del>-22.68</del>	-22.68
125	80	5.22	16 <del>-10.78</del>	-10.78
250	88	12.12	-9 <del>3.12</del>	3.12
500	93	15.52	-3	12.52
1000	94	13.02	0	13.02
2000	87	-1.98	+1	-0.98
4000	82	-33.08	+1	-32.08
8000	76	-92.9	-1	-93.9
16000	75	-93.9	-1	-94.9

Decibel Addition

AdB	Corr for higher level
0-1	3
2-3	2
4-8	1
9-∞	0

final total dBA is SPL = 16 dBA

For the detectability distances the distance R was varied until 50% detectability was reached for selected bands.

Hz	Country		Arid		Near Urban	
	ΔL	R	ΔL	R	ΔL	R
100	36	61 ft	29	29 ft	17	—
123	41	112	37	75	22	—
250	66	2000	52	400	42	130 ft
500	72	3100	64	1400	51	340
1000	76	3900	73	2900	57	650
2000	69	1750	70	1800	57	590
4000	68	—	70	—	60	600
8000	61	—	61	—	61	—
16000	57	—	57	—	57	—

### 4.3.3 Aux. Power Supply estimated

Total requirement of 350 Watts  
for systems in emergency. At  
28 V standard system 6.25  $\frac{\text{Amp}}{\text{hr}}$   
required

$$I = \frac{P}{V} = \frac{(0.5) \frac{350 \text{ W}}{\text{hr}}}{28 \text{ V}} = 6.25 \text{ Amp}$$

allowing a 50% demand average  
for the system.

Energy required for APS

$$(350 \text{ Watt})(30)(60) = 6.3 \times 10^5 \text{ joules}$$

Systems

- ~~1:~~  
2: 23 batt. 14 + 46 batt. 12  
28.75 V + 7.0  $\frac{\text{A}}{\text{hr}}$  at 14.4 lb
- 2: 35 batt. 1 \*  
30 V + 6.3  $\frac{\text{A}}{\text{hr}}$  at 21 lb
- 3: 5 batt. 8  
30 V + 7.5  $\frac{\text{A}}{\text{hr}}$  at 16.5 lb
- 4: 10 batt. 2 + 3 batt. 3  
30 V + 7.5  $\frac{\text{A}}{\text{hr}}$  at 22.9 lb
- 5: 5 batt. 7  
30 V + 6.0  $\frac{\text{A}}{\text{hr}}$  at 13 lb
- ~~6:~~ At 3 x peak rating to  
account for control peaks
- 6: 15 batt. 1  
30 V + 8.1  $\frac{\text{A}}{\text{hr}}$  at 9 lb
- 7: 4 batt. 2 + 1 batt. 3  
30 V + 9  $\frac{\text{A}}{\text{hr}}$  at 8.9 lb.

## 4.4.2 CER cost estimation

Engineering hours - E

$$E = \exp(8.093 + 0.656 \ln S + 0.1 \ln CQ)$$

CQ  $\equiv$  cumulative production

S  $\equiv$  top speed

$$S = 125 \frac{\text{mi}}{\text{hr}} \quad CQ = 1040$$

$$E = \exp(8.093 + 0.656 \ln(125) + 0.1 \ln(1040))$$

$$E = 155,604.3 \text{ hrs}$$

Tooling hours - T

Wt = empty weight

Q = produced quantity

$$Wt = 142 \text{ lb} \quad Q = 1040$$

$$T = \exp(6.08 + 0.764 \ln Wt + 0.092 \ln Q)$$

$$T = \exp(6.08 + 0.764 \ln(142) + 0.092 \ln(1040))$$

$$T = 36511.2 \text{ hrs.}$$

Manufacturing Labor - TL

$$TL = 1000 \exp(0.565 \ln Wt + 0.506 \ln Q)$$

$$TL = 1000 \exp(0.565 \ln(142) + 0.506 \ln(1040)) = 552919 \text{ hrs.}$$

Material

MC  $\equiv$  materials cost in 1973 dollars

$$MC = 1000 \exp(0.622 \ln(\text{WT}) + 0.803 \ln Q)$$

$$MC = 1000 \exp(0.622 \ln(142) + 0.803 \ln(1040))$$

$$MC = \$5772994$$

Development Support - DS (\$) )

$$DS = 1000 \exp(0.2255 \ln(1040) + 1.0987 \ln(142) + 1.0848 \ln(0.7))$$

$$DS = \$300497.8$$

Flight test - FT (\$) )

$$FT = \exp(-2.577) + 0.781 \ln(FQ) + 0.867 \ln WT + 1.5 \ln S)$$

FQ  $\equiv$  # of flight test vehicles

$$FT = \exp(-2.577) + 0.781 \ln(32) + 0.867 \ln(142) + 1.5 \ln(125))$$

$$FT = \$116881$$

Fabor rates (1973 dollars)

Engineering \$18.29  $\frac{1}{hr}$

Zooling \$14.23  $\frac{1}{hr}$

Man. Labor \$12.16  $\frac{1}{hr}$

# A.5.1 NASTRAN DATA CARD FORMAT

Input Data Card CBAR

Simple Beam Element Connection

Description: Defines a simple beam element (BAR) of the structural model.

Format and Example:

1	2	3	4	5	6	7	8	9	10
CBAR	EID	PID	GA	GB	X1,G0	X2	X3	F	abc
CBAR	2	39	7	3	13			2	123
+bc	PA	PB	Z1A	Z2A	Z3A	Z1B	Z2B	Z3B	
+23	.	513							

Field

Contents

- EID Unique element identification number (Integer > 0)
- PID Identification number of a PBAR property card (Default is EID unless BARØR card has nonzero entry in field 3) (Integer > 0 or blank\*)
- GA,GB Grid point identification numbers of connection points (Integer > 0; GA ≠ GB)
- X1,X2,X3 Components of vector  $\vec{v}$ , at end A, (figure 1(a) on page 1.3-15) measured at end A, parallel to the components of the displacement coordinate system for GA, to determine (with the vector from end A to end B) the orientation of the element coordinate system for the bar element (Real,  $X1^2 + X2^2 + X3^2 > 0$  or blank\*, see below).
- G0 Grid point identification number to optionally supply X1, X2, X3 (integer > 0 or blank\*) (see below)
- F Flag to specify the nature of fields 6-8 as follows:

	6	7	8
F = blank*			
F = 1	X1	X2	X3
F = 2	G0	blank/0	blank/0

- PA,PB Pin flags for bar ends A and B, respectively, that are used to insure that the bar cannot resist a force or moment corresponding to the pin flag at that respective end of the bar. (Up to 5 of the unique digits 1-6 anywhere in the field with no imbedded blanks; integer > 0) (These degree of freedom codes refer to the element forces and not global forces. The bar must have stiffness associated with the pin flag. For example, if pin flag 4 is specified, the bar must have a value for J, the torsional constant.)
- Z1A,Z2A,Z3A Components of offset vectors  $\vec{w}_a$  and  $\vec{w}_b$ , respectively, (see figure 1(a), page 1.3-15) in displacement coordinate systems at points GA and GB, respectively. (Real or blank)
- Z1B,Z2B,Z3B

\*See the BARØR card for default options for fields 3, 6, 7, 8 and 9.

Input Data Card C0NM2

Concentrated Mass Element Connection

Description: Defines a concentrated mass at a grid point of the structural model.

Format and Example:

1	2	3	4	5	6	7	8	9	10
C0NM2	EID	G	CID	M	X1	X2	X3	<del>abc</del>	abc
C0NM2	?	15	6	49.7					123
+bc	111	121	122	131	132	153			
+23	16.2		16.2			7.8			

Field

Contents

EID	Element identification number (Integer > 0)
G	Grid point identification number (Integer > 0)
CID	Coordinate system identification number (Integer ≥ 0)
M	Mass Value (Real)
X1,X2,X3	Offset distances for the mass in the coordinate system defined in field 4 (Real)
ijj	Mass moments of inertia measured at the mass c.g. in coordinate system defined by field 4 (Real)

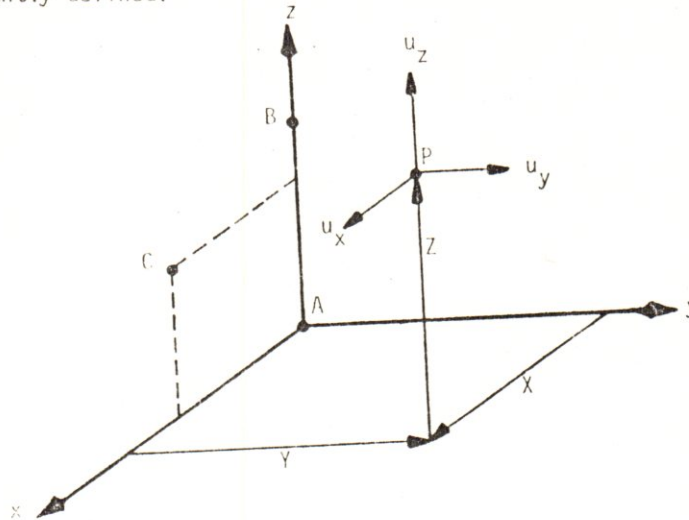
- Remarks:
1. Element identification numbers must be unique with respect to all other element identification numbers.
  2. For a more general means of defining concentrated mass at grid points, see C0M11.
  3. The continuation card may be omitted.



Input Data Card CØRD2R

Rectangular Coordinate System Definition

Description: Defines a rectangular coordinate system by reference to the coordinates of three points. The first point defines the origin. The second point defines the direction of the z-axis. The third point defines a vector which, with the z-axis, defines the x-z plane. The reference coordinate must be independently defined.



Format and Example:

1	2	3	4	5	6	7	8	9	10
CØRD2R	CID	RID	A1	A2	A3	B1	B2	B3	ABC
CØRD2R	3	17	-2.9	1.0	0.0	3.6	0.0	1.0	123
+BC	C1	C2	C3						
+23	5.2	1.0	-2.9						

Field

Contents

- CID Coordinate system identification number (Integer > 0)
- RID Reference to a coordinate system which is defined independently of new coordinate system (Integer ≥ 0 or blank)
- A1,A2,A3  
B1,B2,B3  
C1,C2,C3 Coordinates of three points in coordinate system defined in field 3 (Real)

Remarks:

1. Continuation card must be present.
2. The three points (A1, A2, A3), (B1, B2, B3), (C1, C2, C3) must be unique and non-collinear. Noncollinearity is checked by the geometry processor.
3. Coordinate system identification numbers on all CØRD1R, CØRD1C, CØRD1S, CØRD2R, CØRD2C, and CØRD2S cards must all be unique.
4. An RID of zero references the basic coordinate system.
5. The location of a grid point (P in the sketch) in this coordinate system is given by (X, Y, Z).
6. The displacement coordinate directions at P are shown by (u<sub>x</sub>, u<sub>y</sub>, u<sub>z</sub>).

Input Data Card CQDMEM2

Quadrilateral Element Connection

Description: Defines a quadrilateral membrane element (QDMEM2) of the structural model consisting of four nonoverlapping TRMEM elements.

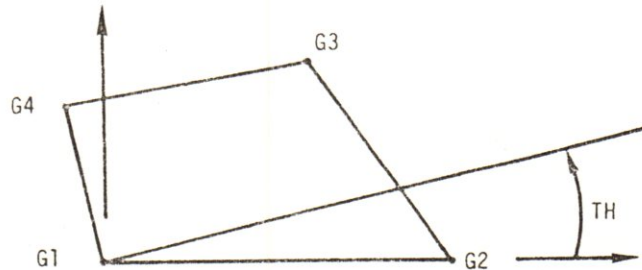
Format and Example:

1	2	3	4	5	6	7	8	9	10
CQDMEM2	EID	PID	G1	G2	G3	G4	.TH		
CQDMEM2	72	13	13	14	15	16	29.2		

Field

Contents

EID Element identification number (Integer > 0)  
 PID Identification number of a PQDMEM2 property card (Default is EID) (Integer > 0)  
 G1,G2,G3,G4 Grid point identification numbers of connection points (Integer > 0;  
 G1 ≠ G2 ≠ G3 ≠ G4)  
 TH Material property orientation angle in degrees (Real)  
 The sketch below gives the sign convention for TH



- Remarks:
1. Element identification numbers must be unique with respect to all other element identification numbers.
  2. Grid points G1 through G4 must be ordered consecutively around the perimeter of the element.
  3. All interior angles must be less than 180 degrees.

Input Data Card CQUAD2

Quadrilateral Element Connection

Description: Defines a homogeneous quadrilateral membrane and bending element (QUAD2) of the structural model.

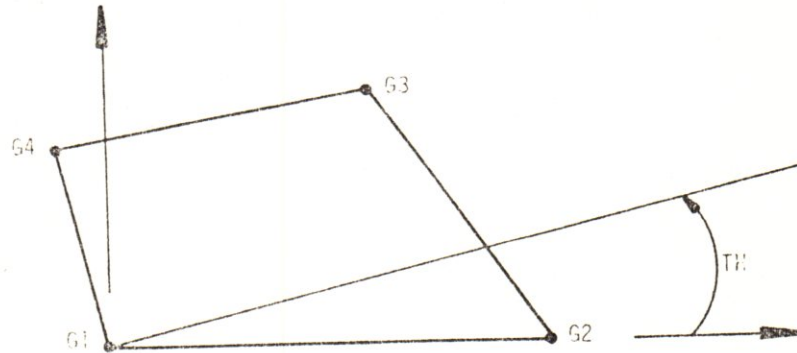
Format and Example:

1	2	3	4	5	6	7	8	9	10
CQUAD2	EID	PID	G1	G2	G3	G4	TH		
CQUAD2	72	13	13	14	15	16	29.2		

Field

Contents

EID Element identification number (Integer > 0)  
PID Identification number of a PQUAD2 property card (Default is EID) (Integer > 0)  
G1,G2,G3,G4 Grid point identification numbers of connection points (Integer > 0;  
G1 ≠ G2 ≠ G3 ≠ G4)  
TH Material property orientation angle in degrees (Real)  
The sketch below gives the sign convention for TH.



- Remarks:
1. Element identification numbers must be unique with respect to all other element identification numbers.
  2. Grid points G1 thru G4 must be ordered consecutively around the perimeter of the element.
  3. All interior angles must be less than 180°.

Input Data Card CTRIA2 Triangular Element Connection

Description: Defines a triangular membrane and bending element (TRIA2) of the structural model.

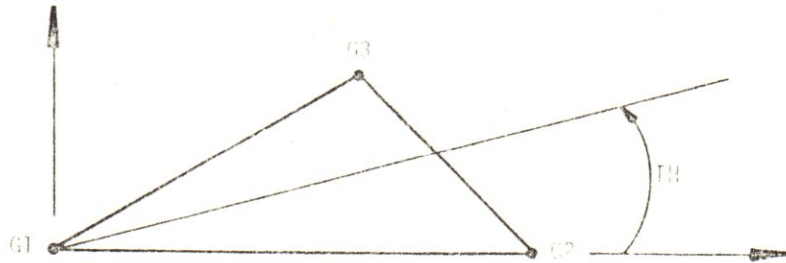
Format and Example:

1	2	3	4	5	6	7	8	9	10
CTRIA2	EID	PID	G1	G2	G3	TH			
CTRIA2	16	2	12	1	3	16.2			

Field

Contents

- EID Element identification number (Integer > 0)
- PID Identification number of a PTRIA2 property card (Default is EID) (Integer > 0)
- G1,G2,G3 Grid point identification numbers of connection points (Integer > 0; G1 ≠ G2 ≠ G3)
- TH Material property orientation angle in degrees (Real) - The sketch below gives the sign convention for TH.



- Remarks:
1. Element identification numbers must be unique with respect to all other element identification numbers.
  2. Interior angles must be less than 180°.

Input Data Card CTRMEM Triangular Element Connection

Description: Defines a triangular membrane element (TRMEM) of the structural model.

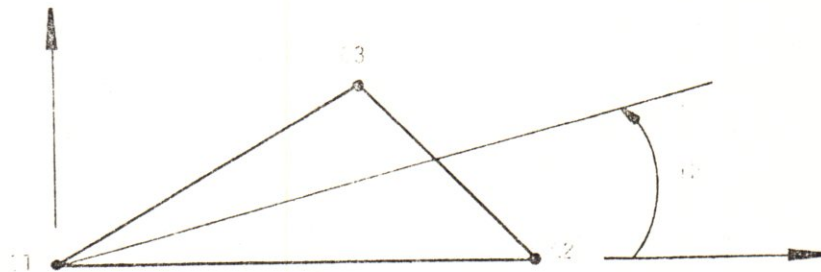
Format and Example:

1	2	3	4	5	6	7	8	9	10
CTRMEM	EID	PID	G1	G2	G3	TH			
CTRMEM	16	2	12	1	3	16.3			

Field

Contents

- EID Element identification number (Integer > 0)
- PID Identification number of a PTRMEM property card (Default is EID) (Integer > 0)
- G1,G2,G3 Grid point identification numbers of connection points (Integer > 0; G1 ≠ G2 ≠ G3)
- TH Material property orientation angle in degrees (Real) - The sketch below gives the sign convention for TH.



- Remarks:
1. Element identification numbers must be unique with respect to all other element identification numbers.
  2. Interior angles must be less than 180°.

Input Data Card FØRCE                      Static Load

Description: Defines a static load at a grid point by specifying a vector.

Format and Example:

1	2	3	4	5	6	7	8	9	10
FØRCE	SID	G	CID	F	N1	N2	N3		
FØRCE	2	5	6	2.9	0.0	1.0	0.0		

Field

Contents

SID	Load set identification number (Integer > 0)
G	Grid point identification number (Integer > 0)
CID	Coordinate system identification number (Integer ≥ 0)
F	Scale factor (Real)
N1,N2,N3	Components of Vector measured in coordinate system defined by CID (Real; N1 <sup>2</sup> + N2 <sup>2</sup> + N3 <sup>2</sup> > 0.0)

Remarks: 1. The static load applied to grid point G is given by

$$\vec{f} = F \vec{N}$$

where  $\vec{N}$  is the vector defined in fields 6, 7 and 8.

2. Load sets must be selected in the Case Control Deck (LOAD=SID) to be used by NASTRAN.
3. A CID of zero references the basic coordinate system.

Input Data Card GRID            Grid Point

Description: Defines the location of a geometric grid point of the structural model, the directions of its displacement, and its permanent single-point constraints.

Format and Example:

1	2	3	4	5	6	7	8	9	10
GRID	ID	CP	X1	X2	X3	CD	PS		
GRID	2	3	1.0	2.0	3.0		316		

<u>Field</u>	<u>Contents</u>
ID	Grid point identification number (Integer > 0)
CP	Identification number of coordinate system in which the location of the grid point is defined (Integer ≥ 0 or blank*).
X1,X2,X3	Location of the grid point in coordinate system CP (Real)
CD	Identification number of coordinate-system in which displacements, degrees of freedom, constraints, and solution vectors are defined at the grid point (Integer ≥ 0 or blank*).
PS	Permanent single-point constraints associated with grid point (any of the digits 1-6 with no imbedded blanks) (Integer ≥ 0 or blank*)

- Remarks:
1. All grid point identification numbers must be unique with respect to all other structural, scalar, and fluid points.
  2. The meaning of X1, X2 and X3 depend on the type of coordinate system, CP, as follows: (see CORD\_\_ card descriptions)

Type	X1	X2	X3
Rectangular	X	Y	Z
Cylindrical	R	θ(degrees)	Z
Spherical	R	θ(degrees)	φ(degrees)

3. The collection of all CD coordinate systems defined on all GRID cards is called the Global Coordinate System. All degrees-of-freedom, constraints, and solution vectors are expressed in the Global Coordinate System.

\* See the GRDSET card for default options for fields 3, 7 and 8.

Input Data Card LØAD

Static Load Combination (Superposition)

Description: Defines a static load as a linear combination of load sets defined via FØRCE, MØMENT, FØRCE1, MØMENT1, FØRCE2, MØMENT2, PLØAD, PLØAD2, SLØAD, RFØRCE and GRAV cards.

Format and Example:

1	2	3	4	5	6	7	8	9	10
LØAD	SID	S	S1	L1	S2	L2	S3	L3	abc
LØAD	101	-0.5	1.0	3	6.2	4			
+bc	S4	L4		-etc.-					

(etc.)

Field

Contents

- SID Load set identification number (Integer > 0)
- S Scale factor (Real)
- Si Scale factors (Real)
- Li Load set identification numbers defined via card types enumerated above (Integer > 0)

Remarks: 1. The load vector defined is given by

$$\{P\} = S \sum_i \{P_{Li}\}$$

- 2. The Li must be unique. The remainder of the physical card containing the last entry must be blank.
- 3. This card must be used if gravity loads (GRAV) are to be used with any of the other types.
- 4. Load sets must be selected in the Case Control Deck (LØAD=SID) to be used by NASTRAN.
- 5. A LØAD card may not reference a set identification number defined by another LØAD card.



Input Data Card MAT1

## Material Property Definition

Description: Defines the material properties for linear, temperature-independent, isotropic materials.

Format and Example:

1	2	3	4	5	6	7	8	9	10
MAT1	MID	E	G	NU	RHØ	A	TREF	GE	+abc
MAT1	17	3.+7	1.9+7		4.28	0.19	5.37+2	0.23	ABC
+abc	ST	SC	SS						
+BC	20.+4	15.+4	12.+4						

FieldContents

MID	Material identification number (Integer > 0)
E	Young's modulus (Real $\geq$ 0.0 or blank)
G	Shear modulus (Real $\geq$ 0.0 or blank)
NU	Poisson's ratio (-1.0 < Real $\leq$ 0.5 or blank)
RHØ	Mass density (Real)
A	Thermal expansion coefficient (Real)
TREF	Thermal expansion reference temperature (Real)
GE	Structural element damping coefficient (Real)
ST, SC, SS	Stress limits for tension, compression and shear (Real) (Used only to compute margins of safety in certain elements; they have no effect on the computational procedures)

- Remarks:
- One of E or G must be positive (i.e., either  $E > 0.0$  or  $G > 0.0$  or both E and G may be  $> 0.0$ ).
  - If any one of E, G or NU is blank, it will be computed to satisfy the identity  $E = 2(1+NU)G$ ; otherwise, values supplied by the user will be used.
  - The material identification number must be unique for all MAT1, MAT2 and MAT3 cards.
  - MAT1 materials may be made temperature dependent by use of the MATT1 card.
  - The mass density, RHØ, will be used to automatically compute mass for all structural elements except the two-dimensional bending only elements TRBSC, TRPLT and QDPLT.
  - If E and NU or G and NU are both blank they will be both given the value 0.0.
  - Weight density may be used in field 6 if the value  $\frac{1}{g}$  is entered on the PARAM card WTMAS, where g is the acceleration of gravity (see Section 3.1.5).

Input Data Card MPC Multipoint Constraint

Description: Defines a multipoint constraint equation of the form

$$\sum_j A_j u_j = 0$$

Format and Example:

1	2	3	4	5	6	7	8	9	10
MPC	SID	G	C	A	G	C	A	<del> </del>	abc
MPC	3	28	3	6.2	2		4.29		+B
+bc	<del> </del>	G	C	A	-etc.-			<del> </del>	
+B		1	4	-2.91					

Field

Contents

- SID Set identification number (Integer > 0)
- G Identification number of grid or scalar point (Integer > 0)
- C Component number - any one of the digits 1-6 in the case of geometric grid points; blank or zero in the case of scalar points (Integer)
- A Coefficient (Real; the first A must be nonzero)

- Remarks:
1. The first coordinate in the sequence is assumed to be the dependent coordinate and must be unique for all equations of the set.
  2. Forces of multipoint constraint are not recovered.
  3. Multipoint constraint sets must be selected in the Case Control Deck (MPC=SID) to be used by NASTRAN.
  4. Dependent coordinates on MPC cards may not appear on OMIT, OMIT1, SUPORT, SPC or SPC1 cards.

Input Data Card PBAR

Simple Beam Property

Description: Defines the properties of a simple beam (bar) which is used to create bar elements via the CBAR card.

Format and Example:

1	2	3	4	5	6	7	8	9	10
PBAR	PID	MID	A	I1	I2	J	NSM	<del> </del>	abc
PBAR	39	6	2.9		5.97				123
+bc	C1	C2	D1	D2	E1	E2	F1	F2	def
+23			2.0	4.0					
+ef	K1	K2	I12						

<u>Field</u>	<u>Contents</u>
PID	Property identification number (Integer > 0)
MID	Material identification number (Integer > 0)
A	Area of bar cross-section (Real)
I1, I2, I12	Area moments of inertia (Real)
J	Torsional constant (Real)
NSM	Nonstructural mass per unit length (Real)
K1, K2	Area factor for shear (Real)
Ci, Di, Ei, Fi	Stress recovery coefficients (Real)

- Remarks:
1. For structural problems, PBAR cards may only reference MAT1 material cards.
  2. See Section 1.3.2 for a discussion of bar element geometry.
  3. For heat transfer problems, PBAR cards may only reference MAT4 or MAT5 material cards.

Input Data Card PLØAD2

Pressure Load

Description: Defines a uniform static pressure load applied to two-dimensional elements. Only QUAD1, QUAD2, QDMEM, QDMEM1, QDMEM2, QDPLT, SHEAR, TRBSC, TRIA1, TRIA2, TRMEM, TRPLT or TWIST elements may have a pressure load applied to them via this card.

Format and Example:

1	2	3	4	5	6	7	8	9	10
PLØAD2	SID	P	EID	EID	EID	EID	EID	EID	
PLØAD2	21	-3.6		4	16		2		

Alternate Form

PLØAD2	SID	P	EID1	"THRU"	EID2				
PLØAD2	1	30.4	16	THRU	48				

Field

Contents

SID            Load set identification number (Integer > 0)  
P                Pressure value (Real)  
EID }  
EID1 }            Element identification number (Integer > 0; EID1 < EID2)  
EID2 }

- Remarks:
1. EID must be 0 or blank for omitted entrys.
  2. Load sets must be selected in the Case Control Deck (LØAD=SID) to be used by NASTRAN.
  3. At least one positive EID must be present on each PLØAD2 card.
  4. If the alternate form is used, all elements EID1 thru EID2 must be two-dimensional.
  5. The pressure load is computed for each element as if the grid points to which the element is connected were specified on a PLØAD card. The grid point sequence specified on the element connection card is assumed for the purpose of computing pressure loads.
  6. All elements referenced must exist.

Input Data Card PQDMEM2

Quadrilateral Membrane Property

Description: Used to define the properties of a quadrilateral membrane. Referenced by the CQDMEM2 card. No bending properties are included.

Format and Example:

1	2	3	4	5	6	7	8	9	10
PQDMEM2	PID	MID	T	NSM	PID	MID	T	NSM	
PQDMEM2	235	2	0.5	0.0					

Field

Contents

PID Property identification number (Integer > 0)  
MID Material identification number (Integer > 0)  
T Thickness of membrane (Real > 0.0)  
NSM Nonstructural mass per unit area (Real)

- Remarks:
1. All PQDMEM2 cards must have unique property identification numbers.
  2. One or two quadrilateral membrane properties may be defined on a single card.

Input Data Card PQUAD2

Homogeneous Quadrilateral Property

Description : Defines the properties of a homogeneous quadrilateral element of the structural model, including bending, membrane and transverse shear effects. Referenced by the CQUAD2 card.

Format and Example:

1	2	3	4	5	6	7	8	9	10
PQUAD2	PID	MID	T	NSM	PID	MID	T	NSM	
PQUAD2	32	16	2.98	9.0	45	16	5.29	6.32	

Field

Contents

PID            Property identification number (Integer > 0)  
MID            Material identification number (Integer > 0)  
T              Thickness (Real > 0.0)  
NSM            Nonstructural mass per unit area (Real)

- Remarks:
1. All PQUAD2 cards must have unique identification numbers.
  2. The thickness used to compute membrane and transverse shear properties is T.
  3. The area moment of inertia per unit width used to compute the bending stiffness is  $T^3/12$ .
  4. Outer fiber distances of  $\pm T/2$  are assumed.
  5. One or two homogeneous quadrilateral properties may be defined on a single card.

Input Data Card PTRIA2

Homogeneous Triangular Element Property

Description: Defines the properties of a homogeneous triangular element of the structural model, including membrane, bending and transverse shear effects. Referenced by the CTRIA2 card.

Format and Example:

1	2	3	4	5	6	7	8	9	10
PTRIA2	PID	MID	T	NSM	PID	MID	T	NSM	
PTRIA2	2	16	3.92	14.7	6	16	2.96		

Field

Contents

PID            Property identification number (Integer > 0)  
MID            Material identification number (Integer > 0)  
T              Thickness (Real > 0.0)  
NSM            Nonstructural mass per unit area (Real)

- Remarks:
1. All PTRIA2 cards must have unique identification numbers.
  2. The thickness used to compute the membrane and transverse shear properties is T.
  3. The area moment of inertia per unit width used to compute the bending stiffness is  $T^3/12$ .
  4. Outer fiber distances of  $\pm T/2$  are assumed.
  5. One or two homogeneous triangular element properties may be defined on a single card.

Input Data Card PTRMEM Triangular Membrane Property

Description: Used to define the properties of a triangular membrane element. Referenced by the CTRMEM card. No bending properties are included.

Format and Example:

1	2	3	4	5	6	7	8	9	10
PTRMEM	PID	MID	T	NSM	PID	MID	T	NSM	
PTRMEM	17	23	4.25	0.2					

<u>Field</u>	<u>Contents</u>
PID	Property identification number (Integer > 0)
MID	Material identification number (Integer > 0)
T	Membrane thickness (Real > 0.0)
NSM	Nonstructural mass per unit area (Real)

- Remarks:
1. All PTRMEM cards must have unique property identification numbers.
  2. One or two triangular membrane properties may be defined on a single card.



Input Data Card SPC1

Single-Point Constraint

Description: Defines sets of single-point constraints.

Format and Example:

1	2	3	4	5	6	7	8	9	10
SPC1	SID	C	G1	G2	G3	G4	G5	G6	abc
SPC1	3	2	1	3	10	9	6	5	ABC
+bc	G7	G8	G9	-etc.-					
+BC	2	8							

Alternate Form

SPC1	SID	C	GID1	"THRU"	GID2				
SPC1	313	12456	6	THRU	32				

Field

Contents

- SID Identification number of single-point constraint set (Integer > 0)
- C Component number (Any unique combination of the digits 1-6 (with no imbedded blanks) when point identification numbers are grid points; must be null if point identification numbers are scalar points)
- Gi, GIDi Grid or scalar point identification numbers (Integer > 0)

- Remarks:
- Note that enforced displacements are not available via this card. As many continuation cards as desired may appear when "THRU" is not used.
  - A coordinate referenced on this card may not appear as a dependent coordinate in a multipoint constraint relation, nor may it be referenced on a SPC, OMIT, OMIT1, SUPORT card.
  - Single-point constraint sets must be selected in the Case Control Deck (SPC=SID) to be used by NASTRAN.
  - SPC degrees of freedom may be redundantly specified as permanent constraints on the GRID card.
  - All grid points referenced by GID1 thru GID2 must exist.

# A.5.2 FUSELAGE PROGRAM LISTING

```

1      $JCB          ,NOEXT,T=28
2      DIMENSION XRIBS(8)
3      DATA XRIBS/8.25,17.63,27.00,36.40,45.80,58.20,65.40,72.00/
4      DATA NRIBS/8/,NSTGR/6/,NGRID/2/,IDBAR/1200/,IDMEM/200/,MBAR1/110/,
5      1MBAR2/10/,MMEM/320/,DTHETA/.5236C/,C/100.0/
6      WRITE(6,6600)
7      CALL GRID(NGRID-1,0.,0.,0.)
8      CALL GRID(NGRID,-1.75,0.,0.)
9      NSTGR1=NSTGR+1
10     DO 2000 I=1,NRIBS
11     CALL COCRDF(C,XRIBS(I),T)
12     CALL GRID(NGRID+2,XRIBS(I),0.,0.)
13     NGRID=NGRID+2
14     DO 1000 J=1,NSTGR1
15     NGRID=NGRID+2;N1=NGRID-2*NSTGR1-2
16     THETA=(J-1)*DTHETA
17     Z=-T*COS(THETA);Y=T*SIN(THETA)
18     Y1=-10.*COS(THETA);Z1=-10.*SIN(THETA)
19     IF(I.NE.4.OR.J.GT.2) GO TO 20
20     Z=-5.30;Y=-Z*TAN(THETA)
21     Y1=-10.0;Z1=0.C
22     GO TO 100
23     20 IF(I.NE.5.CR.J.GT.2) GO TO 40
24     Z=-5.40;Y=-Z*TAN(THETA)
25     Y1=-10.0;Z1=0.C
26     GO TO 100
27     40 IF(I.NE.6.OR.J.GT.2) GO TO 100
28     Z=-5.90;Y=-Z*TAN(THETA)
29     Y1=-10.0;Z1=0.C
30     GO TO 100
31     100 CALL GRID(NGRID,XRIBS(I),Y,Z)
32     IF(J.EQ.1) GO TO 200
33     IF(I.EQ.2.OR.I.EQ.4) GO TO 200
34     IDBAR=IDBAR+1
35     CALL CBAR(IDBAR,MBAR1,NGRID,NGRID-2,10.,0.0,0.0)
36     200 IF(I.EQ.1) GO TO 400
37     IF(J.EQ.1.OR.J.EQ.3.CR.J.EQ.5.CR.J.EQ.7) GO TO 400
38     IDBAR=IDBAR+1
39     CALL CBAR(IDBAR,MBAR2,NGRID,N1,0.0,Y1,Z1)
40     400 IF(I.EQ.1.CR.J.EQ.1) GO TO 1000
41     IDMEM=IDMEM+1
42     CALL CQDMEM(IDMEM,MMEM,NGRID,NGRID-2,N1-2,N1)
43     1000 CONTINUE
44     2000 CONTINUE
45     WRITE(6,6600)
46     6600 FORMAT(1H1)
47     STOP;END
48
49
50
51
52
53
54
55     SUBROUTINE CBAR(IC,IPID,IGA,IGB,X,Y,Z)
56     WRITE(6,6601)IC,IPID,IGA,IGB,-X,Y,Z,1
57     WRITE(7,7701)IC,IPID,IGA,IGB,-X,Y,Z,1
58     6601 FORMAT(1X,'CBAR',4X,4I8,3F8.3,18)
59     7701 FORMAT('CBAR',4X,4I8,3F8.3,18)
60     RETURN
61     END
62
63     SUBROUTINE CQDMEM(IC,IPID,IG1,IG2,IG3,IG4)
64     WRITE(6,6601)IC,IPID,IG1,IG2,IG3,IG4,0.0
65     WRITE(7,7701)IC,IPID,IG1,IG2,IG3,IG4,0.0

```

```
65 6601 FORMAT(1X,'CQDMEM2 ',6I8,F8.3)
66 7701 FORMAT('CQDMEM2 ',6I8,F8.3)
67 RETURN
68 END
```

```
69 SUBROUTINE GRID(ID,X,Y,Z)
70 IF(X.EQ.0.0.AND.Y.EQ.0.0) GO TO 2
71 WRITE(6,6601)ID,-X,Y,Z
72 WRITE(7,7701)ID,-X,Y,Z
73 GO TO 9999
74 2 WRITE(6,6602)ID,-X,Y,Z,12456
75 WRITE(7,7702)ID,-X,Y,Z,12456
76 6601 FORMAT(1X,'GRID',4X,I8,8X,3F8.3)
77 6602 FORMAT(1X,'GRID',4X,I8,8X,3F8.3,8X,I8)
78 7701 FORMAT('GRID',4X,I8,8X,3F8.3)
79 7702 FORMAT('GRID',4X,I8,8X,3F8.3,8X,I8)
80 RETURN
81 END
```

```
82 SUBROUTINE COORDF(C,X,T)
83 DIMENSION XC(18),YC(18)
84 DATA XC/0.,1.25,2.5,5.,7.5,10.,15.,20.,25.,30.,40.,50.,60.,70.,
85 180.,90.,95.,100./
86 DATA YC/0.,2.841,3.922,5.332,6.3,7.024,8.018,8.606,8.912,9.003,
87 18.705,7.941,6.845,5.496,3.935,2.172,1.210,0.189/
88 X1=X/C*100.
89 DO 1000 I=1,18
90 IF(XC(I).LT.X1) GO TO 1000
91 FRAC=(XC(I)-X1)/(XC(I)-XC(I-1))
92 T1=YC(I)-FRAC*(YC(I)-YC(I-1))
93 GO TO 9999
94 1000 CONTINUE
95 9999 T=T1*C/100.
96 RETURN
97 END
```

\$ENTRY

# A.5.3 WING PROGRAM LISTING

```

1      $JCB      ,NOEXT,T=28
2      INTFGEPR*4 C1,C2,G3,G4,G5,G6,G7,G8
3      DIMENSION GRID(3,1000)
4      READ(5,*)B,C1,CSF,CSR,XNR,NR,NGRID1,ICP
5      READ(5,*)NMEM,NPAR,NPLATE
6      READ(5,*)NPMEM,NPBAR1,NPBAR2,NPPLT,NPPLT1,NPMEM1,NPMEM2
7      WRITE(6,6600)
8      NGRID=NGRID1;NSPARG=0;N11=NGRID-2;N21=NGRID-8
11     CSF1=CSF;C=C1*2.;CSP1=CSR+CSF1
14     C2=(CSF+CSR)*C;C3=1.-(CSF+CSR)
16     IF(CSF.EQ.C.0) NSPARG=100000
17     DC 1000 I=1,NP
18     Y=XNR*(I-1)
19     C=2.*C1*(1-Y*Y/(B*B))*0.5
20     N1=NGRID-1;N2=N1-1;N3=N2-1;N4=N3-1;N5=N4-1;N6=N5-1
26     GRID(1,N1)=(CSF1+CSR)*C-C2
27     IF(CSF.EQ.0.0) GO TO 200
28     IF(I.LE.2) GO TO 500
29     IF(NSPARG.NE.0) GO TO 200
30     SLOPE=(GRID(1,N21)-GRID(1,N11))/XNR
31     XINT=GRID(1,N11)
32     CSF=(GRID(1,N1)-(Y*SLOPE+XINT))/C
33     IF(CSF.CT.C.0) GO TO 500
34     NSPARG=NGPID+4
35     200 GRID(1,N2)=-C2
36     GRID(1,N3)=GRID(1,N1)-C
37     GRID(1,N4)=GRID(1,N2)
38     DC 300 J=1,4
39     GRID(2,NGRID-J)=Y
40     300 CONTINUE
41     CALL CCCRDW(C,CSF1,CSR1,Z2,Z3,Z4,Z5)
42     GRID(3,N2)=Z4;GRID(3,N4)=Z5;GRID(3,N3)=GRID(3,N1)=0.0
45     DC 400 J=1,4
46     NJ=NGRID-J
47     CALL SGRID(NJ,ICP,GRID(1,NJ),GRID(2,NJ),GRID(3,NJ),26)
48     400 CONTINUE
49     NGRID=NGRID-4
50     GO TO 1000
51     500 CONTINUE
52     GRID(1,N4)=GRID(1,N1)-C
53     GRID(1,N2)=GRID(1,N6)=GRID(1,N1)-CSF*C
54     GRID(1,N3)=GRID(1,N5)=-C2
55     GRID(3,N1)=GRID(3,N4)=0.0
56     DC 700 J=1,6
57     GRID(2,NGRID-J)=Y
58     700 CONTINUE
59     CALL CCCRDW(C,CSF,CSR1,Z2,Z3,Z5,Z6)
60     GRID(3,N2)=Z2;GRID(3,N3)=Z5;GRID(3,N5)=Z6;GRID(3,N6)=Z3
64     DC 900 J=1,6
65     NJ=NGRID-J
66     CALL SGRID(NJ,ICP,GRID(1,NJ),GRID(2,NJ),GRID(3,NJ),26)
67     900 CONTINUE
68     NGRID=NGRID-6
69     1000 CONTINUE
70     NTIP=NGRID-1
71     GRID(1,NTIP)=-C2;GRID(2,NTIP)=8;GRID(3,NTIP)=0.0
74     CALL SGRID(NTIP,ICP,GRID(1,NTIP),GRID(2,NTIP),GRID(3,NTIP),26)
75     NGRID=NGRID1;NPI=NR-1
77     IF(CSF.EQ.0.0) GO TO 2100
78     DC 2000 I=1,NR1

```

```

79      G1=NGRID-1;G2=NGRID-2;G3=NGRID-8;G4=NGRID-7
83      G5=NGRID-1;G6=NGRID-6;G7=NGRID-12;G8=NGRID-7
87      CALL MEMBRN(NMEM,NPMEM,G1,G2,G3,G4)
88      CALL MEMBRN(NMEM,NPMEM,G5,G6,G7,G8)
89      Z1=(GRID(3,G2)-GRID(3,G6))/2.
90      Z2=(GRID(3,G3)-GRID(3,G7))/2.
91      CALL BAR(NBAR,NFBAR1,G2,G3,Z1,Z2)
92      IF(G3.EQ.NSPARC) GC TC 2100
93      NGRID=NGRID-6
94      2000 CONTINUE
95      2100 NGRID=NGRID-1
96      IF(CSF.EQ.C.O) NGRID=NGRID1
97      DC 3000 I=1,NR1
98      IF(NGRID-1.LE.NSPARG) GO TO 2500
99      G1=NGRID-1;G2=NGRID-2;G3=NGRID-8;G4=NGRID-7
103     G5=NGRID-5;G6=NGRID-4;G7=NGRID-10;G8=NGRID-11
107     CALL MEMBRN(NMEM,NPMEM,G1,G2,G3,G4)
108     CALL MEMBRN(NMEM,NPMEM,G5,G6,G7,G8)
109     G1=NGRID-2;G2=NGRID-3;G3=NGRID-9;G4=NGRID-8
113     G5=NGRID-4;G6=NGRID-3;G7=NGRID-9;G8=NGRID-10
117     CALL MEMBRN(NMEM,NPMEM1,G1,G2,G3,G4)
118     CALL MEMBRN(NMEM,NPMEM1,G5,G6,G7,G8)
119     Z1=(GRID(3,G1)-GRID(3,G5))/2.
120     Z2=(GRID(3,G4)-GRID(3,G8))/2.
121     CALL BAR(NBAR,NFBAR2,G1,G4,Z1,Z2)
122     NGRID=NGRID-6
123     GO TO 3000
124     2500 G1=NGRID-1;G2=NGRID-2;G3=NGRID-6;G4=NGRID-5
128     G5=NGRID-1;G6=NGRID-4;G7=NGRID-8;G8=NGRID-5
132     IF(G1.NE.NSPARC) GO TO 2510
133     G3=G3-1;G4=G4-1;G5=G5-4;G7=G7-1;G8=G8-1
138     2510 CONTINUE
139     CALL MEMBRN(NMEM,NPMEM,G1,G2,G3,G4)
140     CALL MEMBRN(NMEM,NPMEM,G5,G6,G7,G8)
141     Z1=(GRID(3,G2)-GRID(3,G6))/2.
142     Z2=(GRID(3,G3)-GRID(3,G7))/2.
143     CALL BAR(NBAR,NFBAR2,G2,G3,Z1,Z2)
144     G1=G2;G2=G1-1;G3=G3-1;G4=G3+1;G5=G6;G6=G2;G7=G3;G8=G7-1
152     CALL MEMBRN(NMEM,NPMEM1,G1,G2,G3,G4)
153     CALL MEMBRN(NMEM,NPMEM1,G5,G6,G7,G8)
154     IF(NGRID-1.EQ.NSPARG) NGRID=NGRID-1
155     NGRID=NGRID-4
156     3000 CONTINUE
157     IF(CSF.EQ.C.O) GC TC 3100
158     G1=NSPARG+1;G2=NSPARG;G3=NSPARG-5;G4=NSPARG-4
162     CALL TRIMEM(NMEM,NPMEM2,G1,G2,G3)
163     CALL TRIMEM(NMEM,NPMEM2,G1,G4,G3)
164     3100 G1=NTIP+4;G2=NTIP+3;G3=NTIP;G4=NTIP+1;G5=NTIP+2
169     CALL TRIMEM(NMEM,NPMEM2,G1,G2,G3)
170     CALL TRIMEM(NMEM,NPMEM2,G1,G4,G3)
171     CALL TRIMEM(NMEM,NPMEM2,G2,G5,G3)
172     CALL TRIMEM(NMEM,NPMEM2,G4,G5,G3)
173     NGRID=NGRID1
174     DC 4000 I=1,NR
175     G1=NGRID-1;G2=G1-1;G3=G2-1;G4=G3-1;G5=C4-1;G6=C5-1
181     IF(G2.LT.NSPARG) GC TC 3500
182     CALL TRIPLT(NPLATE,NPPL1,G1,G2,G6)
183     CALL TRIPLT(NPLATE,NPPL1,G2,G3,G5,G6)
184     CALL TRIPLT(NPLATE,NPPL1,G3,G4,G5)
185     NGRID=NGRID-6

```

```

186 GO TO 4000
187 3500 CALL TRIPLT(NPLATE,NPPLT,C1,G2,G4)
188 CALL TRIPLT(NPLATE,NPPLT,G2,G3,G4)
189 NGRID=NGRID-4
190 4000 CONTINUE
191 WRITE(6,6600)
192 6600 FORMAT(1H1)
193 STOP
194 END

```

```

195 SUBROUTINE CGCRDW(CHCRD,CSF,CSR,Z1,Z2,Z3,Z4)
196 DIMENSION Z(3,18)
197 DATA Z/0.C,C.C,C.0,1.25,.789,-.789,2.5,1.C89,-1.C89,
15.0,1.481,-1.481,7.5,1.75,-1.75,10.,1.951,-1.951,15.,2.228,-2.228,
220.,2.391,-2.391,25.,2.476,-2.476,30.,2.501,-2.501,40.,2.419,
3-2.419,50.,2.206,-2.206,60.,1.902,-1.902,70.,1.527,-1.527,
480.,1.094,-1.094,90.,.604,-.604,95.,.336,-.336,100.,.053,-.053/
Z1=Z2=Z3=Z4=C.C;C=C+CFD
C1=CSF*100.;C2=CSR*100.
DO 1000 I=1,18
IF(Z1.NE.C.C) GO TO 500
IF(C1.EQ.Z(1,I)) GO TO 200
IF(C1.GT.Z(1,I).AND.C1.GT.Z(1,I+1)) GO TO 1000
ZA=(C1-Z(1,I))/(Z(1,I+1)-Z(1,I))
Z1=ZA*(Z(2,I+1)-Z(2,I))+Z(2,I)
Z2=ZA*(Z(3,I+1)-Z(3,I))+Z(3,I)
GO TO 1000
200 Z1=Z(2,I);Z2=Z(3,I)
GO TO 1000
500 IF(C2.EQ.Z(1,I)) GO TO 700
IF(C2.GT.Z(1,I).AND.C2.GT.Z(1,I+1)) GO TO 1000
ZB=(C2-Z(1,I))/(Z(1,I+1)-Z(1,I))
Z3=ZB*(Z(2,I+1)-Z(2,I))+Z(2,I)
Z4=ZB*(Z(3,I+1)-Z(3,I))+Z(3,I)
GO TO 1100
700 Z3=Z(2,I);Z4=Z(3,I)
GO TO 1100
1000 CONTINUE
1100 C=C/100.;Z1=Z1*C;Z2=Z2*C;Z3=Z3*C;Z4=Z4*C
228 RETURN
229 END

```

```

230 SUBROUTINE SGRID(ID,ICP,X1,X2,X3,IPS)
231 WRITE(6,6601)ID,ICP,X1,X2,-X3,IPS
232 WRITE(7,7701)ID,ICP,X1,X2,-X3,IPS
233 6601 FORMAT(1X,'GRID',4X,2I8,3F8.2,8X,I8)
234 7701 FORMAT('GRID',4X,2I8,3F8.2,8X,I8)
235 RETURN;END

```

```

237 SUBROUTINE PAR(ID,IPID,IGA,IGB,Z1,Z2)
238 ID=ID+1;IF=1;IC1=ID-1000;X1=-100.;X2=X3=0.C
243 WRITE(6,6601)ID,IPID,IGA,IGB,X1,X2,X3,IF,IC1
244 WRITE(7,7701)ID,IPID,IGA,IGB,X1,X2,X3,IF,IC1
245 WRITE(6,6602)ID1,-Z1,-Z2
246 WRITE(7,7702)ID1,-Z1,-Z2
247 6601 FORMAT(1X,'CBAR',4X,4I8,3F8.2,I8,'+CBAR',I3)
248 7701 FORMAT('CBAR',4X,4I8,3F8.2,I8,'+CBAR',I3)

```

```

249      6602 FORMAT(1X,'+CBAR',I3,32X,F8.2,16X,F8.2)
250      7702 FORMAT('+CBAR',I3,32X,F8.2,16X,F8.2)
251      RETURN;END

253      SUBROUTINE TRIMEM(IC,IPID,IG1,IG2,IG3)
254      ID=IC+1;TH=0.0
255      WRITE(6,6601)IC,IPID,IG1,IG2,IG3,TH
256      WRITE(7,7701)IC,IPID,IG1,IG2,IG3,TH
257      6601 FORMAT(1X,'CTRIMEM',I3,518,F8.2)
258      7701 FORMAT('CTRIMEM',I3,518,F8.2)
259      RETURN;END
260

262      SUBROUTINE TRIPLT(IC,IPID,IG1,IG2,IG3)
263      ID=IC+1;TH=0.0
264      WRITE(6,6601)IC,IPID,IG1,IG2,IG3,TH
265      WRITE(7,7701)IC,IPID,IG1,IG2,IG3,TH
266      6601 FORMAT(1X,'CTRIA2',I3,518,F8.2)
267      7701 FORMAT('CTRIA2',I3,518,F8.2)
268      RETURN;END
269

271      SUBROUTINE MEMBEM(IC,IPID,IG1,IG2,IG3,IG4)
272      ID=IC+1;TH=0.0
273      WRITE(6,6601)IC,IPID,IG1,IG2,IG3,IG4,TH
274      WRITE(7,7701)IC,IPID,IG1,IG2,IG3,IG4,TH
275      6601 FORMAT(1X,'CCDMEM2',I3,618,F8.2)
276      7701 FORMAT('CCDMEM2',I3,618,F8.2)
277      RETURN;END
278

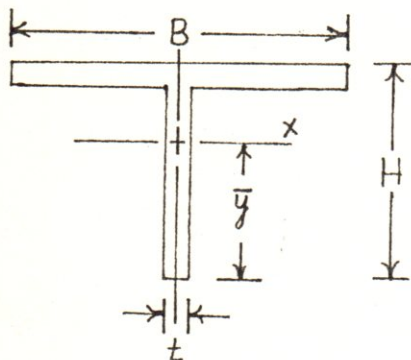
280      SUBROUTINE QDPLT(IC,IPID,IG1,IG2,IG3,IG4)
281      ID=IC+1;TH=0.0
282      WRITE(6,6601)IC,IPID,IG1,IG2,IG3,IG4,TH
283      WRITE(7,7701)IC,IPID,IG1,IG2,IG3,IG4,TH
284      6601 FORMAT(1X,'CQLA2',I3,618,F8.2)
285      7701 FORMAT('CQLA2',I3,618,F8.2)
286      RETURN;END
287

```

\$ENTRY

# A.5.4 CBAR ELEMENT PROPERTIES CALCULATIONS

## FUSELAGE T-SECTION RIBS & STRINGERS



$$B = 0.75''$$

$$H = 0.55''$$

$$t = 0.05''$$

$$\text{Area} = Bt + (H-t)t$$

$$= (0.75)(0.05) + (0.55-0.05)(0.05)$$

$$= \underline{0.0625 \text{ in.}^2}$$

$$\bar{y} = H - \frac{H^2 t + t^2 (B-t)}{2(\text{Area})}$$

$$= 0.55 - \frac{(0.55)^2 (0.05) + (0.05)^2 (0.75-0.05)}{2(0.0625)}$$

$$= \underline{0.415 \text{ in.}}$$

$$I_x = \frac{t \bar{y}^3 + B(H-\bar{y})^3 - (B-t)(H-\bar{y}-t)^3}{3}$$

$$= \frac{(0.05)(0.415)^3 + (0.75)(0.55-0.415)^3 - (0.75-0.05)(0.55-0.415-0.05)^3}{3}$$

$$= \underline{0.00166 \text{ in.}^4}$$

$$I_y = \frac{t B^3 + (H-t)t^3}{12}$$

$$= \frac{(0.05)(0.75)^3 + (0.55-0.05)(0.05)^3}{12}$$

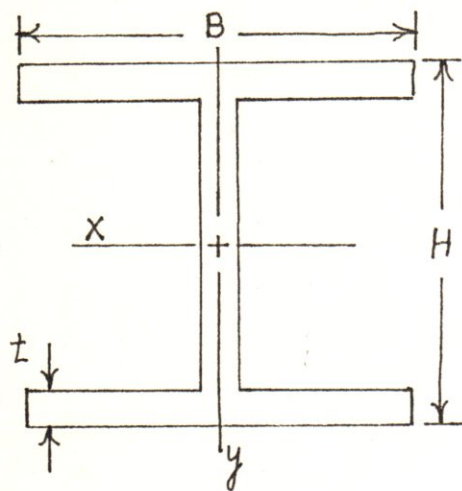
$$= \underline{0.00176 \text{ in.}^4}$$

$$J = I_x + I_y = 0.00342 \text{ in.}^4$$





# MAIN WING SPAR



$$B = H = 1.75''$$

$$t = 0.04''$$

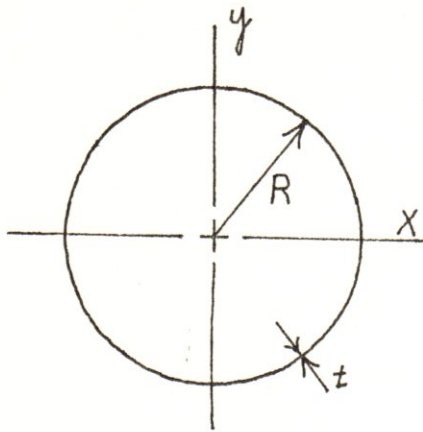
$$\begin{aligned} \text{AREA} &= 2Bt + (H-2t)t \\ &= 2(1.75)(.04) + (1.75-.08)(.04) \\ &= \underline{0.20680 \text{ in}^2} \end{aligned}$$

$$\begin{aligned} I_x &= \frac{BH^3 - (H-2t)^2(B-t)}{12} \\ &= \frac{(1.75)^4 - (1.75-.08)^2(1.75-.04)}{12} \\ &= \underline{0.11789 \text{ in}^4} \end{aligned}$$

$$\begin{aligned} I_y &= \frac{(H-2t)t^3 + 2tB^2}{12} \\ &= \frac{(1.75-.08)(.04)^3 + 2(.04)(1.75)^2}{12} \\ &= \underline{0.03574 \text{ in}^4} \end{aligned}$$

$$J = I_x + I_y = \underline{0.15363 \text{ in}^4}$$

# WING REAR SPAR (INBOARD)



$$R = 0.75''$$

$$r = R - t \\ = 0.74''$$

$$t = 0.01''$$

$$\begin{aligned} \text{AREA} &= \pi (R^2 - r^2) \\ &= \pi [(0.75)^2 - (0.74)^2] \\ &= \underline{0.04681 \text{ in}^2} \end{aligned}$$

$$\begin{aligned} I_x = I_y &= \frac{\pi}{4} (R^4 - r^4) \\ &= \frac{\pi}{4} [(0.75)^4 - (0.74)^4] \\ &= \underline{0.01299 \text{ in}^4} \end{aligned}$$

$$I = 2I_x = \underline{0.02598 \text{ in}^4}$$

PROPOSAL COSTS

PROPOSAL COSTS

1. Personnel

A. 15 weeks for 4 engineering students at

1) 4 hrs/week @ \$10.00 \$ 2400  
2) 15 hrs/week @ \$10.00 \$ 9000

B. 1 week for 4 engineering students at

50 hrs/week @ \$10.00 \$ 2000

Subtotal Personnel \$ 13,400

2. Use of Facilities, Equipment and Supplies

A. Computer \$ 2000

B. References \$ 50

Subtotal Facilities \$ 2050

3. Other Direct Costs

A. Xerograph \$ 75

B. Telephone \$ 40

C. Travel

1) Two trips to Linda Hall Library \$ 60

2) One trip to AVRADCOM \$ 10

Subtotal Other Direct Costs \$ 190

Total Fixed Price \$ 15,635

